

**STUDIES ON EFFECT OF SMALL MOLECULES ON
PROTEIN FOLDING, MISFOLDING AND
AMYLOIDOGENESIS**

by

NANDINI SARKAR

In Partial Fulfillment of the Requirements

for the Degree of

DOCTOR OF PHILOSOPHY



**DEPARTMENT OF BIOTECHNOLOGY
INDIAN INSTITUTE OF TECHNOLOGY GUWAHATI
GUWAHATI 781039, ASSAM, INDIA**

July 2011



... Dedicated to my beloved parents



INDIAN INSTITUTE OF TECHNOLOGY GUWAHATI

DEPARTMENT OF BIOTECHNOLOGY

CERTIFICATE

I hereby declare that the matter embodied in this thesis entitled “*Studies on effect of small molecules on protein folding, misfolding and amyloidogenesis*” is the result of investigations carried out by me in the Department of Biotechnology, Indian Institute of Technology Guwahati, India under the supervision of **Dr. Vikash Kumar Dubey**.

In keeping with the general practice of reporting scientific observations, due acknowledgements have been made wherever the work of other investigators are referred.

Ms. Nandini Sarkar

(Candidate)

Roll No: 07610603

July, 2011



INDIAN INSTITUTE OF TECHNOLOGY GUWAHATI

DEPARTMENT OF BIOTECHNOLOGY

CERTIFICATE

It is certified that the work described in this thesis entitled “*Studies on effect of small molecules on protein folding, misfolding and amyloidogenesis*” by Ms. Nandini **Sarkar** submitted to Indian Institute of Technology Guwahati, India for the award of degree of Doctor of Philosophy is an authentic record of the results obtained from the research work carried out under my supervision at the Department of Biotechnology, Indian Institute of Technology Guwahati, India and this work has not been submitted elsewhere for a degree.

July, 2011

Dr. Vikash Kumar Dubey
(Supervisor)

Acknowledgement

At the outset, I am thankful to Indian Institute of Technology, Guwahati, India and its Department of Biotechnology for having selected me and for providing me the best of facilities for carrying out my doctoral research for a period spanning over four years. I express my respect and gratitude to Dr Gautam Barua, Director, IIT Guwahati.

I would take this opportunity to express my deep sense of gratitude to my supervisor, Dr Vikash Kumar Dubey for his guidance, support and direction. He has been the leading light in my endeavor for meaningful and significant research in the fast growing field of Biotechnology. He has been my constant source of encouragement and inspiration through varying phases of experimental outcome, embedded with occasional pitfalls. I am grateful to the other members of the Doctoral Committee, Dr Kannan Pakshirajan, Dr Utpal Bora and Dr Sanjukta Patra for their valuable suggestions and advices which enabled me to improve my work.

I am thankful to Dr Rukhsana Chowdhury and Amartya at Indian Institute of Chemical Biology, Kolkata for their help with MALDI TOF experiment. I express my gratitude to Prof Soumen Basak of Saha Institute of Nuclear Physics, Kolkata for helping me with CD experiment.

I am grateful to the successive Heads of Department of Biotechnology, Indian Institute of Technology, Guwahati, Prof Pranab Goswami and Prof Arun Goyal for providing me with the departmental facilities for carrying out my research work. I would also like to thank the technical staff of the department for their help and assistance.

I am thankful to my fellow lab members viz, Manjeet, Anil, Abhay, Saudagar, Sushant, Shyamli, Mousumi, Neha, Deblina as well as ex-lab members Bishal and Gayatri for their help and co-operation and also for providing a healthy working environment in the lab. I owe my thanks to Naresh and Vijay Bhaiya for their help with AFM experiments. I am also thankful to Gayatri, ex-BTP for her help with the docking studies. My friends in IITG especially Naresh, Adreeja, Urmila, Purabi, Rachna, Seema, Asim and others deserve special mention for making my stay in the campus lively and enjoyable. Their love and affection has been a constant source of motivation that helped me sail through difficult times.

Last but not the least; I owe personal gratitude to my parents and sister for their endless love, support and encouragement. It is their support, encouragement and good wishes that has helped me to tide over any difficulties that I faced during the past four years and motivated me to move on.

*Nandini Sarkar
July, 2011*

Abbreviations

AD	.	Alzheimer's disease
AFM	.	Atomic Force Microscopy
ANS	.	8-anilino-1-naphthalene sulfonate
AP	.	Aggregation prone
APP	.	Amyloid precursor protein
A β	.	Amyloid beta
BSA	.	Bovine Serum Albumin
CFTR	.	Cystic Fibrosis Transmembrane Conductance Regulator
CR	.	Congo Red
Cyt C	.	Cytochrome C from bovine heart
DKGR	.	2,5 Diketo-D-Gluconate Reductase
DNSCI	.	Dansyl chloride
DTT	.	Dithiothreitol
ER	.	Endoplasmic reticulum
FBS	.	Fetal bovine serum
FTIR	.	Fourier Transform Infra Red
GuHCl	.	Guanidine hydrochloride
HEWL	.	Hen Egg White Lysozyme
MG	.	Molten globule
MTT	.	3-(4,5-dimethyl thiazol-2-yl)-2,5-diphenyl tetrazolium bromide
NMR	.	Nuclear magnetic resonance
STT	.	Sodium tetrathionate
TCEP	.	tris(2-carboxyethyl)phosphine
TEM	.	Transmission electron microscopy
ThT	.	Thioflavin T
TIPT	.	Tetra isopropyl titanate
TTR	.	Transthyretin
β -Glu	.	β -glucocerebrosidase

Contents

Chapter I - Review of literature on protein folding, misfolding and aggregation: Scope and objective of current research	1-30
1.1 Abstract	1
1.2 Review of Literature	2-27
1.2.1 Protein folding	2
1.2.2 Role of intermediate state in protein aggregation	3
1.2.3 Compartmentalization of protein folding	6
1.2.4 Protein aggregation and associated diseases	8
1.2.5 Amyloid fibrils	12
1.2.6 Mechanism of amyloid fibril formation	14
1.2.7 Polymorphism within amyloid fibrils	16
1.2.8 Factors that modulate amyloid formation	17
1.2.9 Therapeutic approach to amyloid diseases	19
1.2.10 Thermodynamics of aggregation	23
1.2.11 Model proteins used in the study	25
1.3 Scope of current research	26
Chapter II - Exploring possibility of promiscuous amyloid inhibitor: Studies on effect of selected compounds on folding and amyloid formation of proteins	31-51
2.1 Abstract	31
2.2 Introduction	32
2.3 Materials and Methods	33
2.3.1 Materials	33
2.3.2 Fluorescence Spectroscopy	33
2.3.3 Thioflavin T assay	34
2.3.4 Equilibrium unfolding study	34
2.3.5 Unfolding kinetics study	34
2.3.6 ANS binding kinetics	35
2.3.7 Atomic Force Microscopy	35
2.3.8 MTT assay	35
2.3.9 Prediction of amyloidogenic regions of model proteins and binding site(s) of rottlerin	36
2.4 Results	37-46
2.4.1 Thioflavin T assay of amyloid progression	37
2.4.2 Atomic Force Microscope Imaging	39
2.4.3 Toxicity assay of HEWL fibrils	40
2.4.4 Thermodynamic basis of amyloid inhibition	40
2.4.5 Alteration in exposed surface hydrophobicity of the aggregate prone state	43
2.4.6 Docking studies to identify potential binding site(s)	45
2.5 Discussions	47

2.6 Conclusions	51
Chapter III - Dissolution of amyloid fibril by rottlerin: A study on Hen Egg White Lysozyme	52-64
3.1 Abstract	52
3.2 Introduction	53
3.3 Materials and Methods	54
3.3.1 Materials	54
3.3.2 Thioflavin T assay	54
3.3.3 Anisotropy study	55
3.3.4 Atomic Force Microscopy	55
3.3.5 ANS binding assay	55
3.3.6 FTIR Spectroscopy	56
3.3.7 Fluorescence quenching	56
3.4 Results	57-62
3.4.1 Disaggregation of HEWL fibril by rottlerin	57
3.4.2 Conformational changes in HEWL fibril induced by rottlerin	58
3.4.3 Characterisation of HEWL and rottlerin interaction	60
3.5 Discussions	62
3.6 Conclusions	64
Chapter IV - Exploring role of disulfide bonds in amyloidogenesis: A study on Hen Egg White Lysozyme	65-82
4.1 Abstract	65
4.2 Introduction	66
4.3 Materials and Methods	67
4.3.1 Materials	67
4.3.2 Thioflavin T assay	67
4.3.3 Atomic Force Microscopy	67
4.3.4 MTT assay	68
4.3.5 ANS binding assay	68
4.3.6 Equilibrium unfolding study	68
4.3.7 Unfolding kinetics study	69
4.3.8 Intrinsic fluorescence study	69
4.4 Results	70-79
4.4.1 Monitoring amyloid progression in presence of STT	70
4.4.2 Monitoring changes in surface hydrophobicity of HEWL	73
4.4.3 Exploring role of disulfide bonds in amyloidogenesis	74
4.4.4 Monitoring effect of STT on stability and unfolding kinetics of HEWL	76
4.4.5 Monitoring conformational changes in HEWL on STT addition	76
4.5 Discussions	80
4.6 Conclusions	82

Chapter V - Effect of curcumin on amyloidogenic property of molten globule like intermediate state of 2,5 Diketo Gluconate Reductase	83-100
5.1 Abstract	83
5.2 Introduction	84
5.3 Materials and Methods	85
5.3.1 Materials	85
5.3.2 Expression of DKGR	85
5.3.3 Purification of DKGR	86
5.3.4 GuHCl unfolding	87
5.3.5 pH denaturation	87
5.3.6 Fluorescence spectroscopy	87
5.3.7 Acrylamide quenching	87
5.3.8 Spectropolarimetry	88
5.3.9 Thioflavin T assay	88
5.3.10 Atomic Force Microscopy	88
5.4 Results	89-97
5.4.1 Characterisation of the folding pathway of DKGR	89
5.4.2 Characterisation of the intermediate state(s) populating the folding pathway	92
5.4.3 Monitoring amyloid progression of DKGR	95
5.5 Discussions	98
5.6 Conclusions	100
Chapter VI - Summary	101-104
Chapter VII – Bibliography	105-118
Publications	119

Review of literature on protein folding, misfolding and amyloid: Scope and objective of current research*.

1.1 Abstract

The correct folding of polypeptides to their native tertiary structure is a prerequisite for proper functioning of the proteins. However, despite several cellular quality control mechanisms, proteins sometimes get misfolded and trapped as aggregates. The transition of proteins from their soluble, globular form to insoluble, fibrillar aggregates is one of the most elusive problems to modern science, which has been subjected to extensive research. These fibrillar aggregates sometimes exhibit highly stable and ordered structures which are known as “amyloids”. Deposition of amyloids in the extracellular matrix has been the starting point of several degenerative diseases such as, Alzheimer’s disease, Parkinson’s disease, Type II diabetes and so on. Currently, efforts are on to develop an efficient mode of therapy against amyloid diseases. The interesting property of amyloids of being highly similar in structural, toxicity, immunogenic and tinctorial properties, irrespective of their source proteins invite the attention towards development of a common mode of therapy.

* Part of the work has been published in *Current Proteomics*, **2010**, 7, 116-120

1.2 Review of Literature

1.2.1 Protein Folding

The inherent ability of a polypeptide chain to fold to its native state with sufficient frequency for it to be able to execute its function in a living organism is one of the most fundamental and remarkable phenomenon of biology (Luheshi and Dobson, 2009). According to Levinthal's Paradox, considering the milliseconds or even microseconds timescale of protein folding, it is impossible for a polypeptide chain to fold by a random search through all its possible configurations as it would take enormously long time (Levinthal, 1968). It was Anfinsen and his co workers who first demonstrated that proteins can fold unassistedly and reversibly to its native three dimensional states based on its amino acid sequence (Anfinsen *et al.*, 1961; Anfinsen, 1973). Thus a driving force must be present within the amino acid sequence of a protein which 'escorts' the polypeptide chain to its uniquely folded native state in minimal timescale.

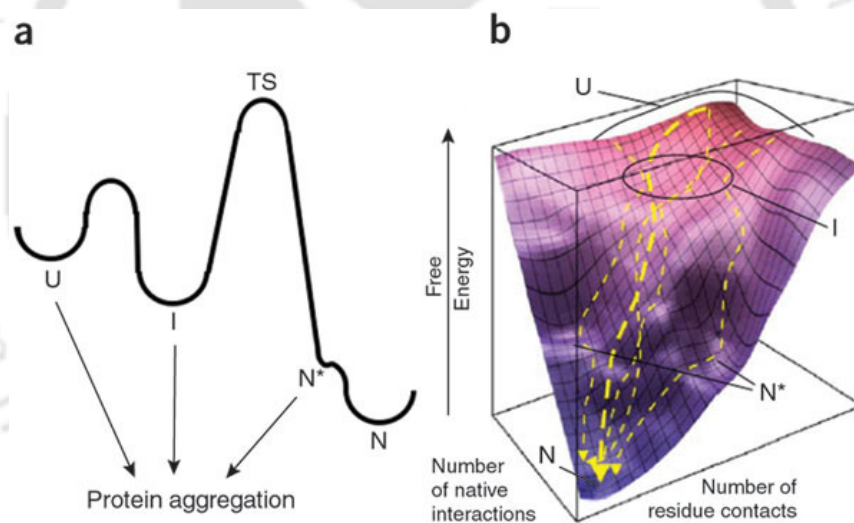


Figure 1.1 Funnel representing an idealized energy landscape for protein folding or a rugged energy landscape with kinetic traps. Molecular chaperones may act to “smooth” rugged landscapes, preventing polypeptide from descending into a kinetic trap, or rescuing it from one. Protein molecules adopting the U, I and N* states or conformations can all self-assemble and consequently trigger amyloid formation, where U, I, N* and N represents unfolded, partially unfolded, locally unfolded and native states respectively. (Adopted with permission from *Nat Chem Biol* 2009, 5: 15–22).

A “folding funnel” or “energy landscape theory” has been proposed for protein folding according to which, the unfolded protein starts from the top of the folding funnel, and during the folding process intramolecular interactions are formed thereby lowering

the free energy as it descends the funnel. The number of possible conformations at each stage is also reduced simplifying the folding process and finally it reaches the unique native state at the lowest energy level. However, in case of larger proteins (generally greater than 100 to 150 amino acids) and few small proteins, the folding funnel is not “smooth” but “rugged” which is due to presence of intermediate state(s) in the folding pathway (Horwich, 2002). During the folding process the protein may get kinetically trapped in local energy minima as intermediate state and has to cross certain energy barrier in order to reach the unique native state at the bottom of the folding funnel. These transiently populated states, known as intermediate states are partially folded protein conformations which have been found to be susceptible to self assembly owing to exposure of hydrophobic core (Oberg *et al.*, 1994).

1.2.2 Role of intermediate state in protein aggregation

These intermediate states are sometimes necessary conformations that a protein must traverse during the folding process in order to reach the native state, in which case the folding pathway is called Non-cooperative or Multistate folding. Whereas in other cases, these states may lie away from a productive pathway and are known as “off-pathway intermediates”. Regardless, when these intermediate states are significantly populated they interact with each other to form aggregates thereby shifting the equilibrium towards protein aggregation, where intermolecular interactions prevail over intramolecular ones. These aggregates are generally classified as either amorphous or highly ordered, the most common form of the latter being “amyloid fibril”. Formation of amyloid is highly dependent on environmental conditions like temperature, ionic strength, pH, peptide or protein concentration etc. (Calamai *et al.*, 2005; Gsponer and Vendruscolo, 2006).

The phenomenon of protein aggregation was first demonstrated by Goldberg and his colleagues in their classic experiment on tetrameric tryptophanase protein (London *et al.*, 1974). They observed that on unfolding tryptophanase with 8 M urea and then diluting into buffer, both refolded native enzyme and inactive aggregate formed. However, with increasing concentration of protein more enzymes were trapped as inactive aggregates. Importantly, these workers showed that the protein partitions in different ways between the native state and the inactive aggregate, depending on the concentration of urea used at the renaturation step. Thus with 3 M urea all the protein

was found in the aggregate state suggesting presence of an intermediate state at this denaturant concentration which is prone to aggregation. They further showed that the self-association of this intermediate is specific, since when BSA or even a crude bacterial extract is denatured in the same tube with the tryptophanase, the enzyme's refolding proceeds exactly as before. To account for both the concentration dependence and the specificity of the aggregation reaction, Goldberg and colleagues proposed that aggregation is driven by the same stereospecific interactions that are required for folding of the polypeptide chain to its native form, but here these interactions occur between two separate polypeptide chains that is, intramolecular contacts become substituted for intermolecular ones. These studies essentially indicate the role of intermediate states in initiating aggregation through intermolecular interactions and further points towards the specificity of these interactions.

It has been suggested that conformations with enhanced flexibility and solvent accessibility are important for initiation of fibrillation indicating partial unfolding of the rigid native structure is a prerequisite for amyloid formation (Pedersen *et al.*, 2004). Till date several studies have shown the role of partially folded intermediate states, populating under mildly denaturing conditions, in initiating fibrillogenesis. β_2 microglobulin fibrillogenesis *in vitro* have been found to be triggered by partially unfolded species with significant secondary structure, non-native tertiary structure, and high surface hydrophobicity which populates at low pH and high ionic strength (McParland *et al.*, 2000). Hen egg white lysozyme fibrillogenesis have been found to be induced by partially unfolded protein conformation populating at low pH and elevated temperature (Wang *et al.*, 2006). Further many studies have shown that these intermediate states demonstrate a molten globule like conformation with high surface hydrophobicity, distinct secondary structures and non-native conformation (Gerber *et al.*, 2007). Also, the hydrophobic interactions among these non-native species have been mainly found to trigger amyloidogenesis (Booth *et al.*, 1997; Bolognesi *et al.*, 2010).

Since amyloid fibrils are characterized by β sheeted conformation irrespective of their native monomeric conformation, proteins are believed to undergo major conformational transition from native structure to predominantly β sheeted structure before oligomerisation (Kayed *et al.*, 1999). Further, self association through the exposed

β strands of the amyloidogenic intermediates is believed to induce fibrillogenesis (Booth *et al.*, 1997). However, a study by Gerber *et al.*, have showed that β oligomer formation is not necessarily preceded by monomeric precursors with β sheet structure but it is formed in the process of oligomerisation triggered by intermolecular contacts between constantly rearranging structures (Gerber *et al.*, 2007). Though in most cases, these intermediates have been found to populate under non-physiological conditions, however few studies have shown presence of partially unfolded monomeric intermediates at close to physiological conditions, which induce aggregation. A study by Quintas *et al.*, have shown dissociation of tetrameric transthyretin (TTR) under close to physiological conditions leads to the formation of a non native monomer which do not exhibit molten globule like conformation and have been found to induce aggregation. This intermediate state showed least thermodynamic stability of all TTR variants, suggesting partial unfolding and conformational fluctuations of molecular species with marginal thermodynamic stability may play crucial role in protein aggregation (Quintas *et al.*, 2001). However, other mechanisms may also be present, as few studies have shown aggregate formation from completely denatured protein state (Silow *et al.*, 1999) or even from native state where locally disordered regions are present (Calloni *et al.*, 2005) or perhaps through domain swapping (Liu *et al.*, 2001). These studies show that protein intermediate states play a vital role in initiating aggregation. When these partially folded intermediate states accumulate significantly under mildly denaturing conditions due to factors like protein mutation, defective quality control machinery of the cell and destabilizing environmental conditions, they interact among themselves through intermolecular interactions leading to aggregate formation. Thus, transiently populated intermediate states are the critical initiators of aggregation in most cases, subsequently leading to amyloid formation.

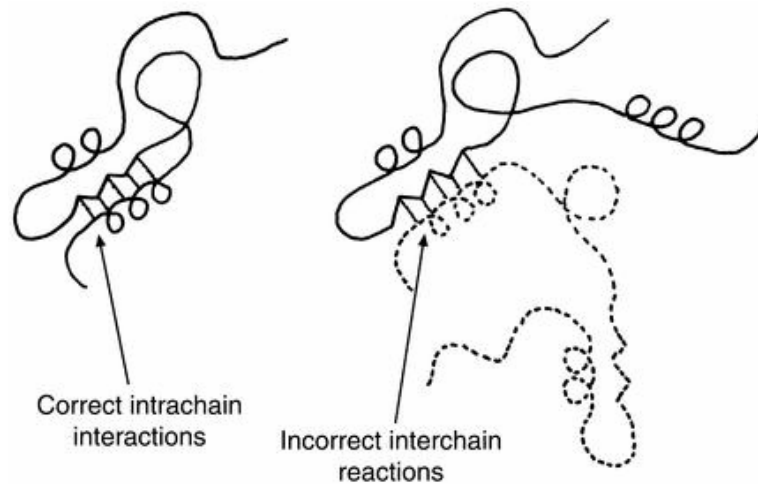


Figure 1.2 Model of Goldberg and coworkers showing intramolecular interactions substituted by intermolecular ones during the process of aggregation (Adopted with permission from *Eur J Biochem* 1974, 47:409-415).

1.2.3 Compartmentalization of protein folding

The folding of the translated linear strand of amino acids in the endoplasmic reticulum (ER) into a fully functional three dimensional protein, and its efficient translocation is one of the most complex challenges facing the cellular protein factory. Preventing accumulation of aggregation prone misfolded protein conformation is the first and most effective intervention point to control protein aggregation. Cells of all kingdoms of life have evolved an elaborate protein quality control system, which acts either to facilitate folding or refolding of misfolded protein species by molecular chaperones or to remove them by proteolytic degradation thereby preventing protein aggregation (Tyedmers *et al.*, 2010). In the cell, proteins are synthesized in the ribosomes from the genetic information encoded in the DNA. Folding *in vivo* is sometimes co-translation, that is, it is initiated before the completion of the protein synthesis when the nascent polypeptide is still attached to the ribosome. However, majority of the folding process occur in the ER. Since incompletely folded proteins are bound to expose regions which are mostly buried in natively folded state, they are prone to aggregation with other molecules in the crowded environment of the cell (Dobson, 2003). Living systems have therefore evolved a range of strategies to prevent such behaviour.

Molecular chaperones like heat shock proteins Hsp 90, Hsp 70 and so on in the ER, play a crucial role in assisting proper protein folding by interacting with partially folded non-native polypeptides, predominantly with the exposed hydrophobic surfaces

and thereby preventing misfolding and aggregation (Hendrick and Hart, 1995). These non-native protein conformations with exposed hydrophobic surfaces are most prone to aggregation. Not only the heat shock proteins prevent aggregation of the partially folded protein structures by binding to the hydrophobic residues, but they also assist in protein folding, triggered upon binding of ATP. If the released protein substrate from the chaperonin complex is still misfolded or incompletely folded, it again binds to another chaperone and retrys the folding process or it is recognized by the cell, ubiquitinated and degraded by the proteasome complex. Thus the sequestration of misfolded proteins allows for the efficient solubilization and refolding or degradation by the components of protein quality control network. Though molecular chaperones assist in proper protein folding, they do not play any role in increasing the rate of individual steps involved in the overall process of folding. There are several classes of folding catalyst that accelerate potentially slow steps in the folding process (Dobson, 2003). Most notable among them are prolyl peptide isomerase that increase the rate of *cis-trans* isomerisation of the peptide bond involved with the proline residue and protein disulfide isomerase which enhance the rate of formation and reorganization of the disulfide bonds (Schiene and Fischer, 2000).

In eukaryotes, most of the proteins synthesized in the cell are destined to be secreted outside into the extra cellular space. These proteins are translocated in the ER where folding takes place before they are secreted outside through the golgi body. The ER has a range of molecular chaperones and folding catalysts that ensure proper folding of the protein. In addition, the newly folded protein has to pass a “quality control” check before they are being exported out (Dobson, 2003). This process is important as there are very few molecular chaperones outside the cell (Wilson and Easterbrook, 2000). This quality-control mechanism comprises of a series of glycosylation and deglycosylation reaction that enables correctly folded protein to be distinguished from the incorrectly folded ones. The importance of this regulatory mechanism lies in the fact that large number of proteins synthesized in the cell fails to pass this regulatory test and are directed for being degraded inside the cell (Schubert, 2000). Further, like the heat shock response, this unfolded protein response is also stimulated under stress and is strongly linked to avoidance of protein misfolding diseases (Bench *et al.*, 2001).

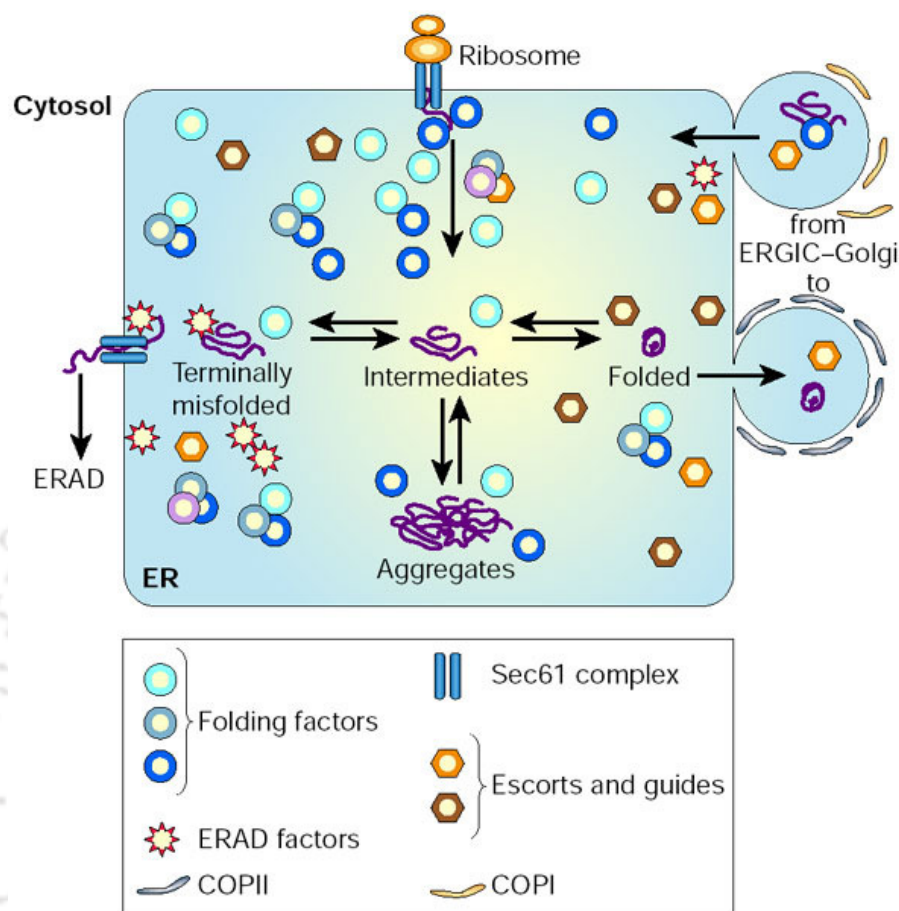


Figure 1.3: Proteins are synthesized by ER-associated ribosomes and co-translationally translocated across the membrane through the Sec61 complex. The ER is rich in chaperones and folding enzymes (folding factors), in molecules involved in mediating transport to the cytosol for proteasomal degradation (ERAD factors) or to the downstream stations of the secretory pathway (Adopted with permission from *Nature* 2003, 426: 891-894).

1.2.4 Protein aggregation and associated diseases

A broad range of diseases arise due to failure of a specific peptide or protein to adopt or remain in its native functional conformational state. Such diseases are collectively known as protein misfolding or protein conformational diseases (Chiti and Dobson, 2006). It is well established that only correctly folded protein can function and folding of proteins *in vivo* may be co-translational or post-translational (Hardesty and Kramer, 2001). Many Heat shock proteins, also called molecular chaperons, such as Hsp70, Hsp90, Hsp40 and other folding catalysts like protein disulfide isomerase, prolyl peptide isomerase etc help in the folding of the protein *in-vivo* (Barral *et al.*, 2004). Some chaperons, like Hsp70 and Hsp100, act on protein aggregates and solubilize them and

provide another chance to refold (Liberek *et al.*, 2008). Only folded proteins are then translocated to the Golgi complex and then delivered to various cellular compartments. The misfolded species of protein is recognized by quality control machinery and degraded by ubiquitine-proteasome pathway. Thus, the protein quality control has important role in maintaining normal function of the cell.

Failure or impaired function of cellular protein quality control machinery results in several diseases (Kaganovich *et al.*, 2008). Such diseases can be broadly classified in two categories. In the first category, protein is misfolded and degraded by quality control machinery of the cell. This results in reduction in quantity of protein that is available to play its normal role. For example, in case of cystic fibrosis, $\Delta F508$ mutation in CFTR Protein results in misfolding of the protein and degraded by ubiquitine-proteasome pathway (Howard and Welch, 2002). The $\alpha 1$ -antitrypsin ($\alpha 1$ -AT) deficiency is other example of this class (Carrell and Lomas, 2002). The second category which includes majority of the protein misfolding diseases involve conversion of specific peptides or proteins from their soluble functional states to insoluble fibrillar aggregates (Chiti and Dobson, 2006; Leandro and Gomes, 2008). When these aggregates deposit extracellularly and are highly ordered, stable structures, they are referred to as “amyloids” leading to several diseases in humans which are collectively known as “amyloidoses” (Rambaran and Serpell, 2008). Till date more than 30 such diseases have been identified which are caused due to deposition of amyloid fibril in the tissues and few of them are listed in Table 1. Thus, protein aggregation appears to be a pathway alternative to protein folding in specific conditions where intermolecular interactions are favored instead of intramolecular interactions.

Although it is clear that amyloid deposition in the tissues results in amyloidoses, but the exact causative agent of the pathogenesis and its mode of action still remain elusive. In many cases it has been suggested that direct interaction of the insoluble fibrillar deposits with the cell membrane leads to the formation of non specific pore-like channels subsequently resulting in membrane permeabilization and eventually cell death (Lashuel, 2005; Engel 2009).

Other hypotheses have been put forward to describe the biochemical basis of the toxicity of amyloid aggregates. Some refer to a number of data indicating cell experiencing toxic aggregates undergo early changes of the intracellular ion content and redox status (Stefani and Dobson, 2003). These data may be a consequence of the presence in the exposed cell of pores modifying membrane permeability (Stefani, 2004). Whereas in some cases, direct deposition of large masses (few kilograms) of fibrils in the tissues have been found to disrupt cellular or organic functions. Studies have also shown that the level of toxicity in Alzheimer's disease does not correlate with the amount of plaque deposited in the brain tissue but with the amount of soluble oligomeric species present (Bucciantini *et al.*, 2002).

Table 1.1 Various diseases resulted from protein aggregation/amyloid formation

PROTEIN INVOLVED	DISEASE/EFFECTED ORGAN
<i>Neurodegenerative Diseases</i>	
Amyloid β -protein ($A\beta$)	Alzheimer's disease
α -Synuclein	Parkinson's disease
Huntingtin polyglutamine sequence	Huntington's disease
Prion protein (PrP)	Creutzfeldt-Jakob disease; mad cow disease
Cystatin C, Gelsolin	Cerebral amyloid angiopathy
ABri	Familial British dementia
<i>Non-neural Diseases</i>	
β -glucocerebrosidase	Spleen, liver, kidneys, lungs, bone marrow etc (Gaucher's disease)
CFTR protein	Lungs (Cystic fibrosis)
p53	Cancer
Transthyretin	Heart, kidney, peripheral neuropathy
Serum amyloid A	Kidney, peripheral neuropathy
Immunoglobulin light chain	Kidney, heart
Immunoglobulin heavy chain	Spleen
Pro-islet amyloid polypeptide (fragments)	Type II diabetes
Medullar carcinoma of thyroid	Procalcitonin
β 2-Microglobulin	Carpal tunnel syndrome, osteoarthropathies
Islet amyloid polypeptide	Diabetic pancreatic islet cells
Fibrinogen α -chain	Kidney
Apolipoprotein A1	Peripheral neuropathy, liver
Atrial natriuretic peptide	Heart

This study suggests that the soluble oligomeric intermediates that precede the formation of matured fibrils are the primary toxic species in amyloidosis compared to the insoluble matured fibrils (Lambert *et al.*, 1998; Hartley *et al.*, 1999). It is clear that conversion of a protein from its soluble state into oligomeric forms will invariably generate a wide distribution of non-native species, the population of which will vary with sequence, time and conditions (Chiti and Dobson, 2006). Also, recent reports indicate common mode of toxicity which is not related to protein sequence but depends on the structural features of the assembly, as non-disease associated protein amyloid can be equally toxic to cells (Canale *et al.*, 2006). These findings provide new insight into the mechanism of pathogenesis of these abnormal protein aggregates and also reveal that the toxicity of protein aggregates may lie in their supramolecular structure and not in their amino acid sequence.

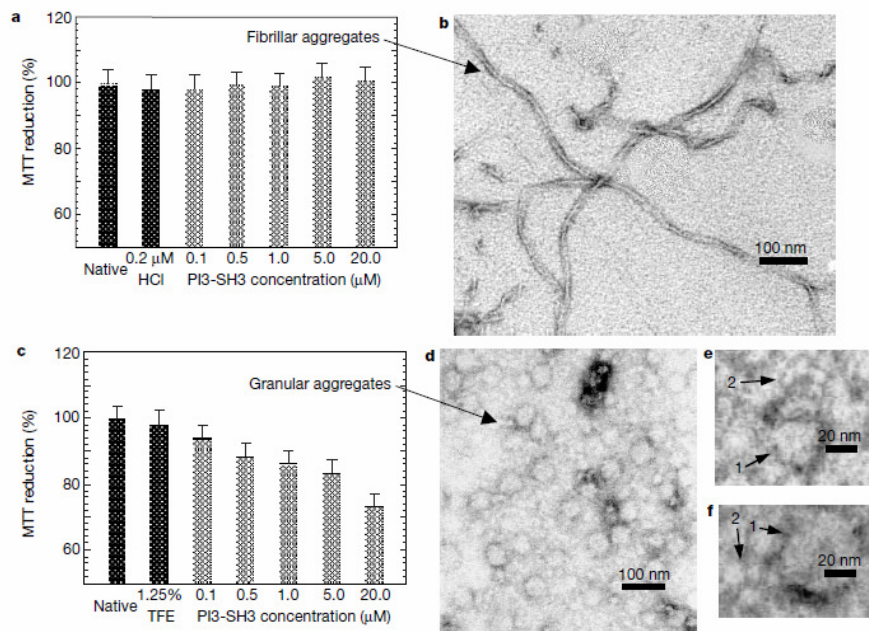


Figure 1.4 MTT assay showing pre fibrillar aggregates, exhibiting beaded chain-like structures, are more toxic than matured fibrils (Adopted with permission from *Nature* 2002, 416: 507-511).

Based on their source organ, amyloid diseases can be broadly classified into three groups - i) neurodegenerative diseases in which amyloid deposits are formed in the brain tissues, ii) nonneuropathic localized amyloidosis in which amyloid deposits are found in a single type of tissue other than the brain, iii) nonneuropathic systemic amyloidosis in which aggregates are found in multiple tissues. Most of amyloid diseases (85%) are

sporadic like Alzheimer's and Parkinson's Disease, some (10%) are hereditary arising from genetic mutations like lysozyme and fibrinogen amyloidosis and others (5%) are transmissible like spongiform encephalopathies (Chiti and Dobson, 2006).

1.2.5 Amyloid Fibrils

For many years the only structural information available about amyloid fibrils came from imaging techniques like TEM and more recently from AFM and X ray diffraction studies (Serpell *et al.*, 1995; Harper *et al.*, 1997; Sunde and Blake, 1997).

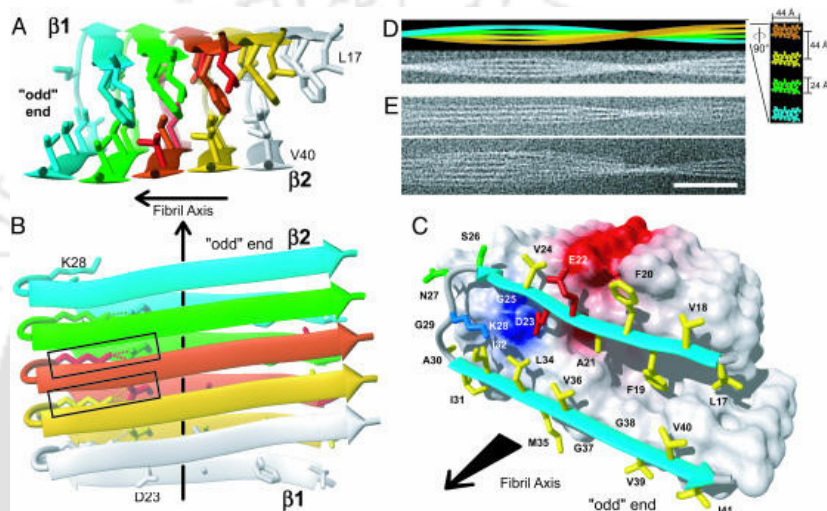


Figure 1.5 3-D structure of the A β (1-42) fibril, showing the arrangement of the β -strands and the inter-atomic distances between the amino acid residues, as obtained from solid state NMR studies (Adopted from *Proc Natl Acad Sci USA* 2005, 102: 17342-17347).

The non-crystalline nature and the large size of amyloid fibrils made them unsuitable candidates for techniques like X-ray crystallography and NMR. However, recent advances in solid state NMR (ssNMR) applications have enabled direct measurements of the inter-atomic distances and the torsion angles present within the amyloid fibrils giving a detailed knowledge of the three dimensional structure of the fibril (Petkova *et al.*, 2002; Jaroniec *et al.*, 2002)). Typically, a matured amyloid fibril consists of 2-5 protofibrils which twist around each other forming a helical rope like structure whose diameter varies from 7-30 nm (Serpell *et al.*, 2000). The cross β sheet structure forms the core of amyloid protofilament (Fandrich *et al.*, 2009). Each protofilament consists of parallel β strands which run perpendicular to the fibrillar axis and is stabilized by cross β sheeted interaction (Sunde and Blake, 1997). These fibrils are characterized by their ability to bind to specific dyes such as Thioflavin T (ThT) and Congo red (CR) which

binds to the cross beta sheet structure of the fibril and thus can be used as analytical tools for fibril detection (Nilsson, 2004). Recent studies have reported that non-disease related proteins can *in vitro* be induced to form fibrillar aggregates under specific mildly denaturing conditions, which exhibit similar morphology, toxicity and dye binding properties as that of disease related proteins (Stefani and Dobson, 2003). These studies suggest that amyloid formation is not a specific but generic property of all polypeptide chains under certain conditions (Dobson, 1999). The fibrils are mainly stabilized by main chain hydrogen bonding between the β strands which run along the fibril axis. This also justifies the independence of amyloid formation on the amino acid sequence of the polypeptide chain, as the side chain interactions play no such significant role in stabilization of the fibrils. However, the propensity of amyloid formation varies from protein to protein based on the hydrophobicity and physicochemical properties of the amino acids. Also, depending on primary sequence and properties of the protein, the condition of amyloid formation may differ significantly.

In many cases precursors of amyloid fibrils known as “prefibrillar aggregates” or “protofibrils” have been found to be the main cause of pathogenesis in amyloid deposition diseases as compared to matured fibrils (Bucciantini *et al.*, 2002). These protofibril, in most cases, have been found to be composed of spherical beaded chain structure which are on the verge of fibril formation and they also exhibit properties characteristic of matured fibril, like ThT and CR binding (Walsh *et al.*, 1997). All these findings further manifest the concept that the structural and functional properties of amyloid fibril is attributed by its supramolecular structural assembly and not by the specific features of the amino acid sequence of the source polypeptide from which it arises . This is in sharp contrast with native structure of proteins where the amino acid sequence is the main guiding factor which determines the unique three dimensional structure as well as the function of the protein. Moreover, Kaye *et al.*, have shown that all amyloid shows immunopositive reaction with anti-amyloid oligomer conformation antibody showing significant structural similarity among them (Kayed *et al.*, 2003).

1.2.6 Mechanism of amyloid fibril formation

To understand the mechanism of amyloid fibril formation it is important to identify and characterize the different monomeric and oligomeric conformational stages that the polypeptide chain undergoes during the aggregation process and understand the key residues or sequence that plays a crucial role in aggregation. Identification and characterization of the oligomeric species that precede the formation of matured fibril is of particular interest due to the growing awareness of the possible role of these prefibrillar structures in amyloid pathogenesis. It has been established experimentally as well as theoretically that amyloid formation occurs via nucleated growth mechanism. Amyloid growth profile is characterized by the presence of an initial lag phase. This lag phase corresponds to the formation of a “nucleus” containing a critical number of molecules. Once this nucleus is formed, it accelerates the fibril growth by addition of monomeric or even oligomeric species to the nucleus, which is represented by an exponential phase in the fibril growth profile following the lag phase (Horwich, 2002; Chiti and Dobson, 2006). This exponential phase is followed by a stationary phase corresponding to the formation of matured fibril with no further elongation taking place.

The duration of the lag phase varies with different polypeptide chains and different aggregation conditions. Further, it has been studied that changes in environmental conditions and even certain mutations in proteins may reduce or eliminate the lag phase (Uversky *et al.*, 2002; Pedersen *et al.*, 2004). Thus, the absence of the lag phase does not necessarily imply that the nucleated growth is not operating, instead it can be due to very slow fibril elongation phase compared to the nucleation phase such that the latter is no longer the rate limiting step in the fibrillation process. Also, the lag phase can be shortened or removed by addition of preformed fibrils to the sample under the aggregation condition, a process known as “seeding”. However, the ability of the preformed fibril to accelerate the aggregation process by seeding mechanism decreases dramatically with increase in the sequence divergence of the polypeptide monomers (Wright *et al.*, 2005).

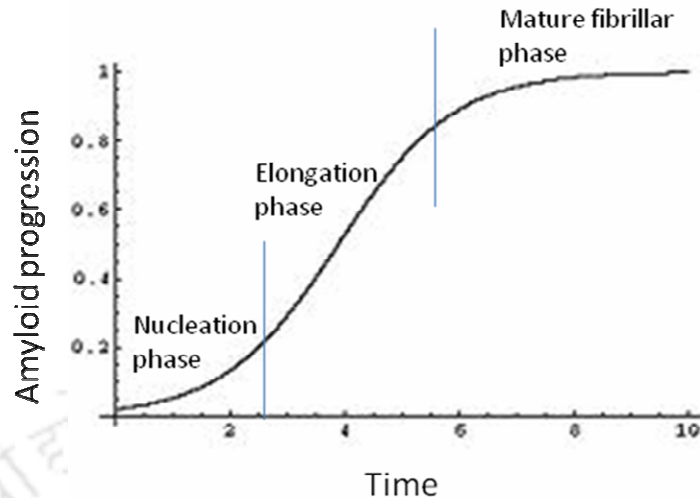


Figure 1.6 A typical growth curve of amyloid fibril showing the different stages- nucleation phase, elongation phase and mature fibrillar phase. Nucleation phase can be removed by addition of pre-formed fibrils by a process called “seeding”.

Formation of mature fibrils is preceded by development of soluble, spherical oligomeric species known as protofibrils. These protofibrils are of substantial clinical importance due to their role in pathogenicity. Studies have revealed that these protofibrils sometimes exhibit spherical beaded structure with 2-5 nm diameter whereas sometimes they exist as beaded linear or circular chain like structure (Chiti and Dobson, 2006). These species have been found to contain mostly β sheeted structure and sufficient structural integrity to bind to characteristic dyes like ThT and CR. Studies have also shown that these prefibrillar structures exhibit more ThT binding and surface hydrophobicity than matured fibrils (Bolognesi *et al.*, 2010). One interesting observation included binding of specific antibodies to protofibrillar species from different sources but not with the native protein structure or the matured fibrils from the same sources (Kayed *et al.*, 2003). This observation necessarily implies a common mechanism to toxicity of all fibrils inviting attention towards development of a common mode of therapy.

During the aggregation process the natively folded protein undergoes partial unfolding forming species which are prone to aggregation. Thus conditions which induce partial unfolding of the native protein such as high temperature, extremes of pH or moderate concentration of organic solvent seem to promote amyloid formation. Further, studies have shown a strong correlation between destabilization of the native state conformation of the protein and its amyloid forming propensity (Chiti *et al.*, 2000). The

partially unfolded intermediates of the proteins exhibit structures with disrupted tertiary but intact secondary conformations as well as high surface hydrophobicity. Fibrillogenesis mainly occurs through the exposed β domain of the monomeric intermediates (Selkoe, 2003). During the process the monomeric protein molecules undergoes major conformational transition from their native secondary structure to predominantly β sheeted structures. In conclusion, fibrillogenesis mainly proceeds from partially unfolded conformations with high surface hydrophobicity. The initial aggregates that are not yet fibrillar in morphology exhibit properties characteristics of amyloid-like structures, notably β sheet conformation and binding to ThT and CR. Further, these aggregates exhibit greater ANS as well as ThT binding and are the main pathogenic species.

1.2.7 Polymorphism within amyloid fibrils

As discussed above, ssNMR and X-ray crystallography have recently made major contributions to our knowledge of the structure of amyloid fibrils. Further, different other biophysical techniques are also employed to obtain a detailed information regarding amyloid structure including the protofibril diameter and mass per unit length, length of the β strands, their arrangement, number of β strands involved in the core structure and so on (Kajava *et al.*, 2005; Saiki *et al.*, 2005; Krishnan *et al.*, 2005). These studies reveal that though amyloids from different source proteins share several common properties such as canonical cross β structure and the frequent presence of repetitive hydrophobic or polar interactions along the fibrillar axis, there exist significant differences in the detailed structure which can be attributable to the influence of the side chains on the structures adopted by the various systems (Chiti and Dobson, 2006). These differences include the length of the β strands, whether they are arranged in parallel or anti-parallel arrangement, conformational properties of loops, turns and other regions not involved in the core structure of the fibril, number of β sheets in the protofilament, number of protofilaments in the fibril, fraction of residues of the polypeptide which is incorporated in the core structure and so on (Chiti and Dobson, 2006). The influence of side chain interaction in fibril structure is demonstrated by the study on polyglutamine fibril where an additional array of hydrogen bonding interactions involving side chains results in fibrillar structure significantly different from the classical amyloid fibrils (Perutz *et al.*,

2002). The structure finally adopted by the fibril is the lowest in free energy and the most kinetically accessible. The interactions of the various side chains with each other and with the solvent are crucial in determining the variations in the fibrillar architecture even though the main chain interactions determine the overall framework within which these variations occur. Thus, the physico-chemical properties of the side chains of the polypeptide seem to play an important role in influencing fibril morphology.

Further, significant variations in amyloid fibril can exist between different fibrils formed from the same peptide or proteins. In case of β_2 -microglobulin, fibrils with distinct morphologies were obtained when the same protein was exposed to different environmental conditions such as protein concentration, pH and ionic strength (Gosal *et al.*, 2005). Similar observations were made with peptide hormone glucagon where morphologically distinct fibrils were obtained at different temperatures (Pedersen *et al.*, 2006). A β peptide causing Alzheimer's disease has also been reported to form structurally distinct fibrils under varying conditions which differ in cross sectional thickness or helical pitch of the fibril (Meinhardt *et al.*, 2009). Further, it has been found that preformed seeds can influence fibril propagation in that particular morphology irrespective of the environmental parameters, resulting in fibrils that inherit the characteristics of the template (Tanaka *et al.*, 2005; Chiti and Dobson, 2006). Thus, fibril morphology is determined by several factors which include environmental parameters like pH, temperature, agitation, and presence of salts or other cosolutes as well as external parameters like addition of preformed seeds. This is in sharp contrast with the native state of a protein which is a unique conformation and significantly more stable for a given sequence than any other alternatives.

1.2.8 Factors that modulate amyloid formation

Despite the cellular quality control machinery some proteins end up forming aggregates. It is due to the fact that some intrinsic properties present in the proteins influence its amyloid forming propensities to some extent. One such important determinant of protein aggregation is the hydrophobicity of the amino acid side chains. Several studies have shown the protein sequences with high hydrophobicity are more prone to amyloid formation, suggesting essential role of hydrophobic interactions in protein aggregation. Further amino acid substitution within regions of the sequence that play a critical role in

amyloidogenesis, resulting in decrease in hydrophobicity of the mutation site, has been found to decrease the amyloid forming propensity (Otzen *et al.*, 2000; Chiti *et al.*, 2002^b).

Another essential determinant of amyloid formation is the net charge of the polypeptide chain. High net charge on the protein, either globally or locally has been found to hinder amyloidogenesis (Broome and Hecht, 2000). Studies have shown that amino acid substitutions that decreased the net charge on the protein, accelerated formation of β sheet containing aggregates that are able to bind to dyes like ThT and CR and vice versa (Chiti *et al.*, 2002^a). Further, compounds that neutralize the overall charge on the protein have also been found to accelerate amyloidogenesis (Goers *et al.*, 2003; Fernandez *et al.*, 2004). Studies have also shown that the pH where fibril formation is maximal for a number of the well characterized proteins is near its pI, where the net charge is negligible (Schmittschmitt and Scholtz, 2003). These studies show that the net charge on the protein plays a critical role in deciding its amyloidogenic propensity.

Apart from hydrophobicity and charge, amino acid sequences which exhibit a greater propensity of forming β sheet structure have a greater tendency to form amyloid (Kallberg *et al.*, 2001; Chiti and Dobson, 2006). Thus, sequences of alternating hydrophobic and hydrophilic residues that favour β sheet formation have been found to be less frequent in natural proteins than expected on a random basis, suggesting that evolutionary selection has reduced the probability of such sequences that have an aggregation propensity (Broome and Hecht, 2000). Based on these parameters several softwares are designed to predict the amyloidogenic propensity of a polypeptide chain based on the physicochemical properties of its amino sequence.

Formation of disulfide bond has also been found to play a critical role in determining amyloid progression. Several disulfide bonded globular proteins have been found to form amyloid under particular conditions. Yamamoto *et al.*, have shown inhibitory effects of reducing agents like DTT and cysteine towards amyloidogenesis of β_2 -microglobulin which is responsible for dialysis-related amyloidosis in humans (Yamamoto *et al.*, 2008). Wang *et al.*, have studied the inhibitory effect of tris(2-carboxyethyl)phosphine (TCEP), a reducing agent towards amyloidogenesis of HEWL at

pH 2.0, through disulfide bond disruption promoting unfolding of HEWL (Wang *et al.*, 2009^b). Further, Kumar *et al.*, have shown the role of 1,4-Dithioerythritol (DTT) in retarding HEWL aggregation at pH 12.2 by disrupting disulfide bonds which were found to stabilize mature fibrils (Kumar *et al.*, 2008). All these studies essentially indicate the critical role of disulfide bonds in modulating fibril formation.

1.2.9 Therapeutic approach to amyloid diseases

Deposition of amyloid plaques in the tissues/organs are the principle cause of several degenerative diseases like Alzheimer disease (AD), spongiform encephalopathies, such as Kuru and Creutzfeldt-Jacob disease, as discussed earlier. Today, we know that the deposits in these conditions contain A β -peptides, prion protein, and transthyretin (TTR) respectively. Joining this list are other proteins as islet amyloid protein in the pancreas of patients with type II diabetes, lysozyme in the liver of patients with systemic amyloidosis, and cystatin C in patients with hereditary cerebral amyloid angiopathy (Kelly, 1996; Horwich, 2002). Many therapeutic efforts are targeted at reducing amyloid plaque production, including inhibiting secretase (for A β amyloid), increasing amyloid clearance with amyloid vaccines, or blocking amyloid aggregation (with antibodies, peptides, or small organic molecules that selectively bind and inhibit amyloid aggregate and fibril formation) (Yang *et al.*, 2005).

Correlation between oxidative stress and amyloid diseases has been reported. Studies indicate imbalances in several metals which have potential to catalyze and stimulate free radical formation are related to amyloid deposition. Thus, it is likely that protein misfolding and amyloid formation in these diseases is a result of redox imbalance. Although not approved for human use so far, the potential for nanoparticles to inhibit formation of amyloid is studied (Pai *et al.*, 2006). Nanocarriers have been developed to deliver drugs which crossed blood brain barrier and decreases oxidative stress by various mechanisms (Shea *et al.*, 2005). Study by Ikeda *et al.*, have shown that biocompatible nanogels 20-30 nm in diameter can prevent aggregation of proteins and inhibit amyloid fibers formation (Ikeda *et al.*, 2006). Moreover, chelator conjugated nanoparticles are reported to cross blood brain barrier, restoring the proper balance of metal ions in the brain (Liu *et al.*, 2006). Many artificial chaperones are reported to assist in protein folding process. Several chemicals have been found to restore defective CFTR

protein. Fischer *et al.* have reported usefulness of trimethylamine oxide while 7,8-benzoflavone and few other chemical compounds have been shown to be useful in restoring function of defective CFTR (Fischer *et al.*, 2001; Dobson, 2003). Gaucher's disease, the most common of the lysosomal storage diseases is caused by few mutations (most common one is N370S) in the enzyme β -glucocerebrosidase (β -Glu), leading to interference with folding in ER and trafficking. The mutant β -Glu does not fold properly in ER pH condition and is thus not translocated to lysosome and degraded by quality control system. The loss of activity results in accumulation of its substrate in lysosome. Sawkar *et al.* have shown that subinhibitory concentrations of *N*-(*n*-nonyl)deoxynojirimycin, an inhibitor of β -Glu, results in significant increase in the activity of N370S β -Glu (Sawkar *et al.*, 2002). It was suggested that *N*-(*n*-nonyl)deoxynojirimycin assists in folding of N370S β -Glu in ER. The correctly folded N370S β -Glu is trafficked to lysosome where the inhibitor is replaced by high concentration of substrate. This appears to be a potential option for enzyme replacement therapy. However, systematic clinical trial is necessary to evaluate efficacy and safety of drugs developed using such strategy. The p53 is a tetramer tumor suppressor protein and controls cell division cycle. Mutations in the p53 gene have been found in more than 50% of human tumors (Hollstein *et al.*, 1991). Few such cancer associated mutants of p53 (G334V; R337H; P53C) have been studied and it was found that these mutants can not form tetramer and make other structural changes in the protein. Mutant forms of p53 protein are prone to amyloid aggregate formation at physiological pH and temperature (Friedler *et al.*, 2002; Higashimoto *et al.*, 2006). Few other mutations in DNA binding core domain are also reported to be cancer associated. The six most common mutations associated to cancer disease are R175H, G245S, R248Q, R249S, R273H, and R282W (Friedler *et al.*, 2002). The literature so far suggests that mutation in p53 results in loss of function due to misfolding followed by amyloid formation. Fersht and colleagues have studied few cancerous mutant forms and identified few peptides which acts like chaperon and prevents misfolding (Friedler *et al.*, 2002). However, this approach of cancer therapy is not sufficiently explored and further studies are needed to identify suitable candidate drugs which may prevent misfolding and/or amyloid formation of cancer related p53 mutants. Alzheimer's disease (AD) is a prevalent neurodegenerative disease and amyloid beta ($A\beta$) deposits are the fundamental cause of the disease. $A\beta$ is β -secretase and γ -secretase cleavage fragment from a larger protein called amyloid precursor protein

(APP), a transmembrane protein that penetrates through the neuron's membrane. APP is critical to neuronal growth, survival and post-injury repair (Priller *et al.*, 2006). There are several therapeutic approaches being targeted including inhibition of secretase, increasing A β clearance by amyloid vaccines or blocking A β aggregation (Yang *et al.*, 2005). Several small compounds or peptides have been reported to inhibit formation of A β aggregate (Yang *et al.*, 2005; Doig, 2007; Takahashi and Mihara, 2008; Torok *et al.*, 2008). Although, the effect of these compounds on the thermodynamic properties of A β or transition state is not studied systematically, these compounds may be potential drugs for AD.

Further, few small polyphenolic compounds have been reported to inhibit amyloid fibril formation *in vitro* and its associated toxicity (Porat *et al.*, 2006). The early findings on the effect of polyphenols on amyloid formation came from small polyphenolic compounds like Congo Red (CR) and Thioflavin T (ThT), both of which were found to specifically interact with amyloids and inhibit its formation to some extent (Lorenzo and Yanker, 1994; Lee, 2002). Later on several other aromatic phenolic compounds were found to show inhibitory effect on amyloid formation *in vitro* such as resveratrol, curcumin, rosmarinic acid, catechin, tannic acid and so on (Porat *et al.*, 2006). These compounds were found to exhibit structural similarities like presence of at least two phenolic rings and more than one –OH groups on the aromatic rings, suggesting some common mode of interaction with amyloid fibrils. Further, they were found to interact with the fibrillar assemblies but not with the monomeric amyloidogenic proteins, suggesting that the inhibitor binding is not sequence dependent but rather conformation dependent. This indicates involvement of some hydrophobic or ring stacking interaction of these phenolic compounds with characteristic cross- β sheet conformation present in amyloid preventing their further elongation. Also, few polyphenolic compounds have exhibited protective effects against amyloid toxicity towards cell culture and primary culture systems, which was mainly attributed to the anti-oxidative properties of the polyphenols (Zhu *et al.*, 2004).

Apart from polyphenols, few quinone derivatives have also been shown to inhibit amyloid formation *in vitro*. Alpha-tocopherol quinone was found to inhibit amyloid beta (A β) fibrillation in a dose dependent manner and attenuate its toxicity towards

neuroblastoma cell lines (Yang *et al.*, 2010). Further, pyrroloquinoline demonstrated significant inhibitory effect on amyloid formation of A β (1-42) and mouse prion protein (Kim *et al.*, 2009). Several quinone based small molecules were also found to be potent amyloid inhibitors like 1,8-dihydroxyanthraquinone which reduced fibrillogenesis and neurotoxicity of β -amyloid proteins (Kwon *et al.*, 2004). Catecholamines like dopamines and L-dopa exhibited inhibitory effect on fibrillogenesis of A β and α -synuclein (Li *et al.*, 2004; Huong *et al.*, 2009). Further, rifampicin and its analogues were shown to inhibit toxicity of pre-formed aggregates of human islet amyloid polypeptide, amylin on PC 12 cells by preventing adhesion of the amylin fibrils with the cell surface by blocking the binding sites (Tomiyama *et al.*, 1997).

Role of few amino acids towards protein aggregation has also been studied (Samuel *et al.*, 1997; Shiraki *et al.*, 2002; Das *et al.*, 2007). Most notable among them is arginine which is found to inhibit aggregation of several proteins and assist in proper refolding of the proteins. Equilibrium studies show that arginine did not stabilize these proteins but suppressed their aggregation and increased their solubility. A mechanism is proposed to account for the inhibitory effect of arginine towards A β (1-42) peptides aggregation where arginine is reported to form molecular clusters in solution which exhibit high surface hydrophobicity by alignment of its methylene groups (Das *et al.*, 2007). These hydrophobic clusters inhibit self association of the peptides by masking the hydrophobic surface of denatured or partially folded protein monomers thereby preventing hydrophobic surface induced aggregation. Apart from arginine, proline is also reported to prevent aggregation in proteins (Schobert and Tschesche, 1978; Samuel *et al.*, 1997; Samuel *et al.*, 2000). Proline is reported to prevent aggregation during protein refolding of HEWL (Samuel *et al.*, 2000). Experimental evidence suggests that proline inhibits protein aggregation by binding to the folding intermediate(s) and trapping the intermediate(s) into “aggregation insensitive” state(s). Thus it acts as a molecular chaperone preventing protein aggregation and assisting in its proper refolding. Proline is also reported to form hydrophillic colloids in solution with a hydrophobic backbone and hydrophillic groups on the surface, exposed to water (Schobert and Tschesche, 1978). It is proposed to enhance solubility of proteins by increasing the water binding capacity of the proline-protein complex.

The similar structural, toxicity, and tinctorial properties of all amyloids irrespective of their source protein invite the attention towards development of a common therapeutic strategy against amyloid diseases. A study by Yang *et al.*, shows the levels of β -amyloid plaque in the brain tissues of transgenic AD mice that were given high doses of curcumin were decreased by around 40% in comparison to those that were not treated with curcumin (Yang *et al.*, 2005). Additionally, there are also circumstantial evidences that curcumin improves mental functions (Ng *et al.*, 2006). These reports so far indicate that the Alzheimer amyloid β ($A\beta$) plaques may be dissolved using curcumin. While these studies have given us some important insights, they do not provide how curcumin prevents amyloid formation. One possible mechanism of inhibition of amyloid formation may be by inhibiting the enzymes (α and γ secretase) involved in sequential cleavage of Amyloid Precursor Protein (APP) to $A\beta$ peptide which is highly aggregation prone. Also, oxidative stress has been found to induce amyloid fibril formation and curcumin being an antioxidant may inhibit amyloid formation (Zhang *et al.*, 2001). Furthermore, curcumin may directly interact with the monomeric protein intermediates and prevent their aggregation.

Another study have shown the inhibitory effects of small molecule compounds like TIPT, clotrimazole, sulconazole, nicardipine, rottlerin on amyloid formation of two prion proteins- yeast prion protein and mouse prion protein, *in vitro* (Feng *et al.*, 2008). However the mechanism of this inhibitory effect is not yet explored. Further, it is also not known whether their amyloid inhibitory effect is specific to these two proteins or can be generalized owing to the similar properties of all amyloids.

1.2.10 Thermodynamics of aggregation

It is generally accepted that in most cases aggregates such as amyloid fibrils originate from ensembles of partially unfolded conformations rather than from the folded and functional states of proteins. Most proteins easily find their native state because the free energy of activation (ΔG^\ddagger), separating the unfolded and transition states is surmountable, and the folded state is substantially more stable than the unfolded state (the difference in free energy, ΔG , dictates the relative populations of folded and unfolded proteins and thus the folding/unfolding rate). For aggregation-prone proteins, it has become clear that the misfolded state can be more stable than the functional three-dimensional structure

under certain conditions, including those associated with a high-denaturation stress (Fandrich *et al.*, 2001). Recent misfolding trap hypothesis suggests wherever amyloid oligomers encounter transiently misfolded proteins with exposed β sheet edges, the oligomers can potentially bind and trap the proteins in their misfolded form (Gruschus, 2008). Promoting oligomer sequestration in amyloid aggregations and upregulating proteases that degrade the peptides both could reduce soluble oligomer levels. Thermodynamics of protein and aggregate/amyloid is explained in Figure 1.7.

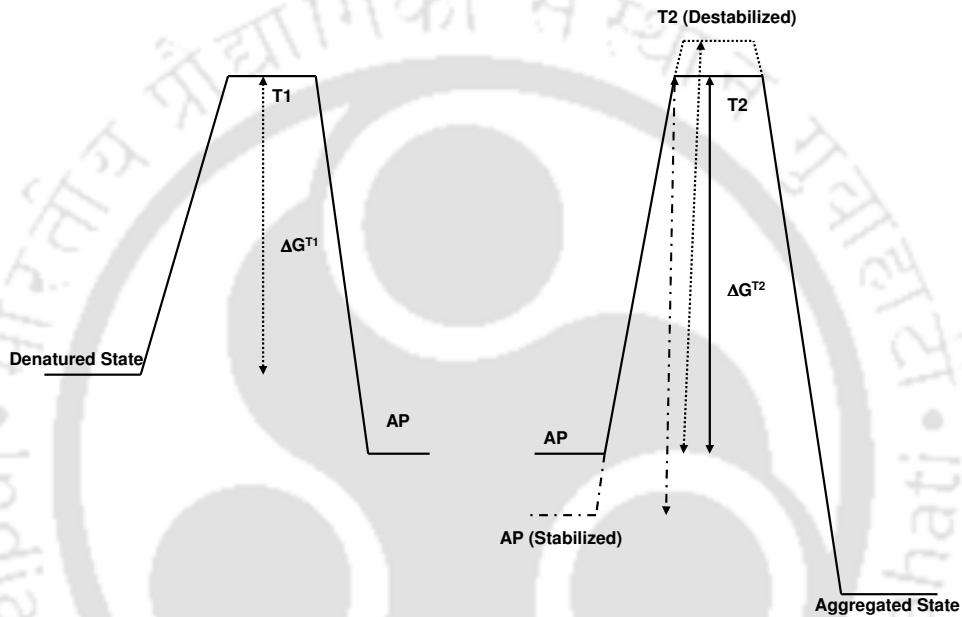


Figure 1.7 Thermodynamics of aggregate formation: Protein folding in aggregation prone (AP) state becomes more favorable to aggregation rather than native state due to mutation or change in cellular environment. Under these conditions the aggregated state becomes thermodynamically more stable and AP states converts in aggregated state. Progression of aggregation may be inhibited by increasing energy barrier between AP state and transition state (T2) between AP and aggregated state. This may be achieved by increasing in stability of AP state or decrease in stability of transition state.

Protein forms misfolded conformation under stressed condition (mutation or change in cellular environment) because misfolded state become thermodynamically more stable than native state or the misfolded state is kinetically trapped i.e, energy barrier for folded state is very high (Fandrich *et al.*, 2001). The misfolded state is thermodynamically more stable in the form of soluble oligomer which ultimately forms more stable insoluble aggregate or amyloid. Chemical chaperones may assist in folding of protein in changed cellular environment and thus prevent misfolding. Additionally, the

thermodynamics of the aggregation provides important clue to fight against associated diseases. Any factor which increases energy barrier between misfolded state and aggregated state significantly will slow down the formation of aggregation and quality control machinery of the cell will have sufficient time to degrade misfolded species. This can be achieved in two ways, either by stabilizing misfolded state conformation or by destabilizing transition state between misfolded and aggregated state (Figure 1.7).

1.2.11 Model proteins used in the study

For the current work *in vitro* studies on protein folding and amyloid formation were carried out using few model proteins. For the study we have selected three model proteins belonging to different protein classes – hen egg white lysozyme (HEWL), cytochrome C from bovine heart (Cyt C) and 2,5 diketo gluconate reductase A (DKGR). These proteins exhibit no similarity relating to their amino acid sequences as well as their native tertiary structure. Further, HEWL and Cyt C are well characterized in terms of their primary, secondary and tertiary structure, folding pathways and amyloid forming conditions.

HEWL is one of the most extensively studied proteins. It is a relatively small enzyme (Mol wt 14.3 KDa) which catalyzes the hydrolysis of beta-glycosidic linkage between N-acetylmuramic acid and N-acetyl glucosamine in the peptidoglycan of the bacterial cell wall. In 1965, Blake *et al.*, solved the three dimensional structure of HEWL, making it the second protein and first structure to be solved by X-ray diffraction methods (Blake *et al.*, 1965). Structurally, it belongs to $\alpha+\beta$ class of proteins where the α and the β domains are linked by a α helix. HEWL is a well characterized protein in terms of its physicochemical properties and is reported to form amyloid under several destabilizing conditions (Artymiuk and Blake, 1981; Redfield and Dobson, 1990; Radford *et al.*, 1992; Goda *et al.*, 2000; Kumar *et al.*, 2009; Wang *et al.*, 2009^a). Further it is homologous to human lysozyme, variants of which lead to hereditary systemic amyloidosis (Pepsys *et al.*, 1993).

Cyt C is a small globular heme protein found loosely associated with the inner membrane of the mitochondrion. It is an essential component of the electron transport chain in the mitochondria and is also involved with the initiation of apoptosis (Liu *et al.*,

1996). Structurally it is a small protein (Mol wt 12.2 KDa) belonging to all α protein class. This protein is well studied in term of its amino acid sequence, three dimensional structure, folding properties and amyloid forming condition (Nakashima *et al.*, 1966; Hoang *et al.*, 2002; Groot and Ventura, 2005; Mirkin *et al.*, 2008). It is known to form amyloid at alkaline pH (pH 9.0) and elevated temperature (75° C) above a concentration of about 90 μ M (Groot and Ventura, 2005).

DKGR is an $(\alpha/\beta)_8$ barrel class of protein which utilizes NADPH as its cofactor. It catalyzes the stereospecific reduction of 2,5 diketo-D-gluconate to 2 keto-L-gulonate which is a tautomeric isomer of ascorbic acid (Vitamin C). Thus, this enzyme can serve as an alternative and simpler method of industrial production of Vitamin C (Grindley *et al.*, 1988). The primary and tertiary structure of the commercially potential enzyme is already studied (Yum *et al.*, 1999; Khurana *et al.*, 1998). However, so far no unfolding and stability studies have been done on this commercially important protein. Here we have expressed this protein in bacterial system *E coli* BL21(DE3) and purified the protein using a novel purification protocol. Further, we have studied the folding pathway and amyloidogenic conditions of this protein. This is the first report of amyloid formation by any alpha/beta barrel protein.

1.3 Scope of current research

The conversion of soluble globular protein to insoluble fibrillar aggregates called “amyloid” is one of the most elusive problems of modern science which has gained immense clinical importance owing to its involvement in several degenerative diseases such as Alzheimer’s disease, Parkinson’s disease, Type II diabetes and so on. Till date over 20 different proteins have been identified which deposit in the tissues forming amyloid fibril and leading to different diseases. These amyloids are found to be highly similar in structural, immunological, toxicity and tinctorial properties despite having originated from polypeptide chains differing in sequence and tertiary structure. Considering the common structural, toxicity, immunogenic and tinctorial properties of amyloids, can it be possible to develop a common mode of therapy for all amyloid forming diseases?

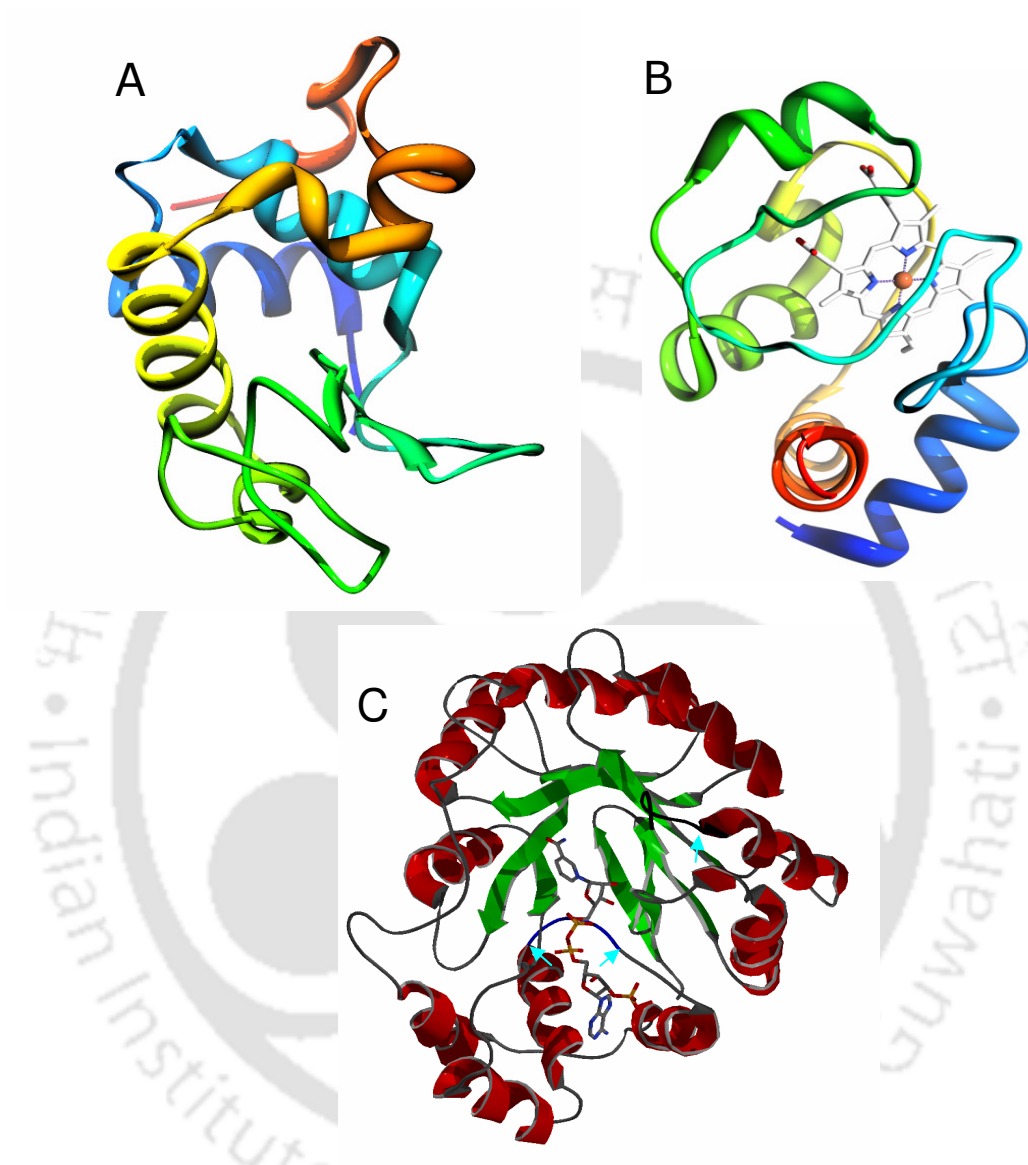


Figure 1.8 Ribbon diagram of (A) hen egg white lysozyme, (B) cytochrome C from bovine heart with the co-crystallized heme group and (C) 2,5 Diketo Gluconate Reductase (DKGR) with the co-crystallized NADPH co-factor. The amyloidogenic regions in DKGR as predicted by the online server called Waltz, are marked by blue arrows. All the three proteins belong to different protein classes and share no structural or sequence similarities.

This was one of the questions I investigated during my PhD research. Further, recent studies have shown that amyloid formation to be an inherent property of all polypeptide chains when subjected to specific partially denaturing conditions. These studies made me more curious to research on possible common mode of therapy against amyloid diseases. Additionally, identification of common drugs which are capable of blocking or inhibiting protein aggregation may be considered as one of the therapeutic approaches directed against amyloid diseases. The present study describes the effect of a few small molecule compounds like clotrimazole, sulconazole and rottlerin towards amyloidogenesis of two model proteins unrelated in terms of structure and sequence such as hen egg white lysozyme and cytochrome c to test promiscuous of amyloid inhibition. Amyloid progression was monitored through Thioflavin T assay (ThT) and Atomic Force Microscope imaging (AFM). Structural alterations in the aggregation-prone intermediate state conformation of the protein in presence of the compounds were monitored through 1-anilino-8-naphthalene sulfonate (ANS) binding studies. Further, we attempted to identify the binding sites between the proteins and the inhibitor through docking studies.

Amyloids are known to be highly stable structures that cannot be reversed easily once formed. Here, we have demonstrated the instantaneous dissolution effect of rottlerin towards pre-formed hen egg white lysozyme fibrils monitored by ThT assay, anisotropy study and AFM imaging. We have also tried to understand the factors that stabilize amyloid fibrils which may provide useful information for development of efficient therapeutics against amyloidosis.

Further, we attempted to explore the role of disulfide bonds in amyloidogenesis through the study of sodium tetrathionate on hen egg white lysozyme amyloidogenesis. Effect of sodium tetrathionate on hen egg white lysozyme amyloidogenesis was monitored through Thioflavin T assay and Atomic Force Microscopy imaging. The underlying mechanism of amyloid fibril inhibition by sodium tetrathionate was investigated showing the critical role of correct disulfide bonds in amyloid formation. These results give insight into the mechanism of amyloid formation and factors that modulate the process of amyloidogenesis.

Further, curcumin, principal curcuminoid of *Curcuma longa*, was reported to inhibit A β plaque deposition in brain. However, the mechanism of action of curcumin is not extensively investigated. This was also included as part of specific aim of my PhD research. We studied the effect of curcumin on amyloidogenic, intermediate state of 2,5 Diketo-D-Gluconate Reductase. In brief, studies on understanding critical parameters that modulate the transition of proteins from its natively folded conformation to misfolded, amyloidogenic conformation and identification of potential inhibitors of amyloidogenesis are important area of my investigation.

The work embodied in this thesis is divided into the following chapters containing the following specific objectives:

I. Exploring possibility of promiscuous amyloid inhibitor: Studies on effect of selected compounds on folding and amyloid formation of proteins:

Small molecule compounds like clotrimazole, sulconazole and rottlerin were studied to see their effect on amyloid progression of model proteins like hen egg white lysozyme (HEWL) and cytochrome c from bovine heart (Cyt C) and to explore the promiscuity of amyloid inhibitor. Further, the effect of these compounds on the energetics of the amyloidogenic state and the transition state were studied with an aim to understand the thermodynamic basis of amyloid inhibition. Changes in the conformational states of the proteins induced by these compounds were also monitored. Further, we attempted to identify the binding sites of the potential inhibitor on the proteins through docking studies.

II. Dissolution of amyloid fibril by rottlerin: A study on hen egg white lysozyme: The effect of rottlerin towards dissolution of amyloid fibril of hen egg white lysozyme formed at alkaline pH, was studied through various techniques like Thioflavin T assay, anisotropy study and AFM imaging. Further, changes in the conformation of HEWL fibril on addition of rottlerin were monitored. We also tried to identify the type of binding interaction between HEWL and rottlerin at alkaline pH.

III. Exploring role of disulfide bonds in amyloidogenesis: A study on hen egg white lysozyme :

Effect of sodium tetrathionate on amyloidogenesis of hen egg white lysozyme was monitored through Thioflavin T assay and AFM. Conformational changes in HEWL structure as well as alteration in the folding pathway of HEWL in presence of sodium tetrathionate were monitored. We tried to understand the underlying mechanism of sodium tetrathionate on amyloid inhibition and elucidate the role of disulfide bonds in determining amyloid progression.

IV. Effect of curcumin on amyloidogenic property of 2,5-Diketo-Gluconate Reductase (DKGR) :

Cloned DKGR gene was expressed in Ecoli strain BL21 (DE3) and purified using a novel purification protocol. The unfolding pathway of purified DKGR was characterized and intermediate states populating the unfolding pathway were identified. Amyloid formation of the intermediate state of DKGR was monitored and effect of curcumin on the amyloid formation was studied using Thioflavin T assay and AFM techniques.

Exploring possibility of promiscuous amyloid inhibitor: Studies on effect of selected compounds on folding and amyloid formation of proteins*.

2.1 Abstract

Fibrillar protein aggregates called amyloids are the hallmark of several degenerative diseases. Identification of common drugs which are capable of blocking or inhibiting protein aggregation may be considered as one of the therapeutic approaches directed against amyloid diseases. The present study describes the effect of a few small molecule compounds like clotrimazole, sulconazole and rottlerin towards amyloidogenesis of two model proteins unrelated in terms of structure and sequence such as hen egg white lysozyme and cytochrome c to test promiscuous of amyloid inhibition. Amyloid progression was monitored through Thioflavin T assay and Atomic Force Microscope imaging. Moreover, the basis of inhibition of fibrillogenesis and structural alterations in the aggregation-prone intermediate in presence of selected compounds were analyzed using various biophysical techniques.

* Part of the work has been published in *Process Biochemistry*, **2011**, 46, 1179-1185

2.2 Introduction

Several diseases are associated with the deposition of insoluble fibrillar protein aggregates known as amyloid fibril. To date over 20 different proteins have been identified that lead to various degenerative diseases by forming amyloid by a pathway alternative to the protein folding, under conditions where the intermolecular interactions are more favoured than the intramolecular ones (Dobson, 2003; Stefani, 2004; Wang *et al.*, 2009^a). These proteins have been found to share no sequence or structural homology. However, irrespective of their origin, amyloids from different proteins have demonstrated strikingly similar structural, and toxicity properties (Kalhor *et al.*, 2009). Moreover, amyloids are also found to share similar tinctorial properties like binding to characteristic dyes like Thioflavin T (ThT), Congo Red which can be attributed to their similar structural properties. Studies have also reported that amyloids exhibit similar immunogenic and toxicity properties, with the soluble prefibrillar structures called 'protofibrils' being the predominant pathogenic species rather than matured fibrils (Goldberg and Lansbury Jr., 2000; Kaye *et al.*, 2003; Bertocini *et al.*, 2005). All these studies provide some evidence to justify the interesting fact that amyloid formation is an inherent property of all polypeptide chains irrespective of the tertiary structure and the amino sequence of the protein from which they have arisen (Kelly, 1996; Chiti and Dobson, 2006). Also, recent studies have shown that proteins not involved with any amyloid forming diseases can *in vitro* be induced to form amyloids very similar in structure and toxicity as compared to amyloid formed by disease related proteins (Bucciantini *et al.*, 2002). Thus, we asked a question considering the common structural, toxicity, immunogenic and tinctorial properties of amyloids, can it be possible to develop a common mode of therapy for all amyloid forming diseases?

The conditions which guide the transition of few proteins from the native state to the aggregation prone state is still a matter of debate but in many cases, molten globule-like intermediate states of proteins with exposed hydrophobic surfaces have been found to play a vital role in aggregation and amyloid formation (Dobson, 2003). Formation of amyloid fibril is a multistep process which starts with oligomerisation of misfolded proteins resulting in soluble aggregates which finally convert into insoluble aggregates or amyloid (Sarkar and Dubey, 2010). Thermodynamics of protein folding and aggregation

pathways provide important clues to combat amyloid diseases. Any factor that can increase the energy barrier between the misfolded state and the aggregated state shall significantly slow down the aggregation process, providing the cellular quality control machinery sufficient time to guide the misfolded protein to the native state conformation or degrade by proteosome complexes (Cohen and Kelly, 2003). This can be achieved in two ways either by stabilizing the misfolded state of the protein or by destabilizing the transition state which lies between the misfolded state and the aggregated state.

Studies by Feng *et al.* have identified few small molecule compounds which have shown inhibitory effect on amyloid fibrillogenesis of two proteins- yeast prion protein and mouse prion protein (Feng *et al.*, 2008). However their mechanism of action still remains elusive and whether their action is specific to those proteins or it can be generalized is also unknown. In the current study we aim to see the effect of few small molecule compounds namely clotrimazole, sulconazole and rottlerin on amyloidogenesis of model proteins e.g, hen egg white lysozyme (HEWL) and cytochrome c from bovine heart (Cyt C). We also aim to understand the thermodynamic basis of inhibition and elucidate the key interactions responsible for preventing protein aggregation into highly ordered fibrils.

2.3 Materials & Methods

2.3.1 Materials

Hen egg white lysozyme (HEWL), cytochrome c (Cyt C) from bovine heart, Rottlerin, Sulconazole, Clotrimazole, Guanidine hydrochloride (GuHCl), Thioflavin T (ThT) and ANS were purchased from Sigma-Aldrich. All other chemicals used were of analytical grade.

2.3.2 Fluorescence Spectroscopy

Fluorescence measurements were taken on Varian Fluorescence Spectrophotometer equipped with stopped flow apparatus. The slit widths for both excitation and emission were kept at 5 nm throughout. To see the effect of the small molecule compounds on the protein, they were added to the sample (1% v/v was added from a stock solution prepared in methanol) such that the final concentration of the compounds is 10 fold of the protein concentration. In the control samples, 1% methanol was added to confirm its

negligible effect on the proteins. All the fluorescence measurements are taken thrice and appropriate blanks are subtracted.

2.3.3 Thioflavin T assay

For Thioflavin T (ThT) assay the proteins were exposed to amyloid forming conditions based on previous reports and aliquots were periodically drawn from the samples for estimation of amyloid formation through ThT fluorescence. HEWL amyloidosis was induced by incubating the protein in 10mM glycine HCl buffer pH 2.0 at 55°C, 30 rpm at a concentration of 35µM as well as 10mM glycine NaOH buffer pH 12.2 at room temperature at a concentration of 70 µM (Arnaudov and Vries, 2005; Kumar *et al.*, 2009). Cyt C amyloidosis was induced by incubating the protein in 10 mM Tris HCl buffer pH 9.0 at 75°C at concentration of 90 µM (Groot and Ventura, 2005). A stock solution of 2.5 mM ThT was prepared in 10 mM phosphate buffer pH 6.5. Samples for fluorimetry were prepared by adding 10 µl of ThT stock solution to appropriate volume of incubated protein sample to make final protein concentration and volume 10 µM and 1000 µl respectively in 10mM phosphate buffer pH 6.5. Samples prepared in this way were incubated for 30 mins at room temperature before taking emission scan from 460 to 610 nm with 450 nm excitation wavelength.

2.3.4 Equilibrium unfolding study

Protein sample was incubated at a desired GuHCl concentration and desired pH for approximately 24 h at 25°C to attain equilibrium. Final concentration of the protein and denaturant, in each sample, were determined by spectrophotometry and refractive index measurements, respectively. Incubated samples were selectively excited at 295 nm for tryptophan and emission was recorded between 300 and 400 nm. The protein concentration was 5 µM for all fluorescence measurements.

2.3.5 Unfolding kinetics study

Unfolding kinetics was monitored by following spectral changes in intrinsic tryptophan fluorescence of the protein samples at 350 nm with excitation at 295 nm, in a stopped flow apparatus. Drive syringes of 500 µl and 2500 µl were used to inject protein and denaturant buffer respectively, resulting in a six-fold dilution of the protein solution. Protein was dissolved in appropriate buffer such that the final protein concentration after

six-fold dilution becomes 5 μM and incubated for a minimum of 6 h. The small molecule compounds were added in the dilution buffer.

2.3.6 ANS binding kinetics

Conformational changes in the protein with respect to its exposed hydrophobic patch, during transition from native state to aggregate prone state was monitored using fluorescent dye ANS (Semisotsov *et al.*, 1991; Khurana and Udgaonkar, 1994). To study the ANS binding kinetics of the proteins, they were incubated at native pH (pH 7.0) for a period of minimum 5h and then transition to aggregation prone state of the protein was induced by diluting it 6 fold in buffer of appropriate pH (pH 2.0 & 12.2 in case of HEWL and pH 9.0 in case of Cyt C) containing 100 fold molar excess of ANS. The final concentration of protein after dilution was maintained at 5 μM . The small molecule compounds were added in the dilution buffer.

2.3.7 Atomic Force Microscopy (AFM)

Samples for AFM were prepared by incubating the proteins under amyloid forming conditions as reported previously, in absence and presence of 10 fold molar excess of the compounds (1% v/v was added from the stock solution prepared in methanol). 10 μl of the incubated sample was added to freshly cleaved mica and kept for few minutes for adsorption of the sample on to the mica sheet before rinsing with deionised water to remove the unadsorbed sample. For negatively charged samples 2 μl of 10 mM MgCl_2 was added to facilitate efficient adsorption of the sample onto the mica sheets. The samples were then dried under nitrogen gas and AFM measurements were taken using Picoplus microscope (Molecular Imaging, USA) operating under non-contact or MAC mode.

2.3.8 MTT assay

Toxicity assay of the fibrils were done on mammalian cell lines – PC12 and HEK 293. HEWL was incubated under amyloidogenic conditions at pH 2.0 with and without rottlerin and aliquots were taken from the incubated sample at different time for MTT assay. Cells were grown in DMEM supplemented with 15% FBS at 37°C and 5% CO_2 according to the standard conditions. Incubated protein (4 μM) was added to the cell culture under exponential phase and grown for 24 h under serum free media. MTT was

added to the culture (10 μ l from MTT stock solution of 5mg/ml was added to 180 μ l culture) and kept for 4 h before taking O.D at 570 nm. The readings were taken in triplicates and appropriate blank readings were subtracted. Positive control consisted of addition of 10 mM Gly-HCl buffer, pH 2.0 at not more than 10 % (v/v) of the culture volume. Assay values for positive control were taken as 100% MTT reduction.

2.3.9 Prediction of amyloidogenic regions of model proteins and prediction of binding site(s) of rottlerin

Amyloidogenic region of the protein was predicted using web server FoldAmyloid, which predicts the sequence(s) on the polypeptide chain which is likely to aggregate based on the physicochemical properties of the amino acid residues (Garbuzynskiy *et al.*, 2010). Binding site of rottlerin was predicted by molecular docking method using AUTODOCK 4.2 (Morris *et al.*, 2009). A blind dock was carried out to predict the modes of binding and the largest cluster (out of 100 Lamarckian genetic algorithm runs) with minimum binding energy was set as the criteria for prediction of binding modes. The force field was parameterized using a large number of protein-inhibitor complexes. The force field evaluates binding in two steps. The ligand and protein start in an unbound conformation. In the first step, the intramolecular energetics are estimated for transition from these unbound states to the conformation of the ligand and protein in the bound state. The second step then evaluates the intermolecular energetics of combining the ligand and protein in their bound conformation. Ligplot, an automatically generates schematic diagrams of protein-ligand interactions, was used to plot bonding and non-bonding interactions of the ligand with receptor in the receptor-ligand complex (Wallace *et al.*, 1997).

2.4 Results

The conversion of soluble globular proteins into insoluble highly ordered fibrillar structures is one of the most remarkable phenomena of protein chemistry which has been subjected to extensive research owing to its contribution in several human diseases. Several compounds have been studied to see their inhibitory effect on amyloid fibrillogenesis but the precise mechanism of inhibition still remains undefined. Here we have tested the inhibitory effects of three small molecule compounds (namely clotrimazole, sulconazole and rottlerin) on amyloid progression and tried to understand the underlying mechanism of inhibition. HEWL and Cyt C are chosen as model proteins for the study owing to the fact that they belong to different class of protein, does not show significant sequence similarity and both the proteins are well characterized in terms of their structural, biochemical, biophysical and amyloidogenic properties (Roux *et al.*, 1997).

2.4.1 Thioflavin T assay of amyloid progression

The amyloid progression was monitored through ThT assay. Figure 2.1 shows the time dependent ThT assay of the proteins in the presence of 10 fold molar excess of the small molecule compounds (considering solubility of these compounds, study with higher molar ratio was not possible). In case of Cyt C, all the three compounds seem to delay fibrillogenesis as compared to the native protein, to nearly similar extent (Figure 2.1A). On reaching the plateau region (stationary phase of amyloid formation) the ThT intensity in presence of the compounds was found to be approx. 50% of the control ThT intensity in all the cases. In case of HEWL at pH 2.0, clotrimazole was found to initially delay fibrillogenesis and later on inhibited amyloid formation by 40-50%. Interesting, in presence of sulconazole and rottlerin, the ThT intensity increased to about 5 times of the native ThT intensity after a characteristic lag phase of 90 h suggesting its promoting effect rather than inhibitory effect on amyloidogenesis at this pH (Figure 2.1B). In case of HEWL at pH 12.2, rottlerin was found to be the most potent inhibitor with an inhibiting efficiency > 65% which seem to remain constant with further incubation time (Figure 2.1C). However, sulconazole and clotrimazole does not have any significant effect at this pH value.

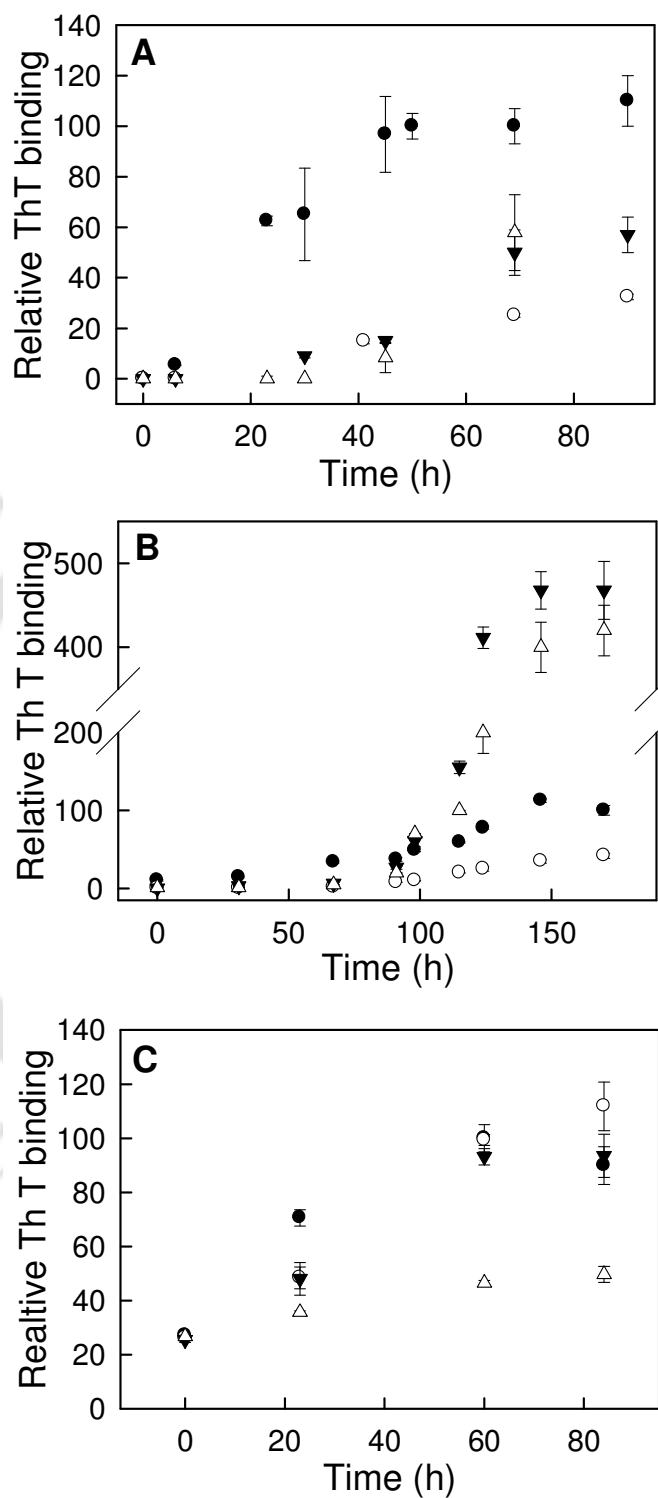


Fig. 2.1 ThT binding assay of (A) Cyt C at pH 9.0, (B) HEWL at pH 2.0 and (C) HEWL at pH 12.2 in absence (●) and presence of 10 fold molar excess of clotrimazole (○), sulconazole (▼) and rottlerin (△).

2.4.2 Atomic Force Microscope imaging

Atomic Force Microscopy (AFM) images of HEWL and Cyt C incubated under amyloid forming conditions in absence and presence of 10 fold molar excess of the compounds are shown in Figure 2.2. Clotrimazole showed less amyloid fibril formation with fibrillar thickness comparable to fibrils populated in absence of the compound. However, in presence of the sulconazole and rottlerin, amount of fibrils formed was considerably less and the fibrils were found to be relatively thicker and shorter (150 nm diameter) as compared to the native fibrils (50 nm diameter) which may account for the high ThT binding observed in presence of the compounds.

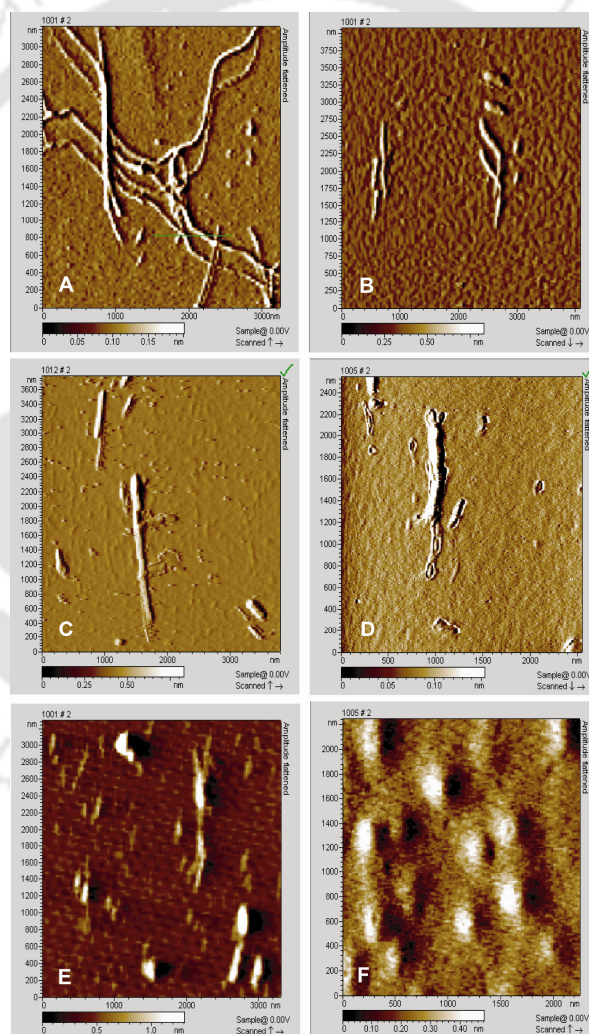


Figure 2.2 AFM images of HEWL samples incubated at pH 2.0 at 35 μ M concentration for 5 days in (A) absence and presence of 10 fold molar excess of (B) clotrimazole, (C) sulconazole and (D) rottlerin, and Cyt C samples incubated at pH 9.0 at 90 μ M concentration for 3 days in (E) absence, and (F) presence of 10 fold molar excess of clotrimazole.

In case of Cyt C, in presence of clotrimazole no fibrillar aggregates were found as compared to the control (absence of any compounds) where both fibrillar and globular aggregates were found to populate.

2.4.3 Toxicity assay of HEWL fibrils

The toxicity of HEWL fibrils formed at pH 2.0 in absence and presence of 10 fold rottlerin were monitored by MTT assay on PC12 and HEK293 cell lines, as shown in Figure 2.3. In case of control fibrils (absence of rottlerin), significant toxicity (approx. 60%) was achieved in prefibrillar stages and no toxicity was found in early and matured stages of fibril formation on PC12 cell line. Similar result was obtained with HEK 293 cell line though the level of toxicity was lesser (approx. 20%). This is in consistent with previously reported data, which shows pre-fibrils are the major pathogenic species in amyloid diseases (Bucciantini *et al.*, 2002). However, in presence of rottlerin, HEWL formed fibrils which exhibited much lesser toxicity compared to the control fibrils at different stages of the aggregation pathway, both in case of PC12 and HEK 293 cell lines.

2.4.4 Thermodynamic basis of amyloid inhibition

We attempt to understand the effects of these compounds on the stability and unfolding kinetics of these proteins employing fluorescence spectroscopy. As shown in (Figure 2.4A), no significant shift in the equilibrium unfolding curve was seen in presence of these compounds in case of HEWL at pH 2.0. However, with HEWL at pH 12.2, considerable stabilizing effect was seen in presence of sulconazole but no shift was seen in the equilibrium unfolding curve with clotrimazole (Figure 2.4B). Also, in case of Cyt C at pH 9.0, 10 fold molar excess of clotrimazole showed significant stabilizing effect on the equilibrium unfolding curve (Figure 2.4C). Sulconazole also exhibited slight stabilizing effect on CytC at pH 9.0, at 10 fold molar excess concentration. Additionally, Cyt C unfolding at pH 9.0 appears to be biphasic in nature which may be attributed to the formation of stable intermediate state (Nallamsetty *et al.*, 2007). Sulconazole and clotrimazole appears to drive the unfolding curve toward monophasic nature. Further, change in the rate constants of unfolding was monitored through kinetic studies. From the unfolding kinetics data of HEWL at pH 2.0 (Figure 2.5A), it can be seen that both clotrimazole and sulconazole significantly reduced the rate of unfolding.

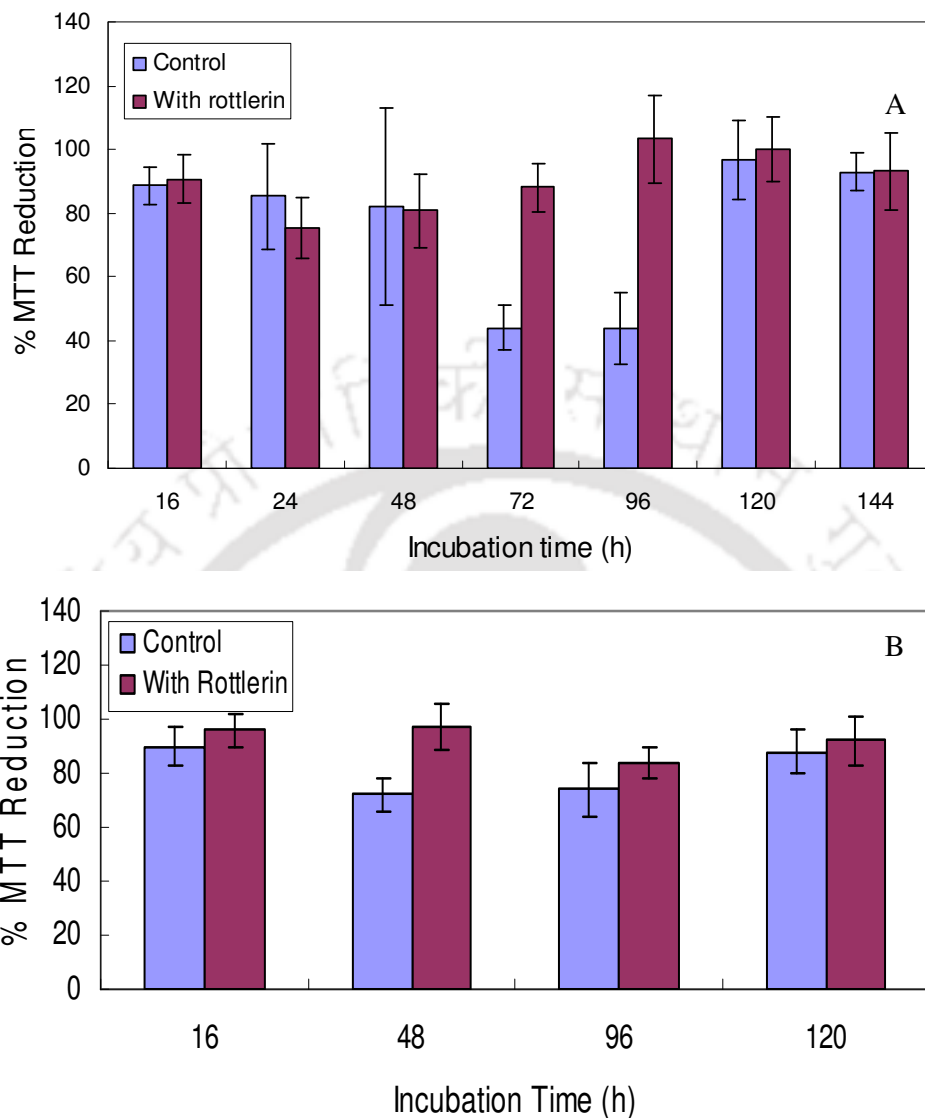


Figure 2.3 MTT assay of HEWL fibrils at different stages in absence (control) and presence of 10 fold rottlerin on PC12 cell line (A) and HEK 293 cell line (B). Readings were taken in triplicates.

However, at pH 12.2, these compounds seem to have no significant effect on unfolding kinetics of HEWL (Figure 2.5B). Further, the curve of unfolding rate constant vs GuHCl concentration clearly shows biphasic nature of unfolding both under control conditions and in presence of the compounds. Effect of rottlerin on equilibrium unfolding and unfolding kinetics could not be studied due to overlapping protein emission and absorption spectra of rottlerin.

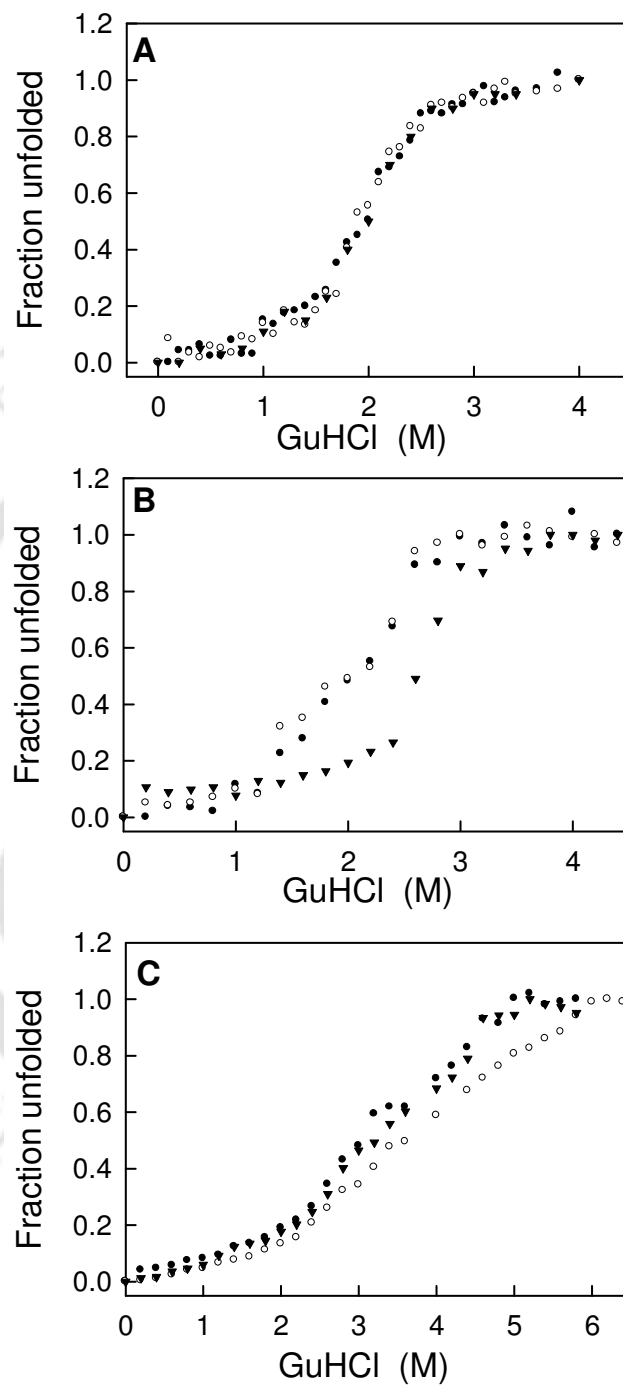


Figure 2.4 Equilibrium unfolding curve of HEWL at (A) pH 2.0, and (B) pH 12.2 in absence (●) and presence of 10 fold molar excess of clotrimazole (○) and sulconazole (▼). (C) Equilibrium unfolding curve of Cyt C at pH 9.0 in absence (●) and presence of 10 fold molar excess of clotrimazole (○) and sulconazole (▼).

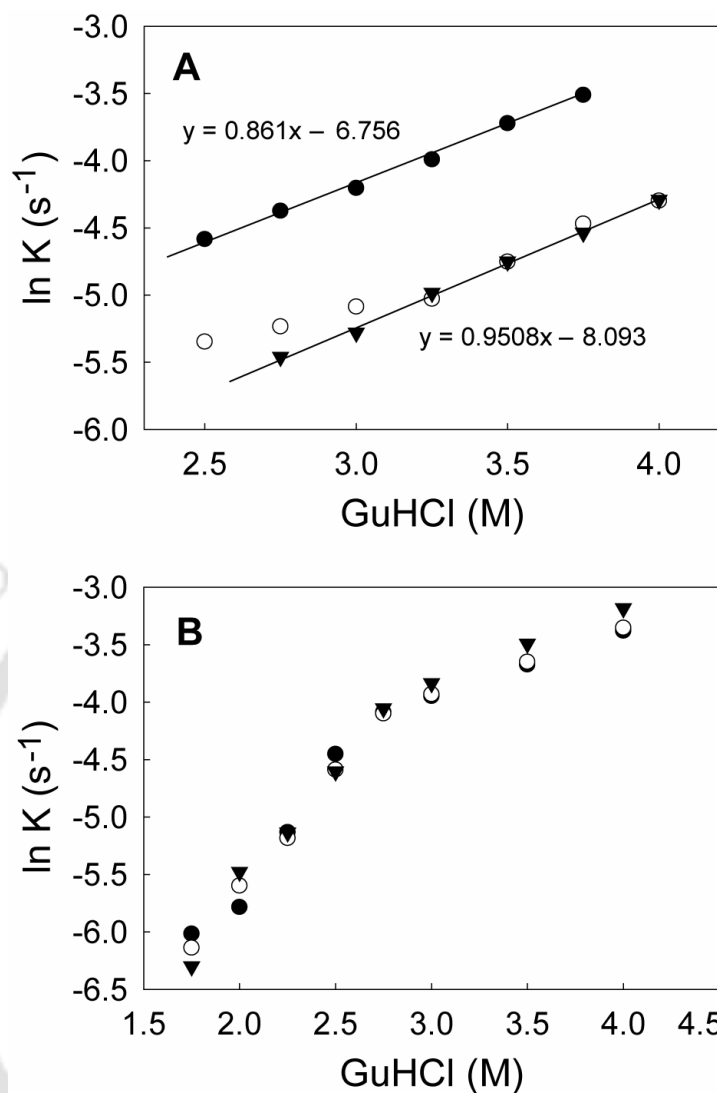


Figure 2.5 Unfolding rate constants as a function of GuHCl concentration of HEWL at pH 2.0 (A) and pH 12.2 (B) in absence (●) and presence of 10 fold molar excess of clotrimazole (○) and sulconazole (▼).

2.4.5 Alteration in the surface hydrophobicity of the aggregation prone state

The exposure of hydrophobic surface in partially unfolded intermediate states of protein has been found to be critical in protein aggregation process. To detect any alteration in protein conformation in terms of exposed hydrophobic surface as well as changes in the kinetics of protein transition, ANS binding kinetics were performed. Protein transition from native state to aggregation prone state was induced by changing the pH of the incubating buffer from pH 7.0 to the desired pH and ANS binding as function of time was recorded during the transition. In case of HEWL at pH 2.0, sulconazole and rottlerin seem to present a conformation with increased exposed hydrophobic surface compared to

the native conformation (in absence of compound) under similar condition, as shown by the enhanced ANS binding (Figure 2.6A). However, clotrimazole seem to have slightly lowering effect on ANS binding. With HEWL at pH 12.2, presence of rottlerin shows no significant ANS binding suggesting that rottlerin interacts with the protein altering its conformation such that minimal hydrophobic cluster is exposed. Also, under the same condition clotrimazole and sulconazole were found to increase the ANS binding of HEWL as evident from the amplitude of the ANS binding kinetics (Figure 2.6B).

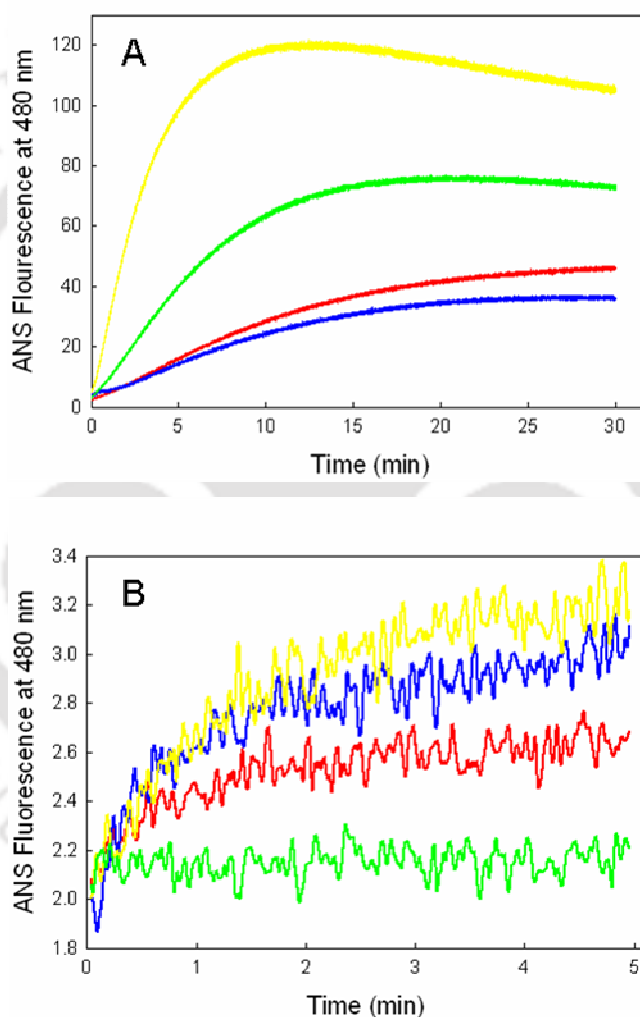


Figure 2.6 ANS binding kinetics of HEWL transition from native state (pH 7.0) to aggregation prone state at pH 2.0 (A) and pH 12.2 (B) in absence (red) and presence of 10 fold molar excess of clotrimazole (blue), sulconazole (yellow) and rottlerin (green).

2.4.6 Docking studies to identify potential binding sites

Analysis of different proteins which form amyloid fibrils suggests that these proteins contain rather small fragments which are required for the amyloidogenesis and certain amino acid sequences are more prone to amyloid formation (Ivanova *et al.*, 2004). Based on this and other studies a FoldAmyloid server was developed for prediction of amyloidogenic regions in a protein or peptide (Garbuzynskiy *et al.*, 2010). This tool to identify amyloidogenic regions of protein has been tested on 144 amyloidogenic and 263 non-amyloidogenic peptides with excellent success. FoldAmyloid web server was used to predict potential regions involved in amyloid formation of model proteins, cytochrome C and hen egg white lysozyme. In case of cytochrome C, region 33-37 (amino acids HGLFG) and 80-84 (amino acids MIFAG) are predicted as amyloidogenic. In case of hen egg white lysozyme, regions 26-30 (amino acids GNWVC), 60-64 (amino acids SRWW), 106-113 (amino acids NAWVAWRN) and 121-129 (amino acids QAWIRGCRL) are predicted as potential amyloidogenic. Further, we carried our molecular docking to see the potential binding sites of rottlerin on these two model protein. Interestingly, molecular docking results show docking of rottlerin in vicinity of these amyloidogenic regions in case of both the model proteins (Figure 2.7). In case of hen egg white lysozyme, the compound exhibits a differential binding pattern, by binding around two different regions, one formed by QAWIRGCAL (121-129) and also around SRWW (60-64) suggesting two molecule of rottlerin may bind per molecule of the protein. Rottlerin single mode of binding to cytochrome C near region formed by the stretch MIFAG (region 80-84) and indicates one molecule rottlerin binding per molecule of Cytochrome C. Although, structures of these compounds are not known in the pH values where they tend to form amyloid, we have docked rottlerin with the available structure of proteins. Our data shows that rottlerin docks near the predicted amyloidogenic region of these proteins (Figure 2.7). Additionally, vicinity of the amyloidogenic region maintains rottlerin binding potential even after change in pH. Additionally, number of rottlerin bound to per molecular of model protein matches well experimentally (Chapter III) and *in silico*. This suggests rottlerin binding sites near amyloidogenic regions are not disrupted on lower pH.

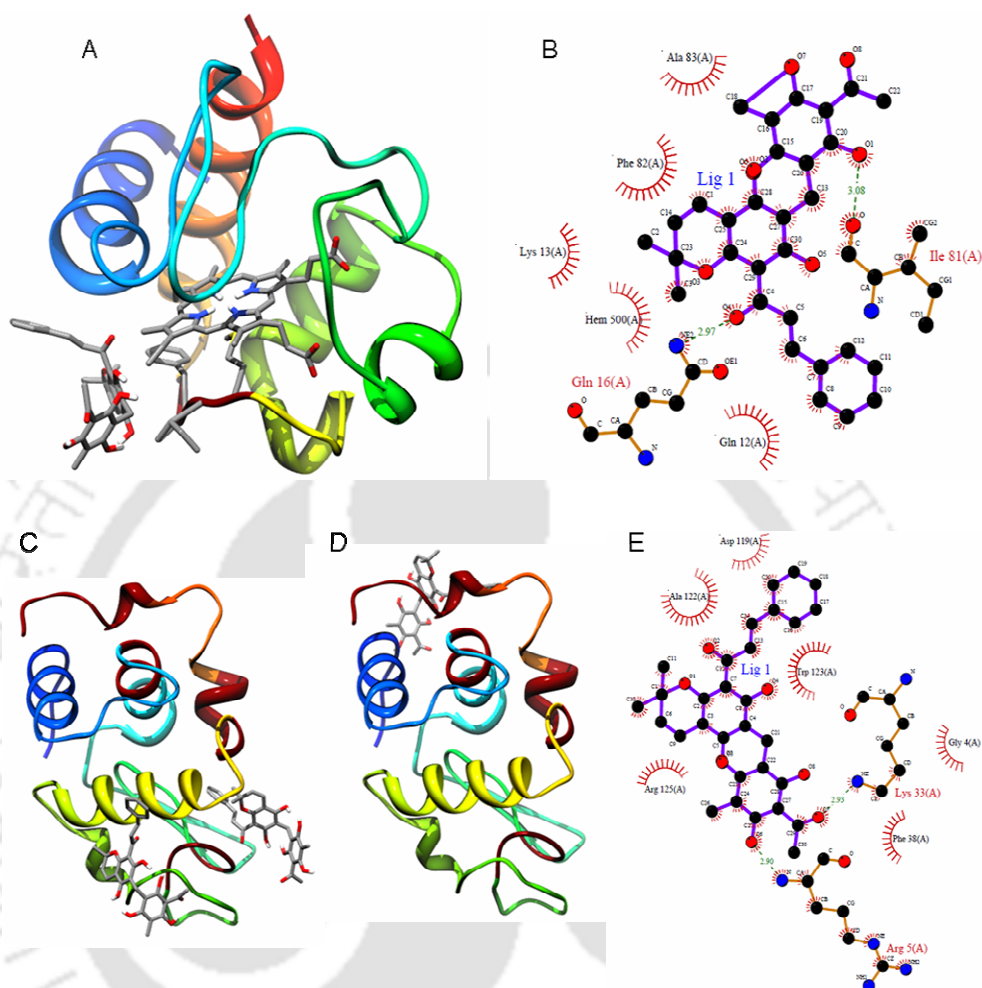


Figure 2.7 Predicted binding mode of rottlerin at amyloidogenic regions of Cyt C and HEWL: Amyloidogenic regions in both the proteins are highlighted in brick red color. **(A)** rottlerin binds to the region formed by the stretch MIFAG of Cyt C (region 80-84). **(B)** The ligplot showing the possible hydrogen bonding and non-bonding interactions of the compound with key residues of the amyloidogenic region of Cyt C. In case of HEWL, the compound exhibits a differential binding pattern, by binding around two different regions, one formed by QAWIRGCAL (121-129) **(C)** and also around SRWW (60-64) **(D)**. **(E)** representative ligplot of rottlerin binding to HEWL. [Binding energy: Rottlerin vs Cyt C - 10.32 Kcal/mol; Rottlerin vs HEWL - 10.71 Kcal/mol].

2.5 Discussions

Gaining insight into the mechanism of amyloid fibril formation and exploring novel directions of inhibition are crucial for preventing amyloid disease development. The similar structural, tinctorial and toxicity properties of all amyloids irrespective of their origin polypeptide chain, invites the attention towards development of a common therapeutic strategy of all amyloid diseases. In the current study, three small molecule compounds with known specific anti amyloidogenic property were tested against two model proteins belonging to different classes.

Of the three compounds, rottlerin was found to be the most effective inhibitor of both HEWL at pH 12.2 and Cyt C at pH 9.0 with an inhibiting efficiency of approx. 70% and 50% respectively. This may indicate involvement of hydroxyl group in preventing aggregation since only rottlerin has hydroxyl groups among the three studied compounds (Morshedi *et al.*, 2007). Additionally, molecular docking results show that rottlerin binds in vicinity of amyloidogenic region of both model proteins suggesting that rottlerin may bind to the protein blocking its aggregation. However, in case of HEWL at pH 2.0, it exhibited reverse effect, enhancing fibril formation as monitored by ThT assay suggesting that the anti-amyloidogenic property of the compound is pH and condition specific. Both sulconazole and rottlerin seem to initially inhibit amyloid formation but later on promoted it suggesting that they act as kinetic but not thermodynamic inhibitor of amyloidogenesis (Cui *et al.*, 2009). Interestingly a correlation was seen with the inhibitory/promoting effect of amyloidogenesis and ANS binding of the compound bound proteins under similar conditions. Compounds which exhibited inhibitory effect in ThT assay were found to significantly reduce the ANS binding as compared to the native condition, like in case of HEWL at pH 12.2 with rottlerin. The fact that rottlerin is inhibiting both ThT binding as well as ANS binding conclusively proves that the reduced ANS binding on rottlerin addition is due to reduction in surface hydrophobicity of the protein and not due to competitive binding of rottlerin with the protein, as it is unlikely that both ThT and ANS will have the same binding site on the protein. On the other hand, compounds which exhibited promoting effect on amyloidogenesis in ThT assay, seem to significantly enhance ANS binding as compared to the native protein, under similar conditions. This observation conclusively proves the fact that exposed hydrophobic cluster of a protein plays a key role in protein aggregation leading to

amyloid formation and that the possible mechanism of inhibition of a compound may consist blocking its exposed hydrophobic surface. Our earlier studies on a $(\alpha/\beta)_8$ -barrel protein, 2,5-Diketo-D-Gluconate Reductase A also suggested role of exposed hydrophobic residues in amyloid formation (Sarkar *et al.*, 2009).

Further, the thermodynamic basis of inhibition/promotion of amyloidogenesis was analysed through equilibrium unfolding and unfolding kinetic studies. These compounds seem to alter the thermodynamic and kinetic aspects of protein folding to varying degrees. Both sulconazole and clotrimazole significantly decreased the rate of unfolding of HEWL at pH 2.0 without altering the thermodynamic stability of the intermediate state (as shown from the equilibrium unfolding curve). Protein unfolds at pH 2.0 with K_u^0 -6.756 and the calculated energy barrier of unfolding between amyloidogenic state at pH 2.0 was 4.733 kJ/mole. In presence of sulconazole, unfolding rate constants show a linear relation with GuHCl concentration suggesting the unfolding to be without any intermediate state. However, the unfolding was found to be much slower with K_u^0 value -8.093. The calculated energy barrier of unfolding was 5.179 kJ/mole. As sulconazole does not show any change in stability of the aggregation prone state by equilibrium unfolding method (Figure 2.4A), the change in energy barrier is likely to be due to destabilization of the transition state. Interestingly, in presence of clotrimazole, unfolding rates are not a linear function of GuHCl concentration. Upward curvature of the unfolding rates with GuHCl concentration suggests that the unfolding of HEWL at pH 2.0 in the presence of clotrimazole passes through parallel unfolding pathways (Fersht, 2000). Also at pH 12.2, HEWL shows non-linear dependence of unfolding rate constant with GuHCl suggesting the unfolding of HEWL at pH 12.2 is a two state process (Dubey *et al.*, 2005). Clotrimazole and sulconazole did not show any effect on unfolding kinetics of HEWL at pH 12.2. Interestingly, sulconazole shows significant stabilization of the amyloidogenic state in the equilibrium unfolding curve, which may increase energy barrier between the amyloidogenic state and amyloid (Figure 2.4B). However, the promoting effect of sulconazole in the later stage of amyloidogenesis is not fully understood and demands more detailed study. However, we hypothesize that although, amyloidogenic state is stabilized by sulconazole, transition state between amyloidogenic state and amyloid is stabilized to greater extent in presence of compound. Thus, the net effect seems to have decreased energy barrier. Also, with Cyt C at pH 9.0

stabilization of the aggregation prone intermediate state was observed in presence clotrimazole as well as sulconazole (slight stabilization) which justifies the inhibitory effect exhibited by these compounds on amyloid formation due to increased energy barrier between the aggregation prone state and the aggregated state.

The morphological characteristics of the structures formed in absence and presence of the small molecule compounds were studied under AFM. In control (absence of any small molecule compounds), HEWL at pH 2.0 after 5 days of incubation exhibited a network of thin, long fibrillar structures characteristic of amyloid fibril with an average diameter of about 50 nm. However, in presence of sulconazole, clotrimazole and rottlerin considerably thicker, shorter fibrils were visible with an average diameter of about 150 nm. Thus, these compounds seem to promote lateral association of protofilaments forming thicker fibril (which give high ThT binding) and thereby reducing fibril elongation. In case of Cyt C, control sample (in absence of any compounds) exhibited presence of both thin fibrillar aggregates as well as globular aggregates. However, in presence of 10 fold molar excess of clotrimazole, no fibrillar aggregates were found confirming its inhibitory effect on fibril formation.

Further, the MTT assay HEWL fibrils formed at pH 2.0 in absence and presence of 10 fold rottlerin shows that the thicker and shorter fibrils seen in AFM in presence of rottlerin also exhibits lesser toxicity compared to the control fibrils, both on PC12 and HEK 293 cell lines. This suggests that in presence of rottlerin at pH 2.0, HEWL is forming fibrils which exhibit different morphological, dye binding and toxicity properties compared to the control fibrils. This confirms that the toxicity of fibrils is mostly related to its structural property and thinner and longer fibrils are toxic compared to the thicker ones.

These compounds are reported to be promiscuous, aggregate-forming compounds. It has been also reported that the compounds sequester enzyme molecules, thereby inhibiting all enzyme activity non-specifically (McGovern *et al.*, 2003). A similar mechanism is suggested for amyloid inhibition (Feng *et al.*, 2008). However, in the molar ratio used for the current study, rottlerin was not found to cause sequestration and non-specific inhibition of several enzymes tested, as shown in Figure 2.8 & Table 1.

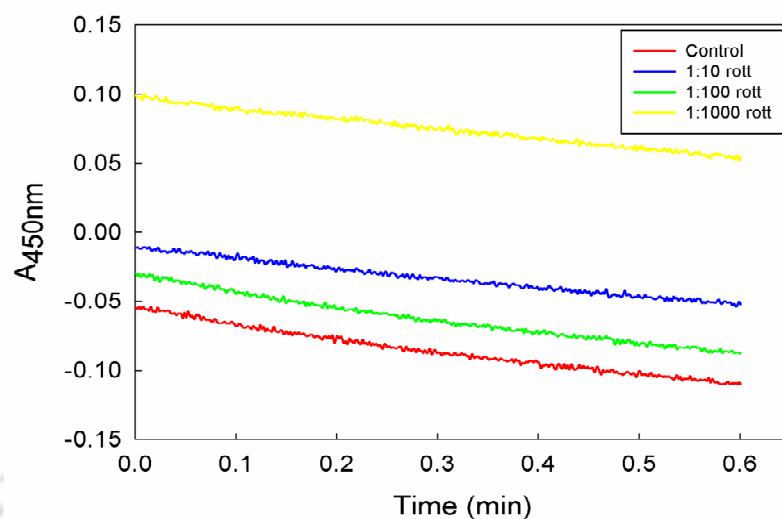


Figure 2.8 Activity assay of HEWL in absence (control) and presence of 10, 100, 1000 fold molar excess of rottlerin. The linear decrease in O.D with time indicates HEWL activity in all the samples.

Table 1: Urease activity assay with Nessler's Reagent showing no change in absorbance at 480 nm with different molar ratios of urease: rottlerin. Appropriate blanks were subtracted in each case.

Urease activity assay	
Sample	A _{480 nm}
Control (without rottlerin)	2.5886
With 10 fold rottlerin	2.5977
With 100 fold rottlerin	2.6344
With 1000 fold rottlerin	2.612

Our in silico results shows that rottlerin binds to amyloidogenic regions of Cyt C and HEWL. Rottlerin binds to Cyt C in the region formed by the stretch MIFAG (region 80-84), the ligplot represents the possible hydrogen bonding and non-bonding interactions of the compounds with key residues of the amyloidogenic region. In case of HEWL, the compound exhibits a differential binding pattern, by binding around two different regions, one formed by QAWIRGCAL (121-129) and also around SRWW (60-64). Although, native protein structure was used for the docking study and it may not be exactly same as amyloid forming state, it is likely that protein retains rottlerin binding potential in vicinity of potential amyloidogenic region. Rottlerin appears to prevent

amyloid formation by masking the hydrophobic region of amyloid forming state which is further substantiated by ANS binding studies.

2.6 Conclusions

In conclusion, the current work describes the effect of small molecule compounds such as clotrimazole, sulconazole and rottlerin on amyloidogenesis of two model protein hen egg white lysozyme and cytochrome c from bovine heart. The compounds exhibited both inhibiting and promoting effect on protein fibrillogenesis under different conditions suggesting the inhibitory effect on amyloidogenesis is both polypeptide chain as well as pH specific. Interestingly, compounds which showed inhibitory effect were found to significantly decrease ANS binding of the protein as compared to the native protein (in absence of compound). Reverse effect was observed in case of compounds with promoting effect confirming that exposed hydrophobic cluster of protein play a vital role in aggregation leading to amyloid formation. The compounds also seem to stabilize the aggregation prone state of the protein in certain cases validating the hypothesis that a possible thermodynamic mechanism of inhibition exists by increasing the energy barrier between the aggregation prone state and the aggregated state. AFM imaging of HEWL at pH 2.0 revealed that these compounds alter fibrillogenesis by forming lesser, thicker and shorter fibrils which also exhibited lesser toxicity of mammalian cell lines as monitored by MTT assay. The current report points out that although amyloids are similar in structure, toxicity and immunological properties, a common inhibitor of amyloid seem to be elusive and further studies are required in the direction.

Dissolution of amyloid fibril by rottlerin: A study on hen egg white lysozyme*.

3.1 Abstract

Deposition of protein fibrillar aggregates called amyloids in the tissue, is the principle cause of several degenerative diseases. Here, we have shown the disaggregation potential of rottlerin towards hen egg white lysozyme (HEWL) fibrils formed under alkaline conditions (pH 12.2). Rottlerin exhibited instantaneous disaggregation effect on pre-formed hen egg white lysozyme fibrils as monitored by Thioflavin T assay, anisotropy study and atomic force microscopy (AFM) imaging. Further we have monitored the conformational changes induced by rottlerin on the fibril in terms of surface hydrophobicity and secondary structure through 8-anilino-1-naphthalene sulfonic acid (ANS) fluorescence and fourier transform infrared spectroscopy studies, respectively. We have also attempted to elucidate the type of interaction between hen egg white lysozyme (HEWL) and rottlerin at pH 12.2 employing techniques like quenching study and transform infrared spectroscopy (FTIR). The current study provides insight into factors which destabilize amyloid fibrils which may in turn help in designing effective therapeutics against amyloidosis.

* Part of the work has been accepted for publication in *Biochimica et Biophysica Acta* - General Subjects, 2011.

3.2 Introduction

Amyloids are highly ordered protein fibrillar aggregates deposition of which leads to several degenerative diseases such as Alzheimer's disease, Parkinson's disease, Type II diabetes and so on. Till date over 20 different proteins have been identified which leads to several diseases by forming insoluble amyloids in the tissues (Dobson, 2003; Stefani, 2004; Sarkar *et al.*, 2010). Moreover, amyloid formation has been found to be a generic property of all polypeptides irrespective of their source protein sequence or tertiary structure (Bucciantini *et al.*, 2002). Further, the similar structural, toxicity and tinctorial properties of different amyloids invite attention towards development of a common therapeutics against amyloid diseases (Goldberg and Lansbury Jr, 2000; Kaye *et al.*, 2003; Bercontini *et al.*, 2005; Kalhor *et al.*, 2009). The mechanism by which the protein amyloid results in cell damage is still a matter of debate. In some cases, the mode of toxicity may be indirect resulting from deposition of huge masses of amyloid fibril in the tissues whereas in other cases the direct interaction of the fibrils with the cell membrane, leads to formation of pores in the membrane, resulting in inappropriate membrane permeabilization and eventually cell death (Lashuel *et al.*, 2002; Dobson, 2003).

Irrespective of the mode of pathogenesis of amyloid, compounds which can inhibit protein aggregation may serve as a potential therapeutic agent against amyloid diseases. Earlier, effect of few compounds like rottlerin, clotrimazole, sulconazole on amyloidogenesis of selected prion proteins has been investigated (Feng *et al.*, 2008). Here, we have shown considerable dissolution effect of rottlerin on pre-formed fibrils of HEWL at pH 12.2. HEWL is a well characterized protein in terms of physicochemical properties and is reported to form amyloid under several destabilizing conditions (Artymiuk and Blake, 1981; Redfield and Dobson, 1990; Radford *et al.*, 1992; Goda *et al.*, 2000; Kumar *et al.*, 2009; Wang *et al.*, 2009^a). Further it is homologous to human lysozyme, variants of which lead to hereditary systemic amyloidosis (Pepsys *et al.*, 1993).

Fibrils are known to be highly stable aggregates which cannot be reversed easily once formed. Only few compounds have been reported to have potential to dissolve pre-formed amyloid. Curcumin has been found to exhibit disaggregation effect on pre formed fibrils of HEWL at pH 2.0 after an incubation period of 2 days (Wang *et al.*, 2009^a). Catecholamines like dopamine have been found to disaggregate fibrils of A β and

α -synuclein after 1 day incubation (Li *et al.*, 2004). Dissolution of fibrils by alcohols have also been studied, where DMSO at 80% (v/v) concentration was found to completely dissolve β_2 -microglobulin fibrils by disrupting hydrophobic interaction over a period of 1 day (Hirota-Nakaoka *et al.*, 2003). However, all of these studies involve slow disaggregation of fibrils by compounds. Here we report for the first time, instantaneous (within 5 minutes) disaggregation of HEWL fibrils formed at alkaline pH by rottlerin as monitored by thioflavin T (ThT) assay, anisotropy and AFM. Structural alterations in HEWL conformation on addition of rottlerin was investigated through ANS and FTIR study. Further, interaction between HEWL and rottlerin at pH 12.2 was characterized through quenching and FTIR study.

3.3 Materials and Methods

3.3.1 Materials

Hen egg white lysozyme (HEWL), Rottlerin, Dansyl Chloride (DNSCI), Thioflavin T (ThT) and ANS were purchased from Sigma-Aldrich. All other chemicals used were of analytical grade.

3.3.2 Thioflavin T assay

HEWL was incubated at pH 12.2 at a concentration of 70 μ M for 120h to induce formation of mature fibrils, as reported earlier (Kumar *et al.*, 2009). Rottlerin stock solution (1% v/v) was added to the pre-formed matured fibrils such that the HEWL: rottlerin molar ratio comes to 1:10. Aliquots were taken from this sample at different time points for ThT assay to monitor dissolution of fibril by rottlerin. A stock solution of 2.5 mM ThT was prepared in 10 mM phosphate buffer pH 6.5. Samples for fluorimetry were prepared by adding 10 μ l of ThT stock solution to appropriate volume of incubated protein sample to make final protein concentration and volume 10 μ M and 1000 μ l respectively in 10 mM phosphate buffer pH 6.5. Fluorescence measurements were taken using Varian Fluorescence Spectrofluorometer keeping the excitation wavelength at 450 nm and collecting emission scan from 460 nm to 600 nm. Slit widths for both excitation and emission were kept at 5 nm.

3.3.3 Anisotropy Study

HEWL labeling with DNSCI: HEWL was covalently labelled with dansyl chloride (DNSCI) using the protocol described by Homchaudhuri *et al.* (Homchaudhuri *et al.*, 2006). Briefly, to 3 mM of HEWL in 1 ml of 0.1 M, pH 9.0 sodium bicarbonate buffer, 50 μ l of 75 mM DNSCI in dimethyl formamide was added. The mixture was kept in dark at 4°C with constant stirring for 3 h. Subsequently, 1.5 ml of 50 mM, pH 7.0 sodium phosphate buffer was added to the reaction mixture. Unlabelled DNSCI was removed by dialysing the mixture against 50 mM, pH 7.0 sodium phosphate buffer. The concentrations of protein and dye in the dye conjugated protein were measured and the molar ratio came to be around 1:1 (Homchaudhuri *et al.*, 2006).

Anisotropy measurement: For steady state fluorescence anisotropy measurements (G factor corrected), the samples were excited at 370 nm for DNSCI and emission measured at 444 nm using Jobin-Yvon Fluoromax-3 spectrofluorometer. The concentration of DNSCI in the final sample was kept at 10 μ M. The slit widths were kept at 1 and 5 nm for excitation and emission respectively.

3.3.4 Atomic Force Microscopy (AFM)

About 10 μ l of the incubated sample was mixed with 2 μ l of 10 mM MgCl₂ and added to freshly cleaved mica and kept for few minutes for adsorption of the sample on to the mica sheet before rinsing with deionised water to remove the unadsorbed sample. The samples were then dried under nitrogen gas and AFM measurements were taken using Picoplus microscope (Molecular Imaging, USA) under non-contact or MAC mode.

3.3.5 ANS binding assay

Change in the exposed hydrophobic surface of the fibrils on addition of rottlerin was monitored through ANS binding study (Semisotnov *et al.*, 1991; Khurana and Udgaonkar, 1994). A stock solution of 2.5 mM ANS was freshly prepared by dissolving appropriate amount of ANS in 50 μ l of methanol and diluting with 950 μ l of distilled water. 180 μ l of this ANS stock was added to the protein sample such that ANS is in 100 fold molar excess of HEWL. The mixture was diluted to 1ml using distilled water and incubated in dark for 30 mins prior to fluorescence scan. Fluorescence measurements were taken using Varian Fluorescence Spectrofluorometer with excitation set at 380 nm

and emission scan from 390 nm to 600 nm. Slit widths were set at 5 nm for both excitation and emission.

3.3.6 FTIR Spectroscopy

HEWL fibrils with and without rottlerin were lyophilised. About 5 mg of the finely powdered samples were pressed into a pellet with 200 mg of potassium bromide and infrared spectra were recorded using FTIR instrument (Perkin Elmer) from 4000 cm^{-1} to 450 cm^{-1} with a resolution of 2 cm^{-1} and 5 scans per sample.

3.3.7 Fluorescence Quenching

HEWL concentration in HEWL-rottlerin mixture was $5\text{ }\mu\text{M}$ whereas concentration of rottlerin was varied from 0 to $50\text{ }\mu\text{M}$ in 50 mM glycine buffer, pH 12.2. The reaction mixture was incubated in dark for 2 h at different temperatures ranging from 20°C to 55°C . Intrinsic fluorescence was measured by exciting the sample at 295 nm and collecting emission scan from 300 nm to 450 nm using Varian Fluorescence Spectrofluorometer. Stern-Volmer plot of the quenching data was plotted. The binding parameters like binding constant (K) and number of binding sites (n) were also calculated from the the plot of $F_0/(F_0-F)$ vs $1/Q$ and $\log[(F_0-F)/F]$ vs $\log Q$ respectively, where Q is the quencher concentration, F_0 is the intrinsic fluorescence in absence of the quencher, F is the intrinsic fluorescence at a particular quencher concentration (Bourassa *et al.*, 2010).

3.4 Results

3.4.1 Disaggregation of HEWL fibril by rottlerin

HEWL fibril formation following incubation in alkaline buffer was confirmed by thioflavin T fluorescence and rottlerin was added to the pre-formed fibril at 10 fold molar excess concentration. Disaggregation of fibril on rottlerin addition was monitored by ThT binding (Figure 3.1). Within about 5 mins of rottlerin addition significant decrease in ThT fluorescence was observed suggesting instantaneous fibril disaggregation by rottlerin. After about 15 mins, the decrease in ThT fluorescence was stabilized indicating no ThT is binding to the protein.

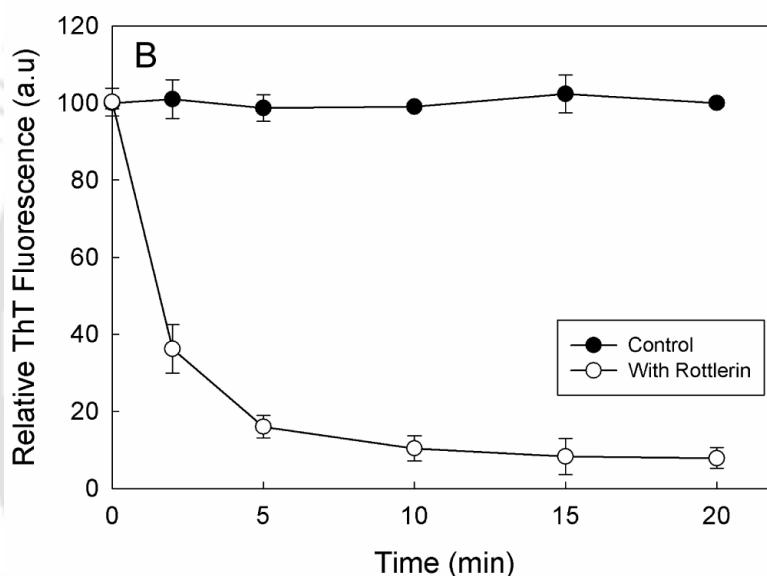


Figure 3.1 ThT binding kinetics of HEWL fibril on addition of rottlerin. HEWL fibrils were grown for 120 h until matured fibrils were formed and rottlerin was added to the pre-formed fibril in 1:10 molar ratio of HEWL: rottlerin. HEWL fibril in absence of rottlerin is denoted as 'Control'. The readings are averaged over three sets of data and the standard deviations are shown.

To further confirm the disaggregation effect of rottlerin on HEWL fibrils, anisotropy experiment was performed (Figure 3.2). Anisotropy measures the rotational mobility of the fluorophore in solution and thus is dependent on the size of the fluorophore-protein complex (Flecha and Levi, 2003). HEWL labeled with DNSCI fluorophore was induced to form fibril and fibrillation was confirmed by ThT fluorescence. Rottlerin was added to the pre-formed fibril and anisotropy was measured. On addition of rottlerin, immediate decrease in anisotropy of the DNSCI labeled HEWL was observed for a period of 1h. After 1h, decrease in anisotropy by almost 0.2 units

suggests that rottlerin has significant disaggregation effect on HEWL fibril. The anisotropy was found to be stabilized after 12h of incubation with rottlerin suggesting complete disaggregation of HEWL fibrils. Though the initial value of anisotropy seems a bit higher which may be due to scattering effect, the decrease in anisotropy value indicates disaggregation of fibrils. AFM was done to further monitor the disaggregation of fibril by rottlerin (Figure 3.3). As seen from Figure 3.3, no amyloid were found in presence of rottlerin whereas in control sample (without rottlerin), elongated thick and short amyloids were seen.

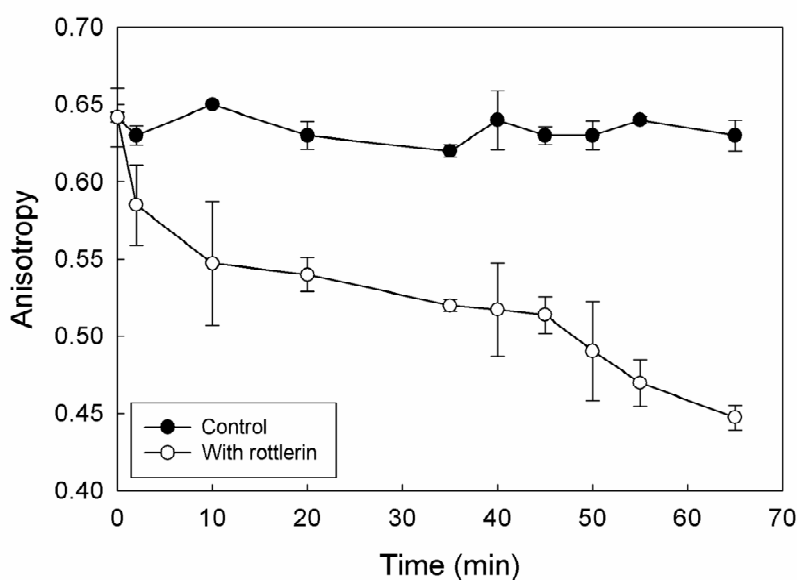


Figure 3.2 Anisotropy change as a function of time of DNSCI labeled HEWL fibril on addition of rottlerin. HEWL fibril in absence of rottlerin is denoted as 'Control'. The readings are averaged over three sets of data and the standard deviations are shown.

3.4.2 Conformational changes in HEWL fibril induced by rottlerin

Changes in the HEWL fibril conformation in terms of exposed hydrophobic surface, on addition of rottlerin was investigated through ANS binding assay. Addition of rottlerin to HEWL fibrils was accompanied by significant reduction (approx 50%) in ANS fluorescence (Figure 3.4). Further, there was a red shift in λ_{\max} from 490 nm (control) to 515 nm (with rottlerin). This suggests that addition of rottlerin is decreasing the exposed hydrophobic surface in HEWL fibril thereby preventing ANS binding.

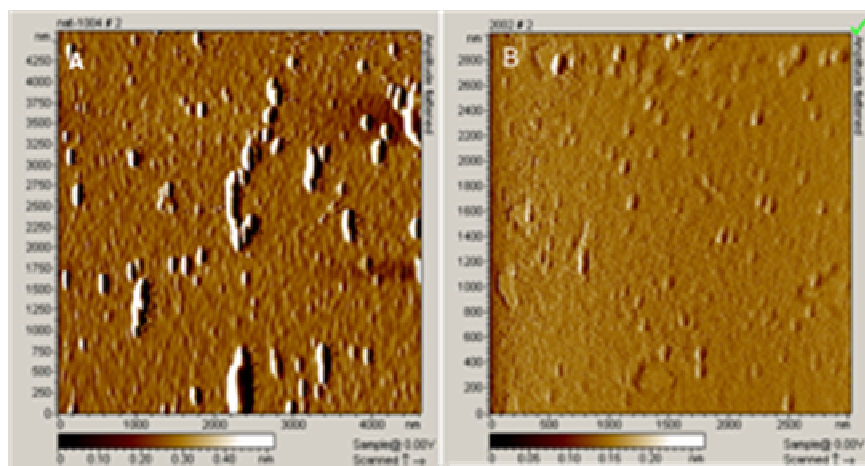


Figure 3.3 AFM of (A) HEWL fibril incubated at pH 12.2 for 120 h showing presence of thick, elongated fibrillar structures and (B) HEWL fibril after addition of 10 fold molar excess of rottlerin where no fibrillar structures were seen.

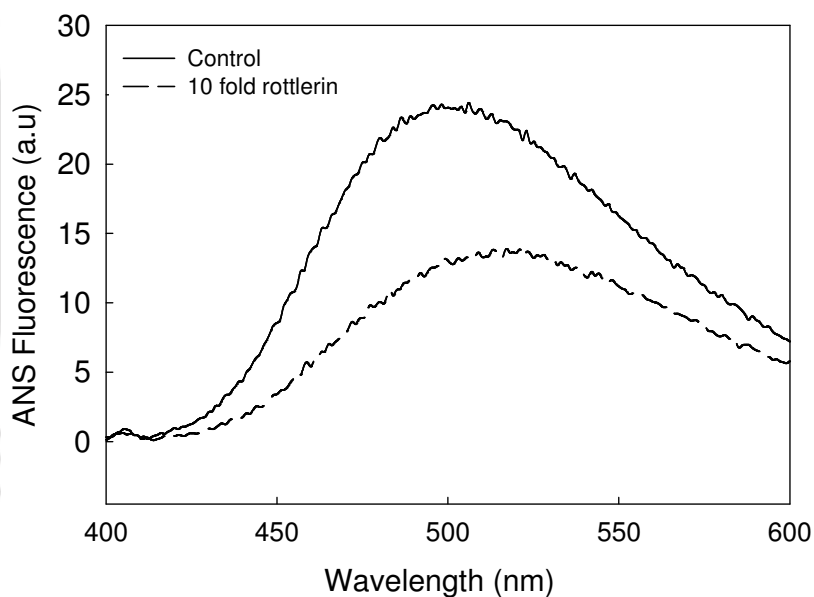


Figure 3.4 ANS spectra of HEWL fibril (control) and on addition of rottlerin. Appropriate blanks are subtracted in each case and the spectra are averaged over three separate readings.

Further, changes in the secondary structure of HEWL fibril on addition of rottlerin were monitored by FTIR spectra (Figure 3.5). A reduction in the peak intensity at 1633 cm^{-1} in FTIR was observed on rottlerin addition to HEWL fibril, as seen from the difference spectra (HEWL fibril and rottlerin complex - HEWL fibril alone). The peak at 1633 cm^{-1} in FTIR is characteristic of β sheet structure of protein (Bouchard *et al.*, 2000; Hiramatsu and Kitagawa, 2005). Thus the reduction in this peak intensity on rottlerin

addition is suggestive of dissolution of fibril by rottlerin as fibrils are rich in β sheeted structure.

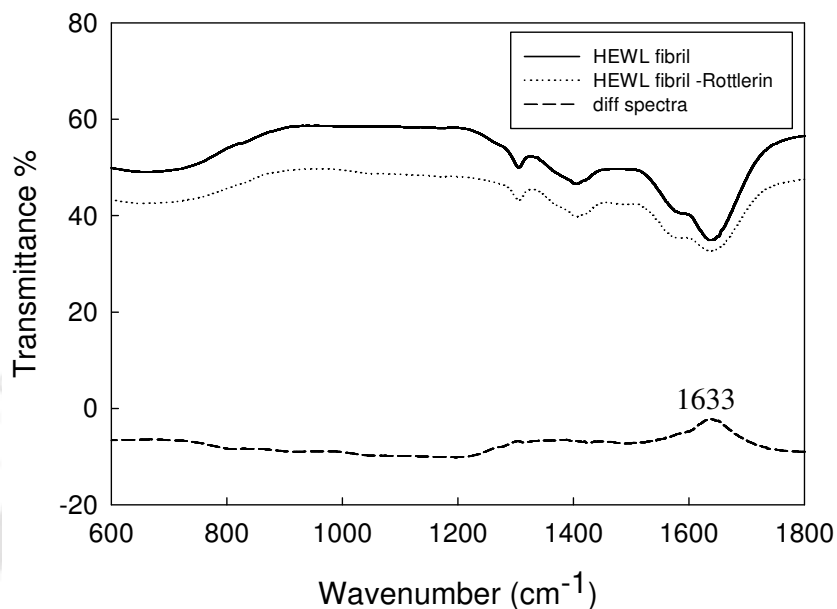


Figure 3.5 FTIR spectra of HEWL fibril in absence and presence of rottlerin and difference spectra between HEWL fibril-rottlerin complex and HEWL fibril alone, showing a reduction in peak intensity at 1633 cm^{-1} indicating decrease in β sheet content of HEWL fibril on rottlerin addition.

3.4.3 Characterization of HEWL and rottlerin interaction

Rottlerin was found to be a quencher of HEWL intrinsic fluorescence at pH 12.2. To gain further insight into the interaction between HEWL and rottlerin, quenching studies were done with varying concentrations of rottlerin at different temperatures (Figure 3.6). Rottlerin seems to exhibit simultaneous dynamic and static quenching on HEWL at pH 12.2, as evident from the upward curvature of the Stern-Volmer plot of the quenching data (Lakowicz, 1983; Papadopoulou, 2005). However the decrease in the quenching rate with increasing temperature is indicative of the involvement of hydrogen bond or Van der Waal's interaction between HEWL and Rottlerin (Wang *et al.*, 2009^a). Binding parameters were also calculated from the quenching data (Figure 3.7), which gave binding constant (K) as $1.64 \times 10^4\text{ (M}^{-1}\text{)}$ and no. of binding sites (n) as 1.98. This is in consistency with our docking study on rottlerin and HEWL which states that rottlerin binds to two sites in HEWL (Sarkar *et al.*, 2011).

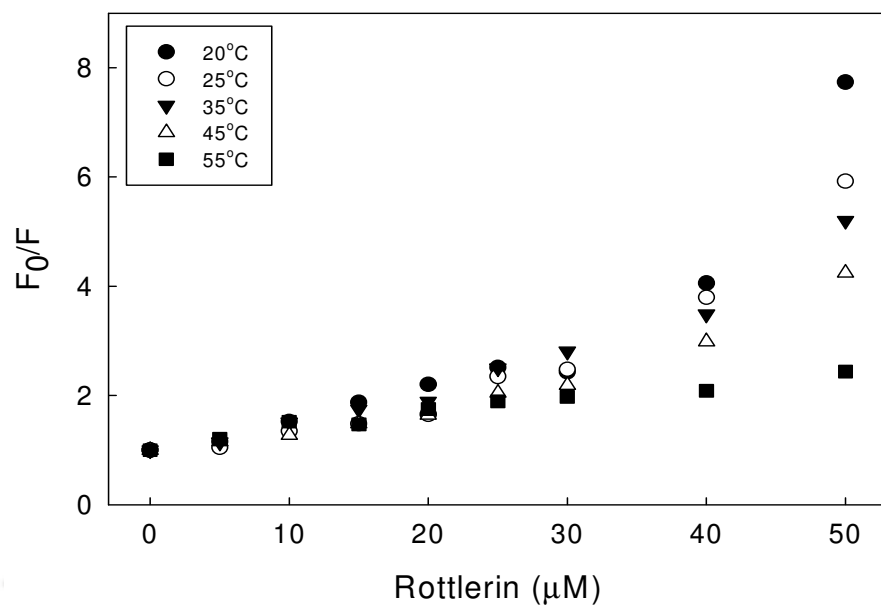


Figure 3.6 Stern-Volmer plot of quenching of HEWL intrinsic fluorescence by rottlerin at pH 12.2 at different temperatures. The readings are averaged over three sets of data and appropriate blanks are subtracted in each case.

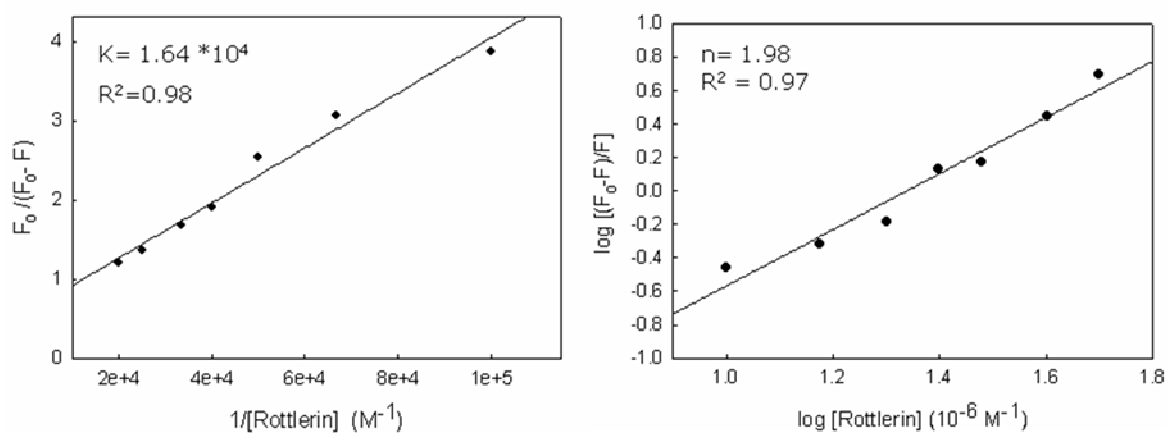


Figure 3.7 Binding parameters calculated from the quenching data of HEWL with rottlerin at pH 12.2 showing a binding constant (K) of $1.64 \times 10^4 \text{ M}^{-1}$ and number of binding sites (n) of 1.98.

FTIR study was done to further characterize the interaction between HEWL and rottlerin at pH 12.2. As seen from Figure 3.8, no major spectral shifts or additional peaks were observed between HEWL and rottlerin complex and HEWL spectra indicating no covalent bonds are being formed between HEWL and rottlerin at pH 12.2. However the difference spectra between HEWL-rottlerin complex and HEWL shows increase in

intensity in protein amide I band at 1657 cm^{-1} and amide II band at 1567 cm^{-1} on addition of rottlerin suggesting that the compound is interacting with protein -C=O , -N-H and -C-N groups (Bourassa *et al.*, 2010).

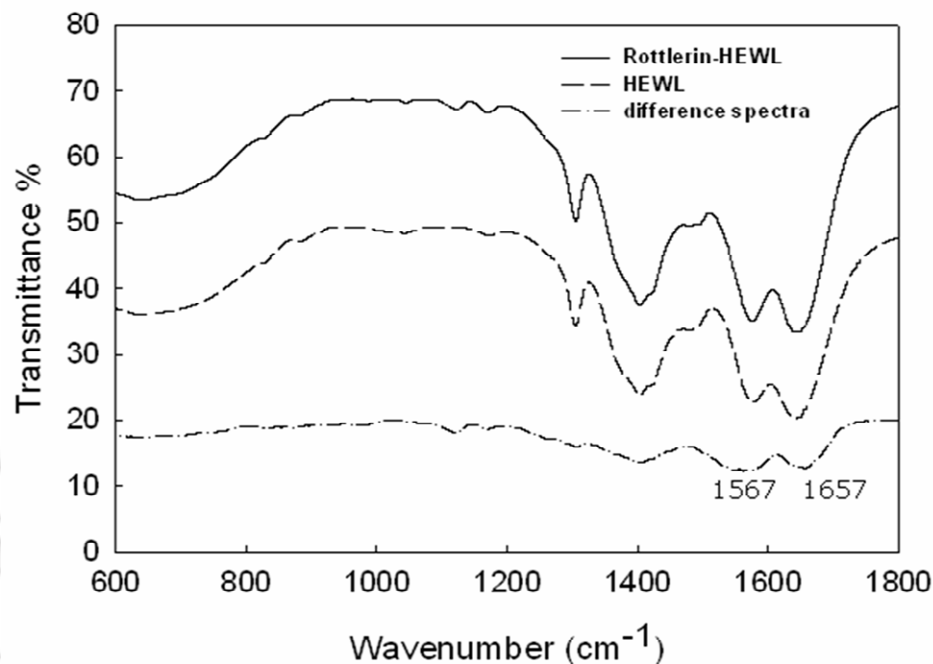


Figure 3.8 FTIR spectra of HEWL-rottlerin complex and HEWL alone at pH 12.2 and the difference spectra between HEWL-rottlerin complex and HEWL. The difference spectra shows two peaks at 1567 cm^{-1} and 1657 cm^{-1} corresponding to amide II and amide I bands respectively.

3.5 Discussions

Amyloids are highly stable fibrillar structures which has gained a lot of clinical importance owing to their involvement in several degenerative diseases (Chatani and Goto, 2005). The extreme stability of amyloids towards chemical or proteolytic degradation is a characteristic feature resulting from backbone hydrogen bonding (Malisauskas *et al.*, 2009). Here we have shown instantaneous disaggregation of pre-formed HEWL fibril by rottlerin at alkaline pH. Further we have tried to investigate the conformational changes induced by rottlerin on HEWL fibrils and the mode of interaction between HEWL and rottlerin. HEWL fibril formation was induced by incubating the protein at pH 12.2 at $70\text{ }\mu\text{M}$ concentration (Kumar *et al.*, 2009). Rottlerin was added to the pre-formed fibril at 10 fold molar excess concentration and ThT fluorescence was measured. Interestingly, after about 10 mins of rottlerin addition there

seem to be complete loss of ThT fluorescence suggesting disaggregation of HEWL fibril (Figure 3.1). To confirm whether the loss of ThT fluorescence on addition of rottlerin was due to competitive binding of rottlerin with fibril preventing ThT binding or due to fibril disaggregation, anisotropy assay was done (Flecha and Levi, 2003; Homchaudhuri *et al.*, 2006). HEWL was tagged with Dansyl Chloride fluorophore (DNSCI), and the tagged HEWL was induced to form fibril under alkaline condition (Kumar *et al.*, 2009). Rottlerin was added to the DNSCI tagged HEWL fibril and anisotropy of the tagged DNSCI was measured at different times of incubation (Figure 3.2). Rottlerin addition was followed by immediate decrease in anisotropy of DNSCI, suggesting decrease in molecular size of DNSCI tagged HEWL fibril complex. However, unlike the ThT assay where decrease in ThT fluorescence was limited to first 10 mins of rottlerin addition, anisotropy was found to decrease gradually upto 1h and finally become stable after about 12 h (total loss in anisotropy being 0.37 units). This suggests that on addition of rottlerin to HEWL fibrils, the fibrils are getting disaggregated to oligomeric species within first 5-10 mins, which no longer shows ThT binding. With longer incubation time, rottlerin is further disaggregating the oligomers to smaller species and finally completely disaggregating them within 12 h. To further confirm the disaggregation potential of rottlerin towards HEWL fibrils, AFM was done. Rottlerin was found to reduce the elongated aggregates of HEWL to monomer species as seen from the AFM images (Figure 3.3).

Exposed hydrophobic surface in protein has been found to be critical in triggering amyloidogenesis (Horwich, 2002; Sarkar *et al.*, 2009). The changes in the surface hydrophobicity of HEWL fibril on rottlerin addition were monitored by ANS fluorescence study. Addition of rottlerin to HEWL fibril was followed by attenuated ANS fluorescence and red shift in λ_{\max} by 25 nm, suggesting that disaggregation of fibril is achieved by reducing the surface hydrophobicity of the HEWL fibril. Further, changes in the secondary structure of HEWL fibril on addition of rottlerin was monitored through FTIR. No additional peaks in the FTIR spectra of HEWL fibril-rottlerin complex and HEWL fibril alone suggests no covalent interaction between HEWL fibril and rottlerin. However, the difference spectra (HEWL fibril and rottlerin complex - HEWL fibril) shows decrease in peak intensity at 1633 cm^{-1} on rottlerin addition which indicates

reduction in β sheet content of HEWL fibril. Thus rottlerin seem to alter the secondary structure of the fibril towards non β sheeted structure thereby destabilizing the fibril.

To gain insight into the type of binding force associated with the interaction between HEWL and rottlerin at pH 12.2 techniques like fluorescence quenching and FTIR were employed. Quenching data of HEWL with rottlerin at different temperatures shows decrease in quenching rate with increasing temperatures. This indicates presence of hydrogen bonding or Van der Waal's interaction between HEWL and rottlerin (Wang *et al.*, 2009^a). The low binding constant ($K = 1.64 \times 10^4 \text{ M}^{-1}$) obtained from the quenching data indicates rottlerin is binding on the protein surface and not penetrating the inner core of the protein. Further increase in amide I (1657 cm^{-1}) and amide II (1567 cm^{-1}) peak intensities of HEWL on addition of rottlerin in FTIR, indicates interaction of rottlerin with $-\text{C}=\text{O}$, $-\text{C}-\text{N}$ and $-\text{N}-\text{H}$ groups of HEWL (Flecha and Levi, 2003). This implies involvement of hydrogen bonding between HEWL and rottlerin interaction at pH 12.2 which is consistent with the quenching data.

3.6 Conclusions

Thus, the current study describes the instantaneous disaggregation potential of rottlerin towards HEWL fibrils formed at alkaline pH. Rottlerin was found to disaggregate pre-formed HEWL fibrils within 10 mins of addition as monitored by Thioflavin T assay. Fibril disaggregation was further confirmed by anisotropy and AFM measurements. Disaggregation was followed by reduction in surface hydrophobicity and β sheet content of the fibril as monitored by ANS and FTIR spectroscopy respectively. Further, HEWL and rottlerin interaction at pH 12.2 was found to be governed by hydrogen bonding as detected by quenching study and FTIR spectroscopy. These studies provide essential insight into factors which destabilize amyloid fibrils which may help in designing effective therapeutics against amyloidosis.

Exploring role of disulfide bonds in amyloidogenesis: A study on hen egg white lysozyme*.

4.1 Abstract

Identification of compounds which can prevent or reduce protein aggregation can serve as a potential therapeutic target. In the present study we have shown inhibitory effect of sodium tetrathionate towards hen egg white lysozyme (HEWL) amyloidogenesis at pH 2.0. Our study reveals that without sulfonation, sodium tetrathionate prevents amyloid fibril progression. Moreover, it shows that correct disulfide bonds rather than exposure of hydrophobic surface in protein plays a critical role in initiating fibrillation process. Inhibitory effect of reducing agent β -mercaptoethanol towards fibrillation process also confirms the involvement of disulfide bond in initiating HEWL amyloidogenesis. These results provide important information towards understanding key interactions that guide amyloidogenesis, which may facilitate development of potential therapeutics.

* Part of the work has been published in *Biochimie*, **2011**, 93, 962-968

4.2 Introduction

Tissue deposition of proteinaceous fibrillar aggregates known as amyloid is the cause of several degenerative diseases in human such as Alzheimer's disease, Parkinson's disease, Type II diabetes and so on. However, the mechanism underlying protein transition from natively folded state to highly ordered amyloidogenic state is still poorly understood. Despite being unrelated in terms of amino acid sequence and three dimensional structures, proteins form amyloids which exhibit strikingly similar structural, toxicity as well as tinctorial properties (Bucciantini *et al.*, 2002). In many cases, partially folded protein intermediate states have been found to be critical precursors of amyloid (Booth *et al.*, 1997; Khurana *et al.*, 2001; Horwich, 2002). Further, many studies have shown a vital role of exposed hydrophobic surface in protein in accelerating self assembly of partially folded protein monomers leading to fibrillogenesis (Li *et al.*, 1999; Kaye *et al.*, 1999; Horwich, 2002; Sarkar *et al.*, 2009;). Owing to the toxicity associated with the formation and deposition of amyloids in the tissues, identification of compounds which can prevent or attenuate fibril formation may serve as a potential therapeutic strategy against amyloid diseases. Furthermore, the mechanism of fibril inhibition may help to gain insight into the fibrillation process and identify the key interactions that guide it.

In the present work we have studied the effect of sodium tetrathionate towards amyloidogenesis of hen egg white lysozyme (HEWL). HEWL is a well characterized protein in terms of physicochemical properties and is reported to form amyloid under several destabilizing conditions (Artymiuk and Blake, 1981; Redfield and Dobson, 1990; Radford *et al.*, 1992; Goda *et al.*, 2000; Kumar *et al.*, 2009; Wang *et al.*, 2009^a). Further it is homologous to human lysozyme, variants of which lead to hereditary systemic amyloidosis (Pepsys *et al.*, 1993). We have used sodium tetrathionate (STT) at pH 2.0 where HEWL is reported to form fibril at elevated temperature (Wang *et al.*, 2009^a; Arnaudov and Vries, 2005). Previously, cysteine sulfonation in Transthyretin (TTR) by STT has been found to reduce amyloidogenesis compared to wild type TTR by stabilizing the tetrameric protein form and reducing its dissociation rate into misfolded monomers which are essential precursors of TTR amyloidogenesis (Zhang and Kelly, 2003). However, the role of cysteine sulfonation in amyloidogenesis has been a matter of debate. A contradictory study by Nakanishi *et al.*, shows cysteine sulfonation triggers

TTR amyloidogenesis through oxidative degradation to dehydroalanine which is highly prone to amyloid formation (Nakanishi *et al.*, 2010). Here we have shown that without sulfonation of the thiol group in HEWL, sodium tetrathionate leads to complete inhibition of fibril formation at pH 2.0. Further, considerable fibril disaggregation was achieved by adding 20 mM STT to prefibrillar species. Also, our results indicate a critical role of disulfide bond rather than exposed hydrophobic surface in the protein in triggering fibrillogenesis at the early stages of fibril formation.

4.3 Materials and methods

4.3.1 Materials

Hen egg white lysozyme (HEWL), Guanidine hydrochloride (GuHCl), Thioflavin T (ThT), DTNB, Sodium Tetrathionate (STT) and ANS were purchased from Sigma-Aldrich. All other chemicals used were of analytical grade.

4.3.2 Thioflavin T assay

HEWL amyloidosis was induced by incubating the protein in pH 2.0 buffer (136.8 mM NaCl, 2.68 mM KCl and 0.01% (w/v) NaN_3) at 55°C, 30 rpm at a concentration of 35 μM as reported earlier (Wang *et al.*, 2009^a). A stock solution of 2.5 mM ThT was prepared in 10 mM phosphate buffer pH 6.5. Samples for fluorimetry were prepared by adding 10 μl of ThT stock solution to appropriate volume of incubated protein sample to make final protein concentration and volume 10 μM and 1000 μl respectively in 10mM phosphate buffer pH 6.5. Samples prepared in this way were incubated for 30 mins at room temperature in dark before taking emission scan from 460 nm to 610 nm with 450 nm excitation wavelength using Cary Eclipse Fluorescence Spectrophotometer from Varian. Appropriate blanks were subtracted in each case.

4.3.3 Atomic Force Microscopy

About 10 μl of the incubated sample was added to freshly cleaved mica and kept for few minutes for adsorption of the sample on to the mica sheet before rinsing with deionised water to remove the unadsorbed sample. The samples were then dried under nitrogen gas and AFM measurements were taken using Picoplus microscope (Molecular Imaging, USA) operating under non-contact or MAC mode.

4.3.4 MTT assay

Toxicity assay of STT towards mammalian cell lines – PC12 and HEK 293 was monitored by MTT assay. Cells were grown in DMEM supplemented with 15% FBS at 37°C and 5% CO₂ according to the standard protocol (Hughes *et al.*, 2000; McLaurin *et al.*, 2000). Varying concentrations of STT was added to the cell culture under exponential phase and grown for 24 h under serum free media. MTT was added to the culture (10 µl from MTT stock solution of 5mg/ml was added to 180 µl culture) and kept for 4 h before taking O.D at 570 nm. The readings were taken in triplicates and appropriate blank readings were subtracted. Positive control consisted of addition of equivalent amount of serum free media to the culture volume. Assay values for positive control were taken as 100%.

4.3.5 ANS binding assay

Exposure of hydrophobic patch in protein during the aggregation process was monitored using fluorescent dye ANS (Semisotnov *et al.*, 1991; Khurana and Udgaonkar, 1994). A stock solution of 20 mM ANS was prepared by dissolving the compound in 100 µl of methanol and then adjusting the volume to 1 ml using deionised water. Samples for ANS assay were prepared by adding ANS from the stock solution to the incubated sample such that protein and ANS final concentration comes to 5 µM and 500 µM respectively. The samples were then incubated in dark for 30 mins before taking fluorescence emission scan from 400 nm to 600 nm at 380 nm excitation wavelength using Cary Eclipse Fluorescence Spectrophotometer from Varian. The slit widths were kept at 5 nm for both excitation and emission.

4.3.6 Equilibrium unfolding study

Protein samples were incubated at desired GuHCl concentration in 50 mM Gly-HCl buffer pH 2.0 for approximately 24 h at 25°C to attain equilibrium. The final concentration of the protein and denaturant, in each sample, were determined by spectrophotometry and refractive index measurements, respectively. Incubated samples were selectively excited at 295 nm for tryptophan and emission was recorded between 315 nm and 400 nm using Jobin-Yvon Fluoromax-3 Spectrophotometer. The final protein concentration was 5 µM for all fluorescence measurements and the slit widths

were kept at 5 nm for both excitation and emission. Appropriate blank samples were subtracted and the readings were taken in triplicates.

4.3.7 Unfolding kinetics study

Unfolding kinetics were monitored by following spectral changes in intrinsic tryptophan fluorescence of the protein samples at 350 nm using Cary Eclipse Fluorescence Spectrophotometer from Varian equipped with stopped flow apparatus. Drive syringes of 500 μ l and 2500 μ l were used to inject protein and denaturant buffer respectively, resulting in a six-fold dilution of the protein solution. Samples were excited at 295 nm and samplings were done at an interval of 0.01s for appropriate time until saturation was reached. HEWL was dissolved in pH 2.0 buffer such that the final protein concentration after six-fold dilution comes to 5 μ M and STT was added to the dilution buffer containing different concentrations of GuHCl. The time course of the kinetics curves were fitted in appropriate equation using the software of Cary Eclipse and the rate constants were calculated and plotted as a function of denaturant concentration.

4.3.8 Intrinsic fluorescence study

HEWL was incubated in absence and presence of 500 μ M STT and 1% β -mercaptoethanol (v/v) under amyloidogenic conditions. Aliquots were taken at regular interval and diluted to a final concentration of 5 μ M protein in pH 2.0 buffer. Intrinsic fluorescence was measured by selectively exciting the sample for tryptophan at 295 nm and taking emission scan from 300 nm to 450 nm using Cary Eclipse Fluorescence Spectrophotometer from Varian. Slit widths were kept at 5 nm for both excitation and emission.

4.4 Results

4.4.1 Monitoring amyloid progression in presence of STT

The progression of amyloid was monitored through ThT assay and AFM. As shown in Figure 4.1, the ThT intensity seemed to increase dramatically for first 60 h in case of control (HEWL without addition of STT) after which it attained stationary phase. However, presence of STT at a concentration of 100 μM seemed to significantly reduce ThT intensity, with the stationary phase intensity being 40% (approx.) of the control intensity. Further, complete inhibition of fibril formation was achieved with and beyond 500 μM STT for as long as 160h. Also, effect of 20 mM STT towards disaggregation of pre-fibrils was examined by addition of STT on pre-formed fibrils (fibrils were grown for 20h). 20 mM STT seem to have significant disaggregating effect on prefibrillar species of HEWL as monitored by ThT binding data after an incubation period of about 116 h (Figure 4.2).

The ThT data was further substantiated through the AFM data of HEWL incubated at pH 2.0 buffer for 180 h in presence of 0, 100, 500 μM of STT as well as of fibril dissolution with 20 mM STT (Figure 4.3). As seen from Figure 4.3, a network of fibrillar structures were found in control HEWL whereas relatively lesser and thinner fibrils were seen in presence of 100 μM STT, in agreement with ThT data. No fibrillar structures were seen in presence of 500 μM STT confirming the fibril inhibition potential of STT at these concentrations. Also, in case of dissolution data with 20 mM STT, complete absence of fibrillar structures confirms the disaggregation potential of STT at this concentration. To monitor STT as a potential therapeutic target, its toxicity towards mammalian cell line PC12 was assessed through MTT assay. As seen from Figure 4.4, STT was found to be non toxic to PC12 cells for up to 2 mM concentration suggesting its potential as a prospective drug target.

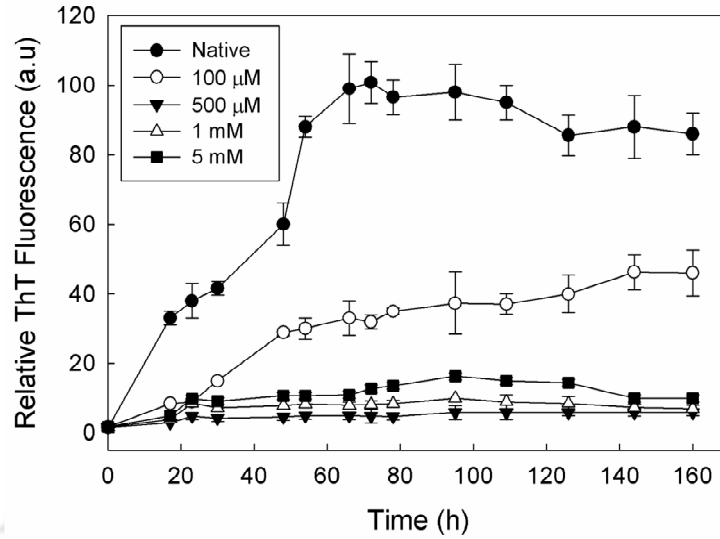


Figure 4.1 ThT assay of hen egg white lysozyme incubated at pH 2.0 under amyloidogenic conditions in absence (control) and presence of different concentrations of sodium tetrathionate. Each reading was taken thrice and error bars are shown.

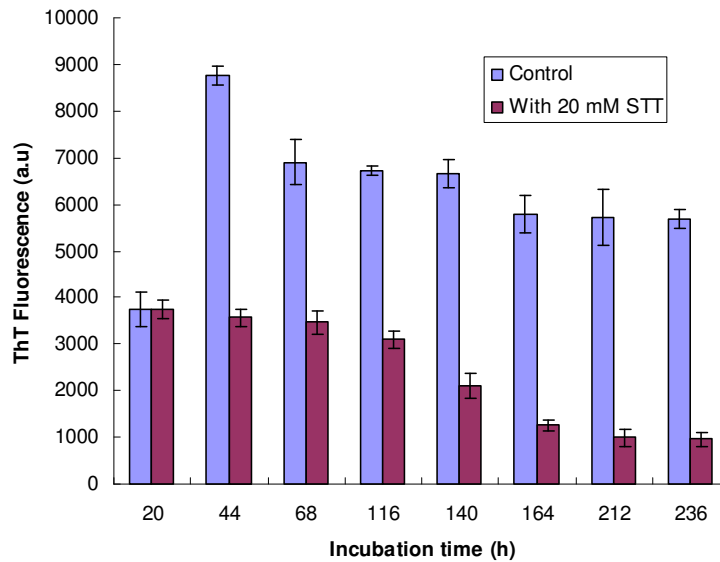


Figure 4.2 ThT assay showing dissolution effect of 20 mM sodium tetrathionate on 20 h old hen egg white lysozyme fibrils prefibrils at pH 2.0. The data shown is the average of three sets of readings.

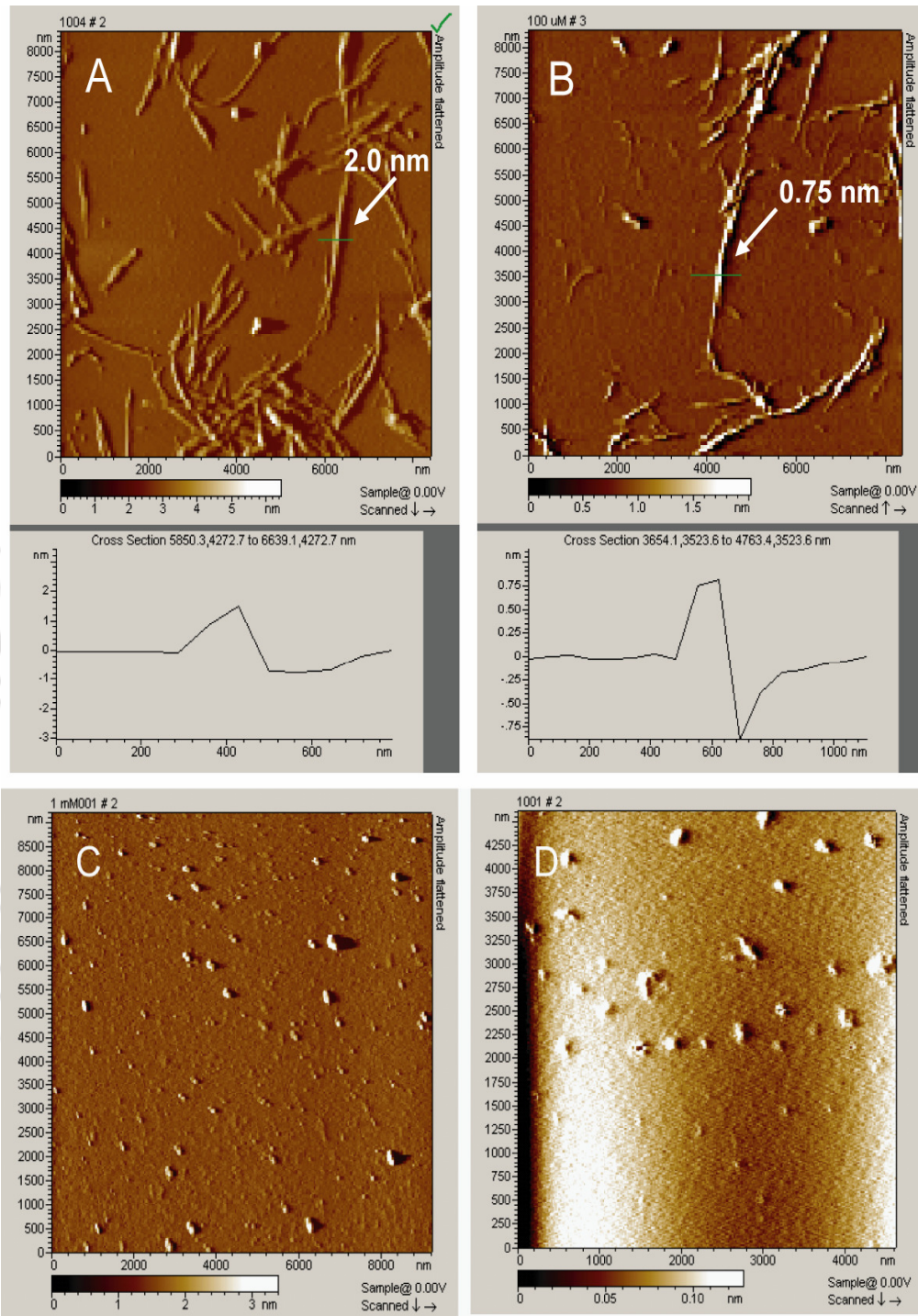


Figure 4.3 AFM of HEWL incubated at pH 2.0 under amyloidogenic conditions for 180 h in absence (A) and presence of 100 μM (B) and 500 μM (C) STT, and dissolution of HEWL prefibrils with 20 mM STT after an incubation time of 240 h (D). The height of the fibrils is indicated with arrows.

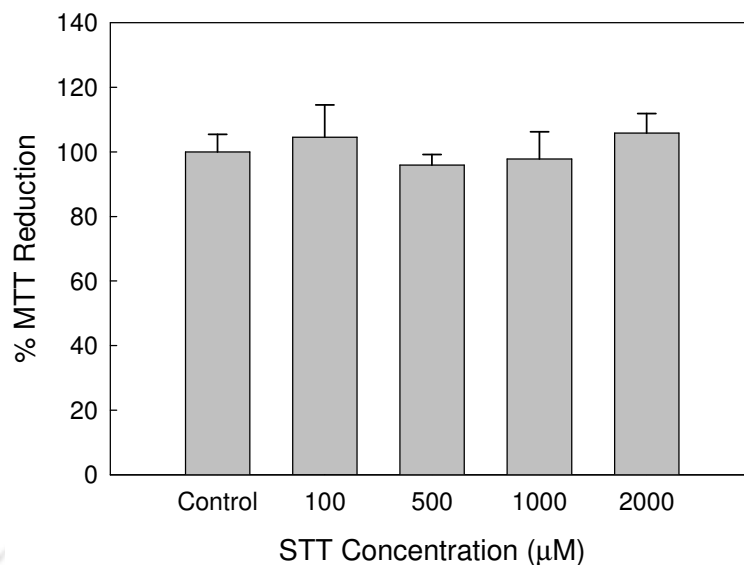


Figure 4.4 MTT assay of different concentrations of STT on PC12 cell line. Each readings were taken in triplicates and appropriate blanks were subtracted.

4.4.2 Monitoring changes in surface hydrophobicity of HEWL

Exposure of hydrophobic surface in proteins has been found to be a key driving force towards aggregation and subsequent fibrillation process (Bolognesi *et al.*, 2010). To study the role of exposed hydrophobic surface in HEWL amyloidogenesis at pH 2.0, ANS binding assay was performed with time in absence and presence of different concentrations of STT (Figure 4.5). In control HEWL, ANS binding intensity increased upto 50 h after which it showed slight decrease confirming prefibrillar aggregates exhibit more exposed hydrophobic surface than matured fibrils (Bolognesi *et al.*, 2010). Interestingly, there seem to be no correlation between the fibril inhibition potential of STT and the ANS binding data. The ANS binding kinetics of control HEWL and in presence of 1 mM STT were found to be similar despite of complete inhibition of fibril formation of HEWL at these STT concentrations. Also, the ANS binding profiles of HEWL in presence of 100 μM and 500 μM STT were similar inspite of significant difference in ThT as well as AFM data. This result clearly suggests the involvement of some other factor apart from exposed hydrophobic surface in proteins in triggering fibril formation.

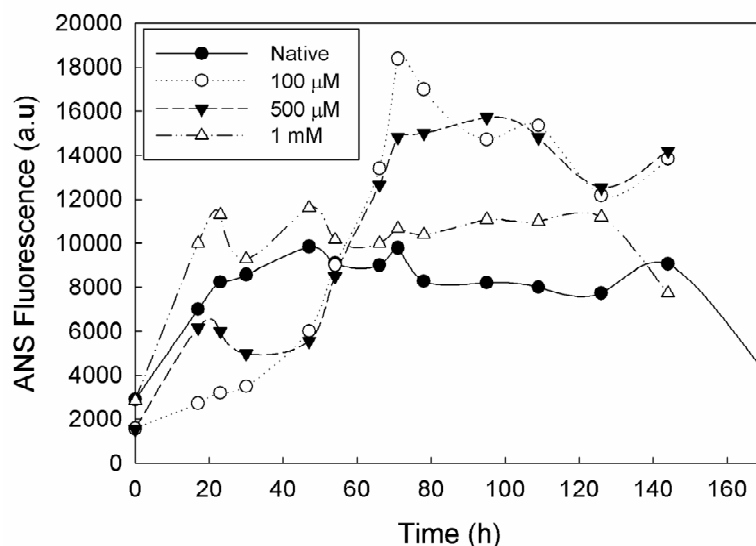


Figure 4.5 ANS binding assay of HEWL incubated at pH 2.0 under amyloidogenic conditions in absence (control) and presence of different concentrations of STT. The data represent average of three sets of readings

4.4.3 Exploring role of disulfide bonds in amyloidogenesis

To confirm the role of disulfide bond in initiating fibril formation, reducing agent like β -mercaptoethanol was added to HEWL incubated at pH 2.0 under amyloid forming conditions (Figure 4.6). Co-incubation of HEWL with β -mercaptoethanol completely inhibited fibril formation suggesting the role of disulfide bond during the early stages of aggregation process in initiating fibrillation process.

To access if the amyloid inhibition is result of HEWL sulfonation, mass spectrometry analysis was performed which did not show any change in mass (Figure 4.7). Thus, possibility of sulfonation by STT was ruled out. Further, to assess the changes conferred on HEWL by STT, HEWL was treated with STT at pH 2.0 for 2 h and subsequently STT was removed by dialysis. Amyloid formation was monitored with the STT treated and dialysed HEWL through ThT assay (Figure 4.8), which showed complete inhibition of amyloid formation suggesting that STT is irreversibly altering HEWL, making it resistant to amyloid formation.

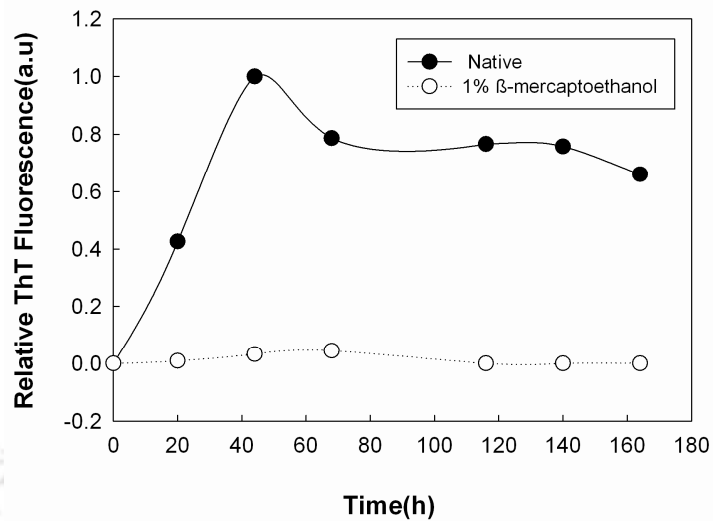


Figure 4.6 ThT assay of HEWL incubated at pH 2.0 under amyloidogenic conditions in absence and presence of 1% (v/v) β -mercaptoethanol. The readings are averaged over three sets of data and appropriate blanks are subtracted in each case.

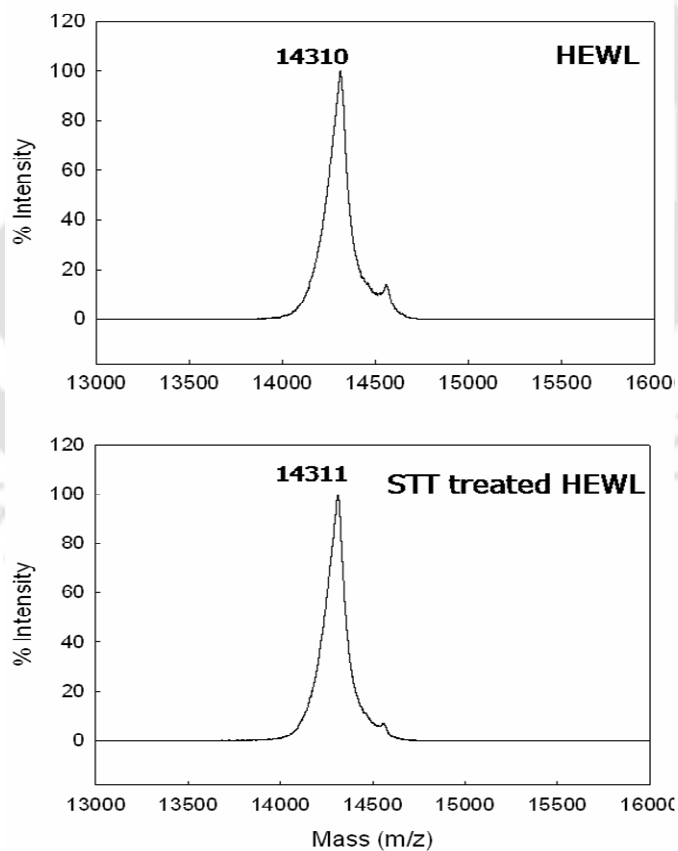


Figure 4.7 MALDI TOF spectra of STT treated and untreated HEWL showing no shift in peak at 14310 m/z corresponding to HEWL.

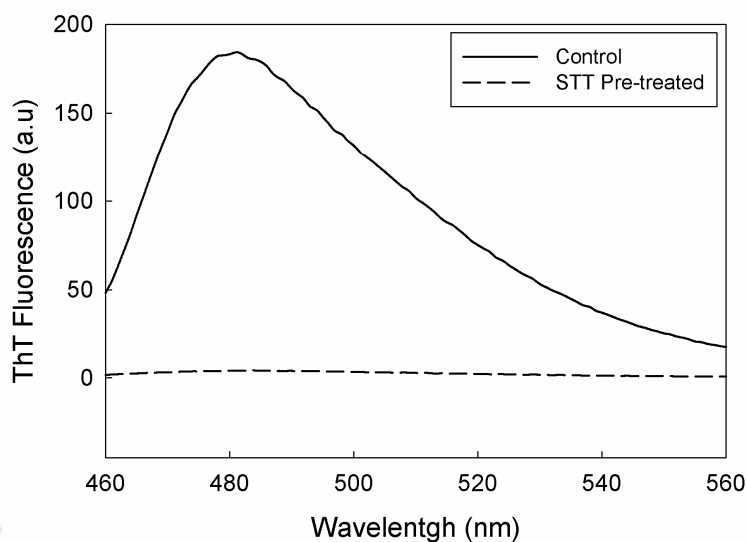


Figure 4.8 ThT fluorescence spectra of untreated HEWL (control) and STT treated and dialysed HEWL, incubated under amyloidogenic conditions for a period of 140 h.

4.4.4 Monitoring effect of STT on stability and unfolding kinetics of HEWL

The effect of STT towards the energetics of the intermediate and transition states of HEWL at pH 2.0 was detected through equilibrium unfolding and unfolding kinetic studies. As seen from the equilibrium unfolding data (Figure 4.9A), presence of 500 μM STT significantly destabilized the HEWL conformation populating at pH 2.0. Additionally, HEWL seems to unfold in non-cooperative manner which is indication of folding intermediate (Nallamsetty *et al.*, 2007). However, unfolding curve in presence of 500 μM STT seems to be cooperative. Further, the unfolding kinetics data as a function of GuHCl concentrations shows no change in presence of 500 μM STT (Figure 4.9B). This suggests that STT has destabilizing effect on both intermediate as well as transition states of HEWL at pH 2.0 to similar extent keeping energy barrier of unfolding unchanged.

4.4.5 Monitoring conformational changes in HEWL on STT addition

The change in the tertiary structure of HEWL induced by addition of STT and β -mercaptoethanol under amyloidogenic conditions were monitored through intrinsic fluorescence. On addition of 500 μM STT after 6 h, there is a red shift in maximal emission wavelength (λ_{max}) from 339 to 349 nm, indicative of exposure of tryptophan residues to a more polar environment (Figure 4.10).

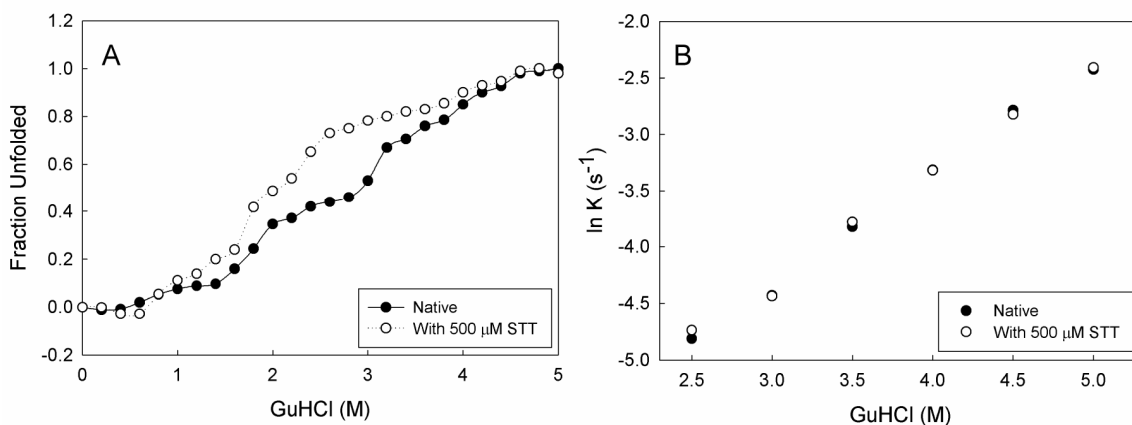


Figure 4.9 Equilibrium unfolding curve (A) and unfolding kinetics (B) of HEWL at pH 2.0 in absence (control) and presence of 500 μM STT as a function of GuHCl concentration. The readings are averaged over three sets of data and appropriate blanks are subtracted in each case.

Similar effect was seen with 1% (v/v) β -mercaptoethanol, but in the control sample no such shift was found. Interestingly, in presence of STT the intrinsic fluorescence intensity reduced significantly within 6 h of incubation whereas in presence of β -mercaptoethanol, intensity was slightly higher than that of the control sample. This suggests that though STT and β -mercaptoethanol is altering the conformation of HEWL to a more solvent exposed hydrophobic core conformation, the conformation induced by STT is different from that of β -mercaptoethanol (STT was found to have no quenching effect in HEWL). On further incubation, there was found to be no significant change in the intrinsic fluorescence of HEWL.

Change in the exposed hydrophobic surface of HEWL on addition of β -mercaptoethanol under amyloidogenic condition was also monitored through ANS fluorescence (Figure 4.11). Initially, after 6 h of incubation ANS fluorescence of HEWL in presence of 1% (v/v) β -mercaptoethanol was significantly higher than the control sample indicating presence of a conformation with highly exposed hydrophobic surface. However, the intensity decreased gradually with time after a period of about 31 h. In case of the control, initially ANS was much lower compared to HEWL in presence β -mercaptoethanol. However, it started shooting up gradually with time and finally was significantly higher than the β -mercaptoethanol reduced sample.

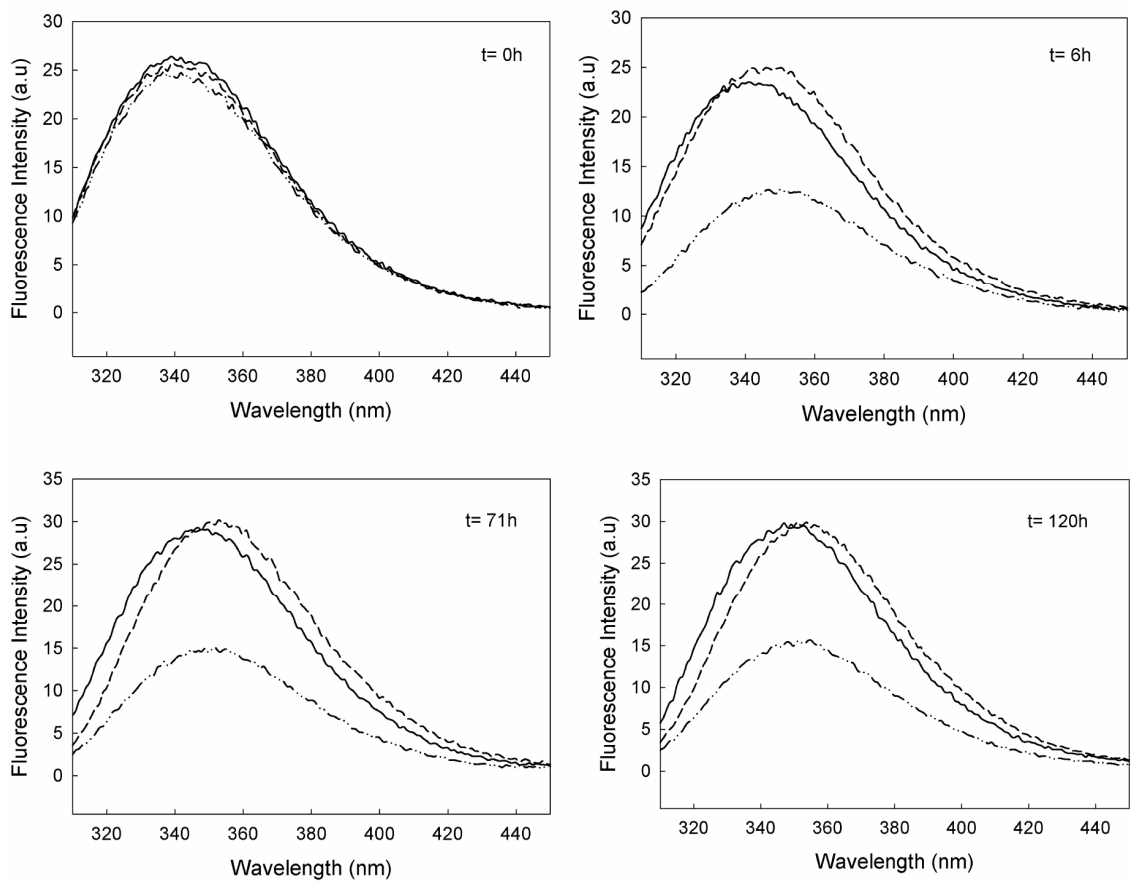


Figure 4.10 Intrinsic fluorescence spectra of HEWL incubated in absence (continuous line) and presence of 500 μM STT (double dotted line) and 1% (v/v) β -mercaptoethanol (broken line), under amyloidogenic conditions. The time of incubation is denoted by t.

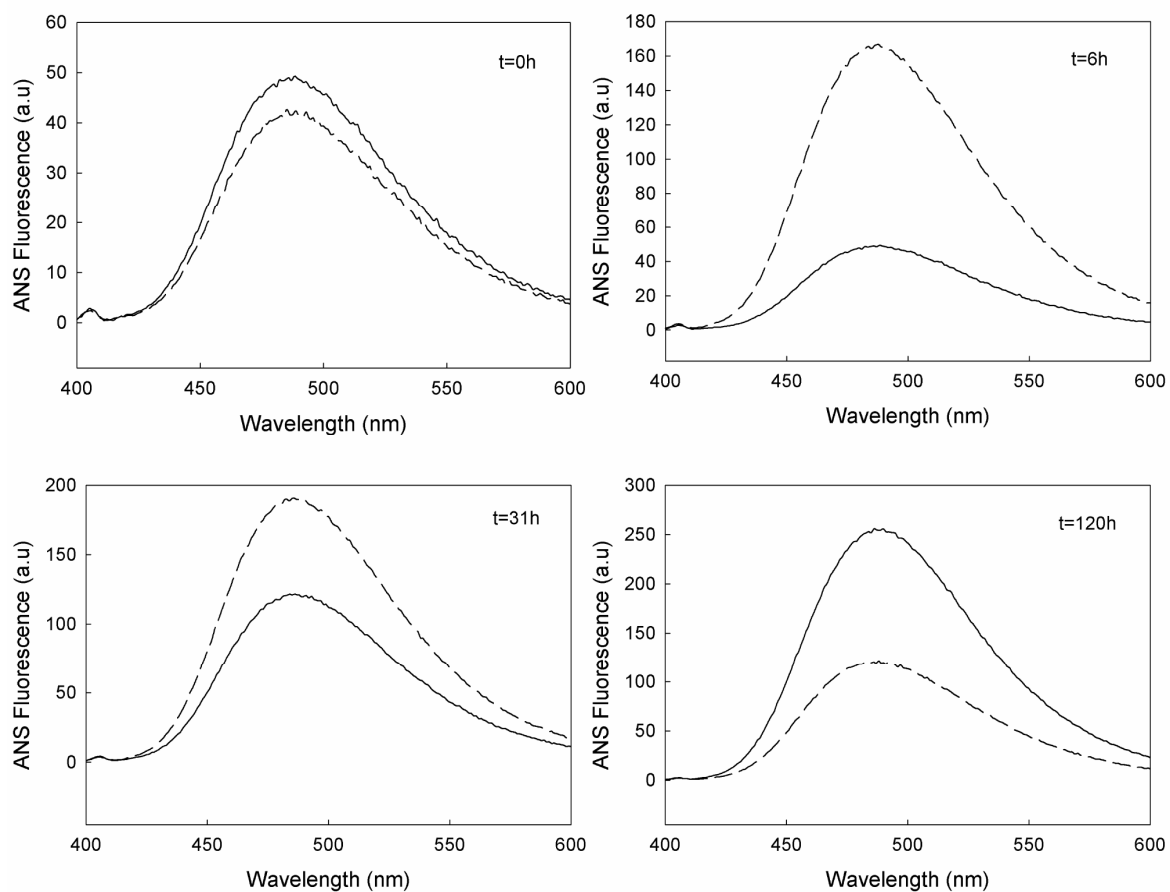


Figure 4.11 ANS fluorescence spectra of HEWL incubated in absence (continuous line) and presence of 1% (v/v) β-mercaptoethanol (broken line) under amyloidogenic conditions. The time of incubation is denoted by t.

4.5 Discussions

Several disulfide bonded globular proteins have been found to form amyloid under particular conditions (Yamamoto *et al.*, 2008; Wang *et al.*, 2009^b). Yamamoto *et al.*, have shown inhibitory effects of reducing agents like DTT and cysteine towards amyloidogenesis of β_2 -microglobulin which is responsible for dialysis-related amyloidosis in humans (Yamamoto *et al.*, 2008). Wang *et al.*, have studied the inhibitory effect of tris(2-carboxyethyl)phosphine (TCEP), a reducing agent towards amyloidogenesis of HEWL at pH 2.0 through disulfide bond disruption promoting unfolding of HEWL (Wang *et al.*, 2009^b). Further, Kumar *et al.*, have shown the role of 1,4-Dithioerythritol (DTT) in retarding HEWL aggregation at pH 12.2 by disrupting disulfide bonds which were found to stabilize mature fibrils (Kumar *et al.*, 2008). All the studies essentially indicate the role of disulfide bonds in stabilising fibrils. However, in most cases inhibition of fibril formation is accompanied by reduced ANS binding indicating that the compounds are promoting protein unfolding by disrupting disulfide bonds. This reduces exposed hydrophobic surface in protein which is known to initiate aggregation process.

Interestingly, in this study inhibition of HEWL amyloidogenesis by STT is not accompanied by reduced ANS binding as seen from Figure 4.5. STT was found to completely inhibit HEWL fibrillation at a concentration of 500 μM as seen from ThT and AFM data. However, the ANS binding kinetics of HEWL incubated with STT and control HEWL (without STT) were found to be similar. This observation necessarily indicates the role of another factor apart from exposed hydrophobic surface in HEWL in initiating fibrillation process. Also, 20 mM STT was able to disaggregate 70% of the prefibrillar species of HEWL. Initially, addition of 20mM STT to 20h old HEWL prefibrils seem to arrest further fibril growth as compared to the control fibril. Later, it seemed to disaggregate already formed fibrillar species as evident from the ThT data (Figure 4.2). This delayed disaggregation property may be due to slow diffusion of STT towards the inner core of fibrillar assembly.

To verify the role of disulfide bond in fibrillation process, reducing agent β -mercaptoethanol was added to HEWL incubated at pH 2.0 at a concentration of 1% (v/v). No fibril formation was seen by ThT assay (Figure 4.6) which confirms essential

role of disulfide bonds in determining amyloid formation. Sodium tetrathionate is reported to sulfonate free sulfhydryl group present in protein forming a sulfonated intermediate (Hermanson, 2008). If any other free sulfhydryls are present in the vicinity, this sulfonated intermediate facilitates formation of disulfide bond with the free sulfhydryl group with the release of thiosulfate group (Hermanson, 2008). Sodium tetrathionate (STT) does not seem to sulfonate HEWL at pH 2.0 as observed from the mass spectrometry data. Additionally, when STT was removed by dialysis, HEWL does not show amyloidogenesis. This suggests some irreversible modification in protein by STT other than sulfonation which does not change molecular mass. One such possibility is alteration in disulfide pattern. We believe, sodium tetrathionate (STT) facilitates mixing of intramolecular disulfide bonds in HEWL resulting in wrong disulfide bond formation, making it resistant to fibril formation. Possibility of intermolecular disulfide mixing is ruled out as there was no mass difference found in mass spectrometry data. Thus, formation of correct disulfide bond is essential in inducing amyloidogenesis. Once intramolecular mixing of disulfides is done, the protein amyloid is not formed even when STT is removed by dialysis. Addition of reagents such as DTT, or β -mercaptoethanol provides high reducing environment and reduces disulfide bonds and thereby prevents fibril growth. In brief, amyloidogenic protein with all disulfide bonds reduced or wrongly formed disulfide bond appears to be resistant to amyloid formation. The current study points out towards vital role of correct disulfide bond in amyloidogenic protein in progression of amyloid formation.

Effect of STT on the stability and unfolding kinetics of HEWL at pH 2.0 were studied. As seen from the equilibrium unfolding data, STT seem to significantly destabilize HEWL at pH 2.0. However, the unfolding kinetics data shows no effect of STT on the unfolding rate constants at different denaturant concentrations suggesting no change in energy difference between transition states of unfolding of protein at pH 2.0. Thus, STT appear to destabilize both the intermediate as well as the transition states of HEWL at this pH to similar extent to keep energy difference between protein at pH 2.0 and unfolded state unchanged. This indicates role of correct disulfide bond in stabilizing both the intermediate and transition states of the protein populating at pH 2.0 during the unfolding process. The intrinsic fluorescence spectra of HEWL in absence and presence of STT and β -mercaptoethanol under amyloidogenic conditions reveal about the changes

in the tertiary structure of HEWL induced by the compounds. After 6h of incubation, both STT and β -mercaptoethanol alter the conformation of HEWL to a more solvent exposed hydrophobic core conformation as seen by the red shift in λ_{\max} . However, in case of STT the fluorescence intensity is significantly reduced as compared to β -mercaptoethanol suggesting that the two conformations are different.

On further incubation there seem to be no significant change in λ_{\max} and fluorescence intensity of HEWL in presence of STT as well as β -mercaptoethanol. Exposure of hydrophobic surface in HEWL on addition of 1% β -mercaptoethanol was studied through ANS fluorescence (Figure 4.11). The study shows that β -mercaptoethanol induces structural alteration in HEWL further exposing its hydrophobic surface. However, it does not seem to promote complete protein unfolding as evident from the high ANS fluorescence. The control sample (in absence of β -mercaptoethanol) exhibited a different pattern of ANS binding kinetics. Initially, the control ANS was much lower than that of the β -mercaptoethanol reduced HEWL. However, it later started increasing with time indicating fibril formation.

4.6 Conclusions

In the present study we have shown the inhibitory effect of STT towards HEWL amyloidogenesis at pH 2.0 at a concentration of 500 μ M. 20 mM STT also showed considerable disaggregation effect on already formed HEWL fibrils. STT seem to facilitate formation of intramolecular disulfide bond mixing in HEWL at pH 2.0, rendering it resistant to fibril formation. Further, the ANS binding assay reveals that formation of proper disulfide bond is critical in inducing HEWL fibrillation rather than exposed hydrophobic surface. The crucial role of disulfide bonds in initiating of amyloidogenesis is further confirmed through the fibril inhibitory effect of reducing agent like β -mercaptoethanol. Equilibrium unfolding curve shows considerable destabilizing effect of STT on HEWL conformation at pH 2.0 as well as transition of unfolding path of HEWL from non-cooperative to relatively cooperative. These studies give insight into a new mechanism of fibrillation process which may be considered in development of potential therapeutics against amyloidosis.

Effect of curcumin on amyloidogenic property to molten globule like intermediate state of 2,5 Diketo Gluconate Reductase *.

5.1 Abstract

Structure-function of 2,5-diketo-D-gluconate reductase A (DKGR) was investigated by equilibrium unfolding. Additionally, amyloidogenic property of the protein was also investigated. We have identified a molten globule like intermediate of DKGR enzyme at pH 2.5 which is prominently β -sheet structure. The molten globule state of the protein shows amyloidogenic property above 50 μ M protein concentration. Interestingly, 1:1 molar ratio of curcumin prevents amyloid formation as shown by Thioflavin-T assay and atomic force microscopy (AFM). To best of our knowledge, this is first report about amyloid formation by $(\alpha/\beta)_8$ -barrel protein. Results presented here indicate that molten globule state has important role in amyloid formation and potential application of curcumin in protein biotechnology as well as therapeutics against amyloid diseases.

* Part of the work has been published in *Biol Chem.* **2009**, 390, 1057-1061.

5.2 Introduction

Turmeric (*Curcuma longa*) is used in Indian traditional medicine for treatment of several diseases. Curcumin is the principal curcuminoid of Turmeric. In the last few decades, there has been considerable interest in the biological activities of curcumin. Many studies report significant anti-inflammatory, antioxidant, anticancer, and immunomodulatory properties of curcumin *in vitro* and in animal models and humans. Worldwide, there are over 1000 published animal and human studies, both *in vivo* and *in vitro* in which the effects of curcumin on various diseases have been examined (Mishra and Palanivelu, 2008).

Amyloid plaques are characteristic of several diseases like Alzheimer disease (AD), spongiform encephalopathies, such as kuru and Creutzfeldt-Jacob disease. The deposits in these conditions contain A β -peptides, prion protein, and transthyretin (TTR), respectively. Joining this list is such other diseases also (Kelly, 1996; Horwich, 2002). Therefore, many therapeutic efforts are targeted at reducing progression of amyloid production (Yang *et al.*, 200). The mechanism by which the protein amyloid results in cell damage is still a matter of debate. However, recent reports indicate common mode of toxicity which is not related to protein sequence as non-disease-associated proteins can also be equally toxic to cell. Thus, it is suggested that the toxicity of aggregated species could be general phenomenon of aggregated species primarily related to the structural nature of the aggregates rather than to the specific sequences of the proteins from which they arise (Bucciantini *et al.*, 2002). On the other hand, all amyloid appears to have very similar structure which is stabilized by backbone interactions (Horwich, 2002). Thus, considering common mode of toxicity and similar structure of amyloids, can we have a common therapeutics for all amyloid diseases?

A recent study by Yang *et al.*, shows the levels of β -amyloid in AD mice that were given low doses of curcumin were decreased by around 40% in comparison to those that were not treated with curcumin (Yang *et al.*, 2005). However, it is not clear if the effect is specific to Alzheimer's β peptide or generalized to all proteins. Moreover, it was also not clear if curcumin inhibits β -amyloid formation by inhibiting amyloid progression or by inhibiting secretase activity (secretase cleavage of Alzheimer precursor protein and generates Alzheimer's β -peptide, which is mostly prone to aggregation). Additionally, there are also circumstantial evidences that curcumin improves mental functions (Ng *et al.*, 2006).

The molecular mechanism of amyloid formation and the role of intermediate states during this transition remain elusive. In the current work, we have used DKGR as a model system for the study. This enzyme belongs to $(\alpha/\beta)_8$ barrel class of protein and utilizes NADPH as its cofactor. So far, no unfolding and stability studies have been done on this commercially important protein which catalyzes the stereospecific reduction of 2,5 diketo-D-gluconate to 2 keto-L-gulonate, which is a tautomeric isomer of ascorbic acid (vitamin C). Our results shed some light on the folding pathway of DKGR in specific and $(\alpha/\beta)_8$ barrel proteins in general.

We have identified an amyloidogenic molten globule like state of DKGR and shown that molten globule like intermediate states in proteins play a vital role in amyloidogenesis. Further, we have shown that curcumin acts like chaperone and inhibits the amyloid formation by directly interacting with the amyloidogenic intermediate state and thereby preventing aggregation.

5.3 Materials and methods

5.3.1 Materials

2,5-DKGR A in the pET-21a(+) expression vector was generously provided by Prof. Michael Blaber. ANS, GuHCl, Thioflavin T (ThT) and acrylamide were purchased from Sigma Chemicals. Concentrations of GuHCl were determined from the refractive index of the solution (Pace, 1990). All other reagents that were used were of analytical grade.

5.3.2 Expression of DKGR

2,5 Diketo Gluconate Reductase (DKGR) A gene cloned in pET-21a (+) expression vector was transformed in *E coli* strain BL 21(DE3). The transformed BL 21 cells were grown in M9 Minimal Media containing ampicillin marker (50 $\mu\text{g}/\text{ml}$ conc.) at 37°C temp., till the O.D of the culture reached 0.3, when it was transferred to 20°C temperature. When the O.D of the culture reached 0.5, it was induced with 1mM IPTG and grown overnight until the O.D was around 1.2. The cells were then harvested by centrifugation at 6000 rpm for 20 mins at 4°C temp and the pellet was dissolved in 20mM Tris 5mM EDTA buffer pH 8.0 (40 ml was added to 2 litre culture pellet and to this 100 μl sigma cocktail protease inhibitor was added). The cells were lysed by sonication. The lysed cells were centrifuged at 10,000 rpm for 30 mins at 4°C temp and the supernatant obtained was stored at 4°C temp for purification.

5.3.3 Purification of DKGR

The purification method for DKGR was already reported by Miller *et al* (Miller et al., 1987). However, we could not follow the reported purification protocol due to unavailability of the affinity matrix Amicon Red and thus, we developed a novel method of DKGR purification. The enzyme was purified following a novel purification protocol of ion exchange chromatography (DEAE Sepharose) followed by gel filtration chromatography (Sephadex G 75).

5.3.3.1 Anion Exchange Chromatography: The cell lysate obtained after sonication was loaded in a 20 ml DEAE Sepharose matrix pre-equilibrated with 20mM Tris buffer pH 8.0 in a FPLC setup. After loading, the column was washed with 60 ml of 20mM Tris buffer pH 8.0 to remove the unbound proteins. Elution was performed by NaCl gradient from 0 M to 0.7 M NaCl in 20mM Tris buffer pH 8.0 with total elution volume of 800 ml, collecting 10 ml fractions. The purity of the peak fractions were checked by 12% SDS PAGE gel. Fractions 30, 31, 32 (eluted at around 0.25 M – 0.3 M NaCl) were found to contain DKGR in partial purified state. These fractions were then pooled and dialysed extensively against 20 mM Tris buffer (pH 8.0), to remove the salt present in the sample.

5.3.3.2 Gel Filtration Chromatography: The dialysed sample was loaded in a 100 ml Sephadex G75 column pre-equilibrated with 250 ml of 50 mM sodium phosphate buffer pH 7.0 containing 0.25 M NaCl (small amount of NaCl was added to prevent intermolecular interaction between the monomeric protein molecules leading to aggregation). Elution was done with three column volume of equilibration buffer, collecting 5 ml fractions each. The homogeneity of the peak fractions were checked by 12% SDS PAGE gel. The fractions 10 and 11 have been found to contain completely pure DKGR. These fractions were then pooled and dialyzed extensively against 50 mM phosphate buffer pH 7.0 to remove the traces of NaCl. Activity assay of dialysed fractions was done as per the method of Sonoyama and Kobayashi (1987) to confirm presence of DKGR (Sonoyama and Kobayashi, 1987).

5.3.4 GuHCl unfolding

Protein sample was incubated at a desired GuHCl concentration for approximately 24 h at 25°C to attain equilibrium. Final concentration of the protein and denaturant, in each sample, were determined by spectrophotometry and refractive index measurements, respectively.

5.3.5 pH denaturation

Acid denaturation of the enzyme was carried out as a function of pH using KCl-HCl (pH 0.5-1.5), Gly-HCl (pH 2.0-3.5), sodium acetate (pH 4.0-5.5), sodium phosphate (pH 6.0-8.0), Tris-HCl (pH 8.5-10.5), and Gly-NaOH (pH 11.0-12.5). Concentrations of all buffers were 50 mM. A stock solution of the protein was added to the appropriate buffer and the mixture was incubated for 24 h at 25 °C. The final pH and concentration of the protein in each sample were measured again.

5.3.6 Fluorescence spectroscopy

5.3.6.1 Intrinsic fluorescence: Intrinsic fluorescence measurements were taken using Jobin Yvon Fluoromax-3 Spectrofluorimeter. Protein was excited at 295nm and emission was recorded between 300 and 400 nm with 5nm slit widths for both excitation and emission. The protein concentration was 5 µM for all fluorescence measurements.

5.3.6.2 ANS fluorescence: Exposure of hydrophobic surfaces in the enzyme was measured by its ability to bind to the fluorescent dye ANS (Semisotnov *et al.*, 1991; Khurana and Udgaonkar, 1994). Protein was incubated with a 100-fold molar excess of ANS for more than 30 min at room temperature in dark and ANS fluorescence was measured using Jobin Yvon Fluoromax-3 Spectrofluorimeter. The excitation wavelength was 380 nm and emission spectra were collected between 400 and 600 nm. Slit widths for both excitation and emission were 5 nm.

5.3.7 Acrylamide quenching

DKGR was incubated at different pH conditions with varying concentrations of acrylamide at room temperature for 2 h. Intrinsic fluorescence of the incubated samples were taken using Jobin Yvon Fluoromax-3 Spectrofluorimeter with emission scan from

310 to 400 nm and excitation at 295 nm wavelength. Slit widths were kept at 5 nm for both excitation and emission and protein concentration was kept at 5 μM .

5.3.8 Spectropolarimetry

CD measurements were done on a Jasco J715 or Jasco J500 spectropolarimeter equipped with a constant temperature cell holder. Conformational changes in the secondary structure of the protein were monitored in the region between 200 and 250 nm with a protein concentration of 5 μM in a cuvette of 1mm path length while changes in the tertiary structure were observed in a cuvette with a path length of 10 mm in the region between 260 and 320 nm at a protein concentration of 10 μM . After subtracting appropriate blanks, mean residue ellipticities were calculated, using the formula,

$$[\theta] = \theta_{\text{obs}} \times 100/cl,$$

where, θ_{obs} is the observed ellipticity in degrees, c is the concentration of protein (Moles) and l is the path length in centimeters (Balasubramanian and Kumar, 1976).

5.3.9 Thioflavin T assay

DKGR was incubated at a concentration 30-150 μM in 10 mM Gly-HCl buffer at pH 2.5 and allowed to stand at 37°C without agitation. For studying effect of curcumin on amyloid formation, 150 μM of curcumin was added in at maximum protein concentration, (150 μM) sample. Aliquots were periodically drawn for analysis. Stock solution of 2.5 mM ThT was prepared in 10 mM potassium phosphate buffer, pH 6.5. Samples for fluorimetry were prepared by the addition of 20 μl of ThT stock solution to appropriate volume of incubated protein sample to make final protein concentration and volume 15 μM and 1000 μl respectively in 10 mM phosphate buffer. Samples prepared in this way were incubated for 30 min at room temperature followed by an emission scan from 470–560 nm with an excitation wavelength of 450 nm, using Jobin Yvon Fluoromax-3 Spectrofluorimeter. Appropriate blank samples were subtracted in each case. ThT binding relative to maximum value in all cases are calculated and plotted.

5.3.10 Atomic Force Microscopy (AFM)

Prior to experiment, protein at 60 μM concentration was incubated for 50 h at pH 7.0, pH 2.5 and pH 2.5 with curcumin in 1:1 molar ration. AFM was performed using an ambient air scanning probe microscope operating in non-contact mode, using Picoplus

microscope (Molecular Imaging, USA). For data collection, 10 μ l of the sample was deposited on a freshly prepared thin layer of mica film and dried under nitrogen for 2 h. The sample at pH 7.0 was added with 2 μ l of 1 mM magnesium chloride at mica layer for effective adsorption.

5.4 Results

5.4.1 Characterisation of the folding pathway of DKGR

Lot of research is currently focused on the properties of the partially unfolded states of proteins, particularly which can be populated in the mild denaturing conditions as these intermediates may be starting point for protein folding process or amyloid/aggregate formation. Our current investigation clearly indicates existence of an amyloidogenic intermediate state of DKGR at pH 2.5 and the role of curcumin as inhibitor of amyloid formation. DKGR was successfully purified following a novel two step purification method of anion exchange chromatography followed by gel filtration chromatography. Purification was confirmed by 12% SDS PAGE which clearly indicated DKGR purified to homogeneity. Activity assay of the purified fractions further confirmed the presence of DKGR.

The GuHCl induced equilibrium unfolding curve of DKGR at pH 7.0 is shown in Figure 5.5. The equilibrium unfolding curve clearly shows a biphasic nature indicating the presence of intermediate state in the unfolding pathway. The intrinsic fluorescence spectrum of DKGR at neutral pH has an emission maximum (λ_{max}) at 338 nm indicating burial of tryptophan (Figure 5.6).

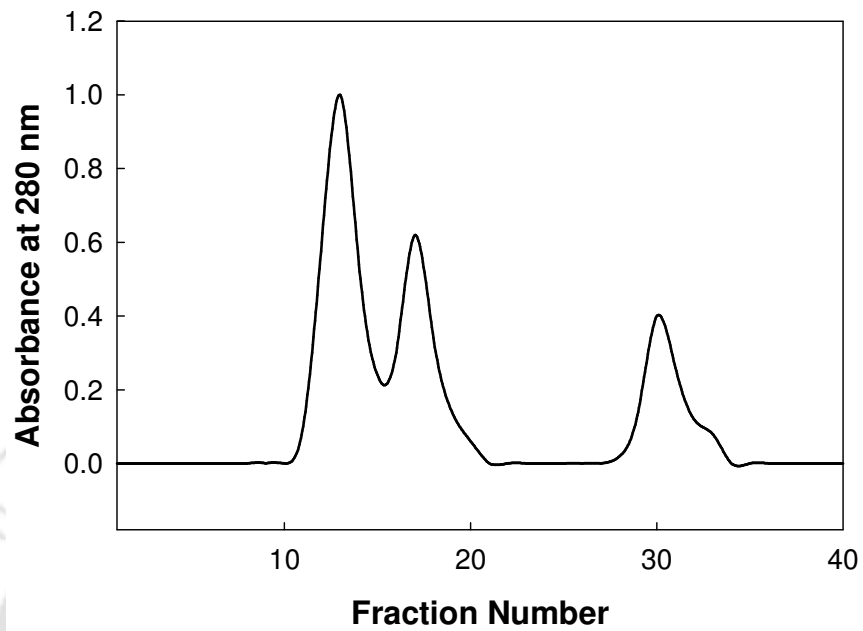


Figure 5.1 Elution profile of the cell lysate in anion exchange (DEAE Sepharose) chromatography across NaCl gradient from 0 M to 0.7 M in total 800 ml elution volume and 10 ml fraction size. Fractions 30, 31, 32 were found to contain partially purified DKGR.

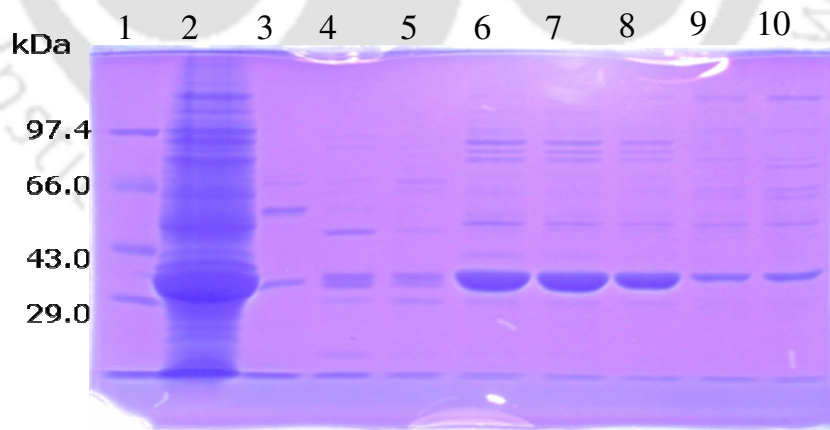


Figure 5.2 SDS PAGE of the peak fractions obtained from anion exchange chromatography with 12% gel. The lanes marked from 1 to 10 contain protein marker, cell lysate, fractions- 13, 16, 17, 30, 31, 32, 35, 37 respectively.

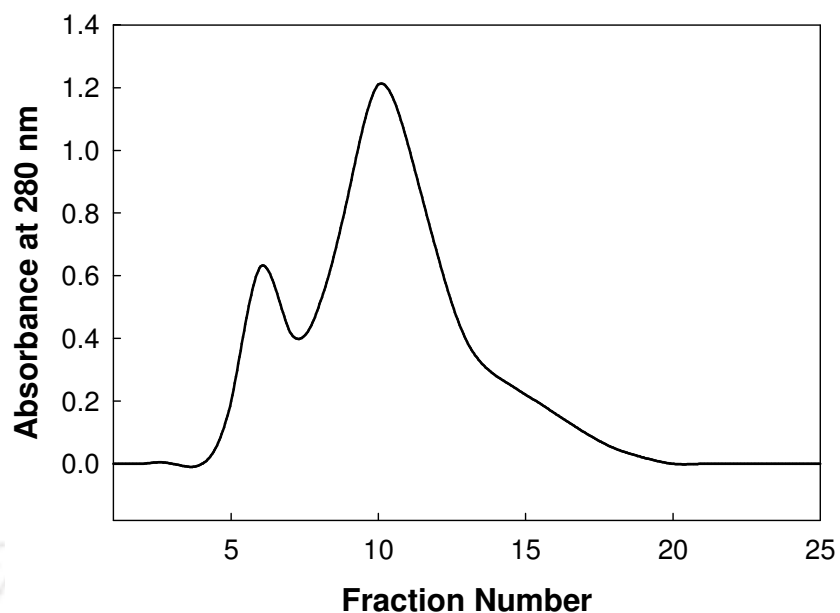


Figure 5.3 Elution profile of the pooled fractions in gel filtration chromatography using Sephadex G-75 matrix. Fractions 10 and 11 have been found to contain completely pure DKGR.

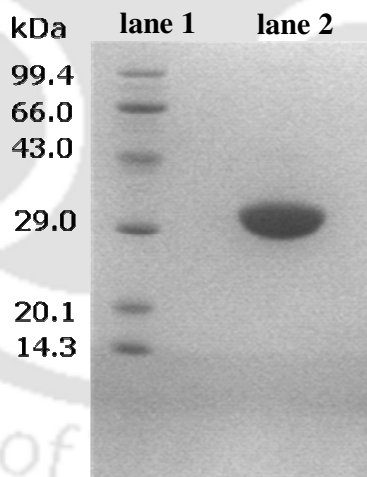


Figure 5.4 SDS PAGE of the peak fractions obtained in gel filtration chromatography with 12% gel. Lane 1 has protein marker and lane 2 has pooled fractions 10 and 11. These fractions were found to contain completely pure DKGR.

There is approximately 20% decrease in fluorescence intensity along with a red shift of 18nm in emission maximum (from 338 nm in native state to 356 nm in denatured state) upon complete unfolding of protein in presence of 1.5M GuHCl which remains

constant when GuHCl was further increased. Presence of intermediate state in the unfolding pathway can be observed in GuHCl range from 0.3 M to 0.6 M.

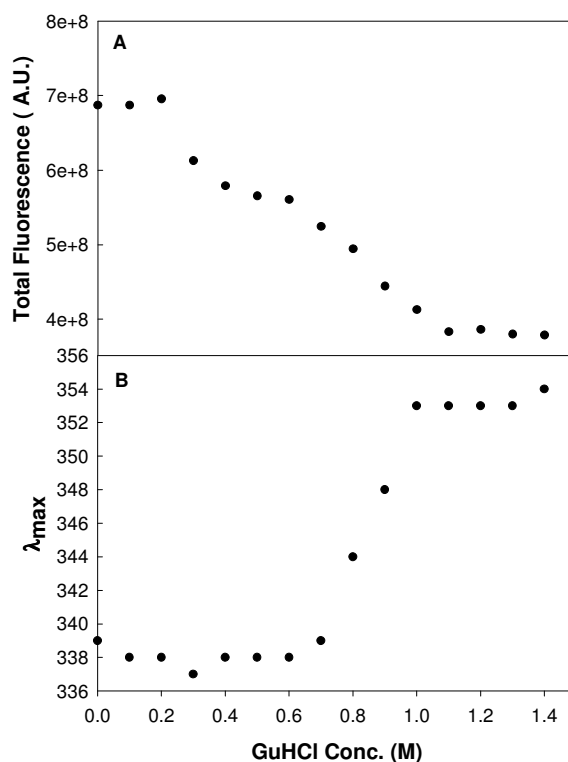


Figure 5.5 GuHCl induced equilibrium unfolding curve of DKGR showing changes in total fluorescence (A), and wavelength maxima, λ_{max} (B) with varying GuHCl concentration. Readings were taken in triplicates and appropriate blanks were subtracted in each case.

5.4.2 Characterisation of the intermediate state(s) populating the folding pathway

The pH induced conformational changes of DKGR by fluorescence are shown in Figure 5.7. The changes in fluorescence properties upon acid denaturation of DKGR follows multi step pattern. The first transition between pH 6.0-2.5 resulting in acid intermediate state 1 (AI₁) and second transition between pH 2.5-1.0 resulting in acid intermediate state 2 (AI₂). The ANS binding assay was performed to monitored exposure of hydrophobic surfaces. The fluorescence emission of ANS is known to increase when the dye binds to the hydrophobic regions of a protein (Stryere, 1965). Both of the intermediate states (AI₁ and AI₂) show high ANS binding but their intrinsic fluorescent properties are different (Figure 5.7A). This indicates that they are two distinct intermediate states. Moreover, they show distinct curves in acrylamide quenching data indicating two different solvent

exposed conformations (Figure 5.8). The pH induced transition of DKGR in alkaline range when monitored by fluorescence also seems to be cooperative. The transition occurred between pH 8.0 to pH 10.0 which corresponds to formation of alkaline denatured state. The secondary and tertiary structure of the protein at pH 2.5 were monitored by far-UV and near UV CD respectively and shown in Figure 5.9. The AI₁ state shows significant secondary structure as monitored by far UV-CD and characteristic of β -sheet. Additionally, AI₁ state shows a strong ANS fluorescence intensity (Figure 5.7C). All these characteristics are consistent with properties of molten-globule state (Dubey and Jagannadham, 2003).

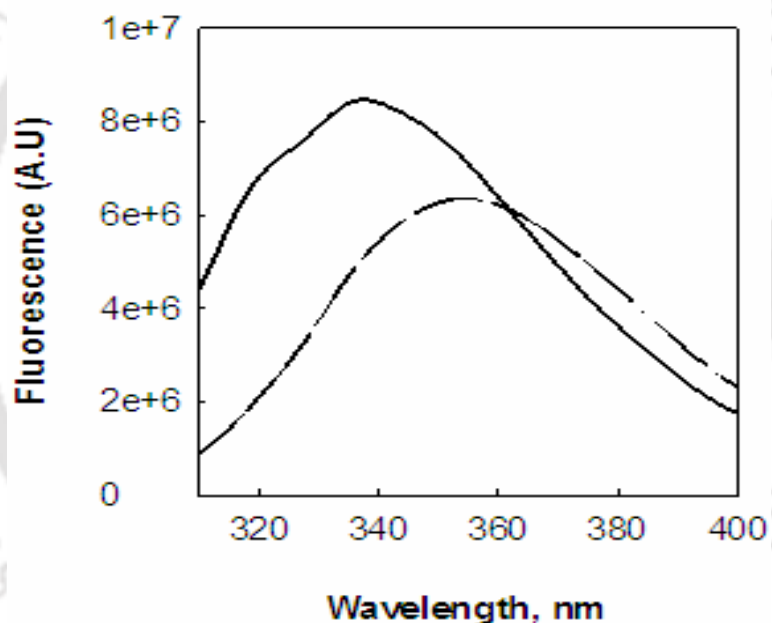


Figure 5.6 Intrinsic fluorescence spectra of native DKGR at pH 7.0 (continuous line) and completely denatured DKGR with 2.5 M GuHCl at pH 7.0 (broken line). Appropriate blanks were subtracted in each case.

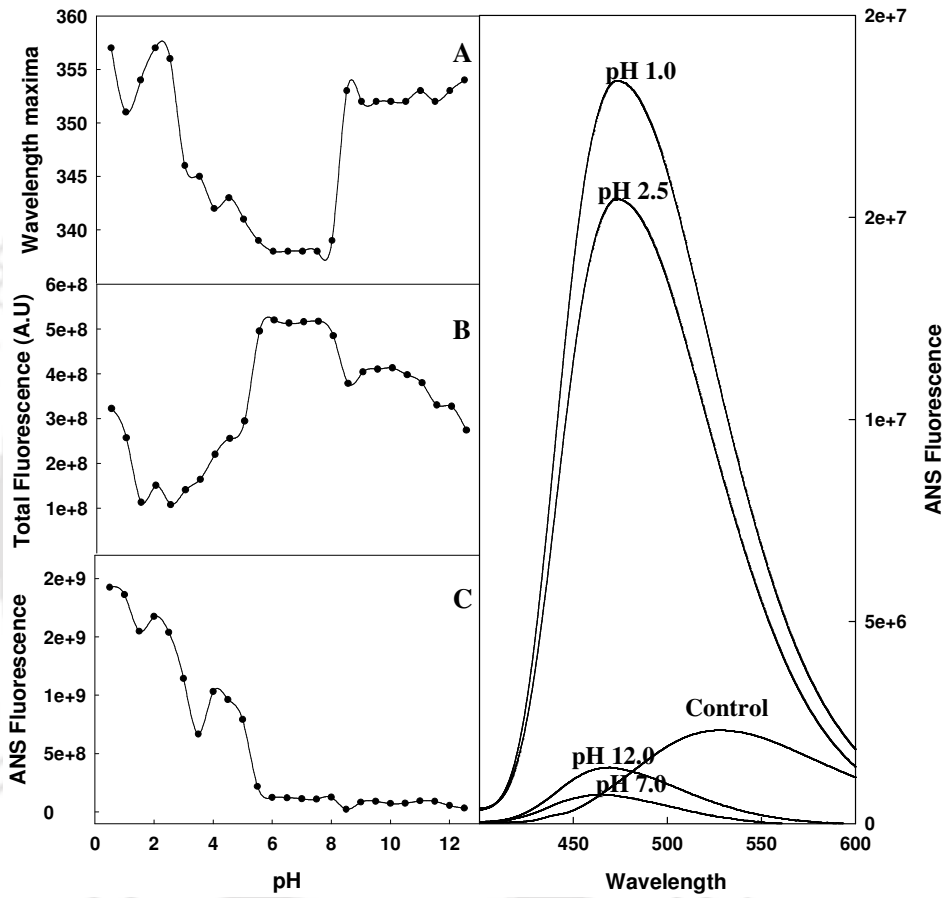


Figure 5.7 pH induced equilibrium unfolding of DKGR showing changes in (A) λ_{max} (B) total intrinsic fluorescence and (C) total ANS fluorescence with varying pH and (D) shows ANS fluorescence spectra at different pH.

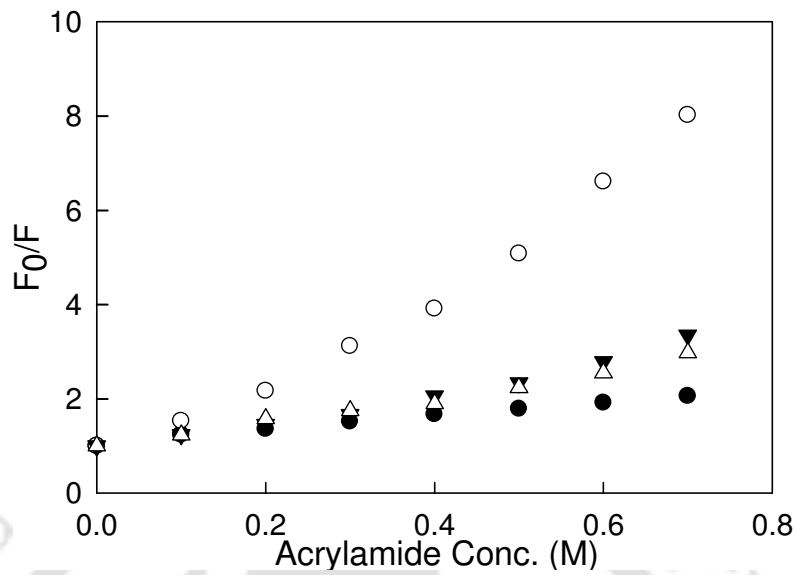


Figure 5.8 Plot of F_0/F of DKGR vs acrylamide concentration at (●) pH 7.0, (○) pH 7.0 with 2.5 M GuHCl, (▼) pH 2.5, and (△) pH 1.0. The readings were taken in triplicates and appropriate blanks were subtracted.

5.4.3 Monitoring amyloid progression of DKGR

ThT is reported to bind specifically to amyloids and show an increase in the fluorescence intensity at 482 nm when excited at 450nm (Eisert *et al.*, 2006). ThT binding of DKGR at pH 2.5 at various concentrations as a function of time is shown in Figure 5.10A and Figure 5.10B. Strong ThT binding was seen after 48 h when protein was incubated at pH 2.5 at concentrations 50 μ M and 150 μ M. Moreover, no ThT binding was seen at 30 μ M protein when incubated in the same pH condition. Interestingly, when 150 μ M of protein was incubated at pH 2.5 with curcumin in equal molar ratio, no significant ThT binding was seen.

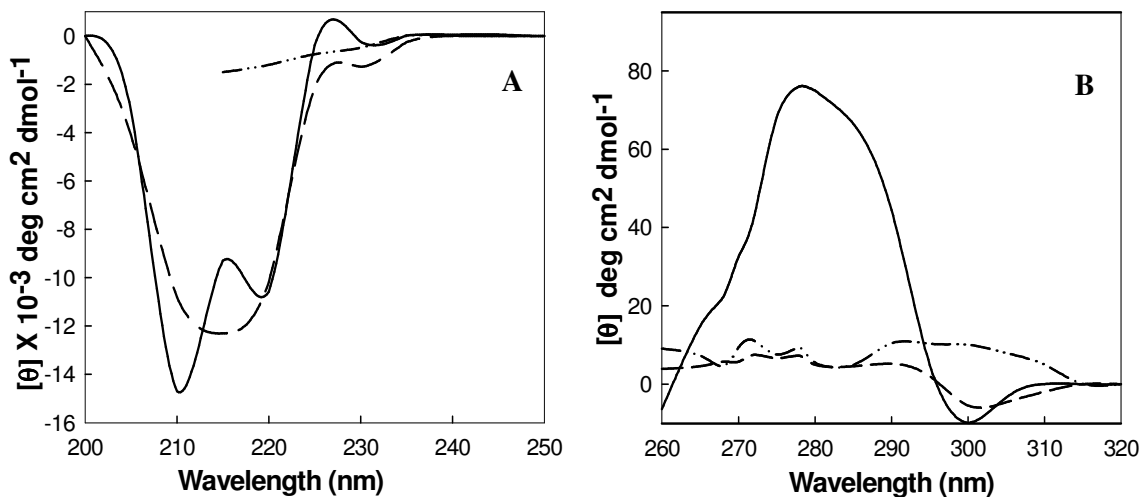


Figure 5.9 (A) Far UV and (B) Near UV CD spectra of DKGR at pH 7.0 (continuous line), pH 2.5 (broken line) and in presence of 6 M GuHCl (double dotted line). Blank spectra were subtracted in each case.

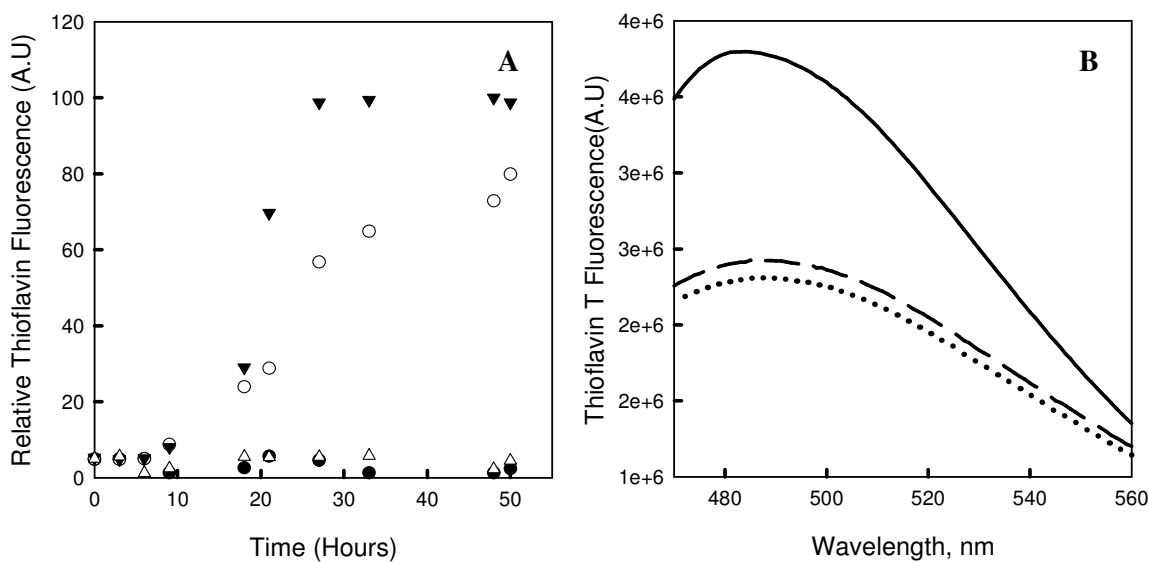


Figure 5.10 (A) Thioflavin-T binding assay of DKGR at concentrations of 30 μM (\bullet), 50 μM (\circ), 150 μM (\blacktriangledown) and 150 μM with 1:1 molar ratio of curcumin (\triangle) in 10 mM Gly-HCl buffer at pH 2.5. (B) Thioflavin-T fluorescence spectra of samples after 50 h of incubation. Continuous line, broken line and dotted line represents 150 μM protein, 150 μM protein with 1:1 molar ratio curcumin and 30 μM protein samples respectively.

Atomic Force Microscopy (AFM) images of DKGR at 60 μM concentration at pH 2.5 in presence or absence of equimolar curcumin after 50 h of incubation are shown in Figure 5.11. DKGR at 60 μM concentration at pH 7.0 after 50 h of incubation was used as control. The AFM image clearly shows amyloid formation at pH 2.5 at 60 μM concentration in absence of curcumin. Control sample and sample at pH 2.5 at 60 μM concentration with curcumin did not show any sign of amyloid formation. Thus, curcumin seems to prevent formation of amyloid.

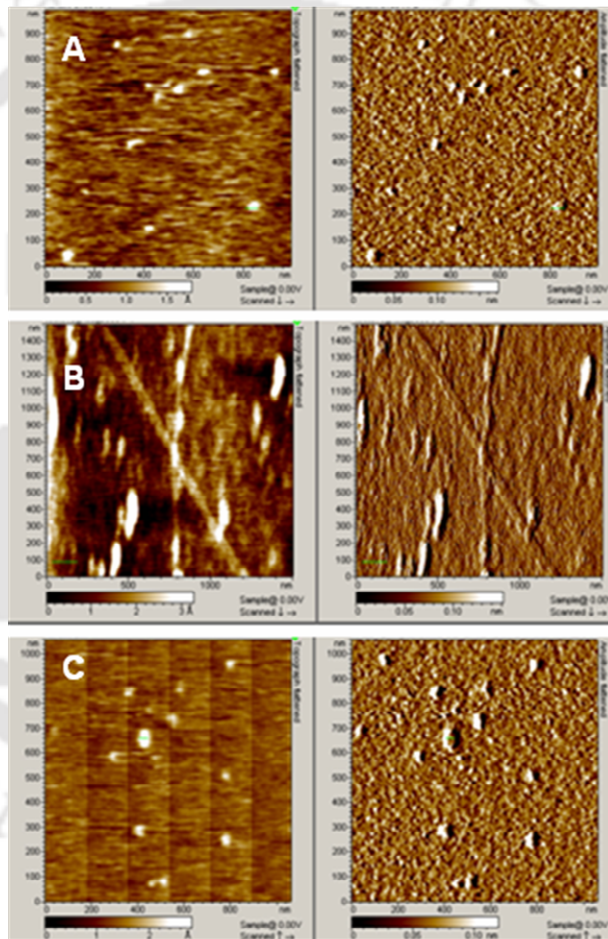
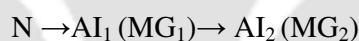


Figure 5.11 Atomic Force Microscopy (AFM) images of (A) 60 μM of DKGR at pH 7.0 (as control sample) (B) 60 μM of DKGR at pH 2.5 (C) 60 μM of DKGR at pH 2.5 with 1:1 molar curcumin. AFM images are collected after 50 h of incubation.

5.5 Discussions

A range of human diseases is associated with protein amyloid formation that results in the malfunctioning of the cellular machinery (Thomas *et al.*, 1995). In addition to significance in medicine, protein amyloid/aggregation is a fundamental problem in biotechnology as well. For example, heterologous expression of proteins in bacteria, the *de novo* design of novel proteins, or the rational modification of existing proteins, is frequently frustrated by the fact that the polypeptide chains aggregate into large assemblies including inclusion bodies or amyloid fibrils (West *et al.*, 1999; Carriò and Villaverde, 2002; Schlieker *et al.*, 2002). Thus, identification of key factor/interaction contributing to amyloid/aggregate formation and development of strategy for overcoming the problem has a potential application in therapeutics and protein biotechnology. Intermediate states are key to understanding the molecular mechanisms governing protein misfolding and their role in protein misfolding and aggregation is poorly understood. We have used DKGR as model system for the study. Ribbon diagram of DKGR is shown in Figure 5.12, which shows $(\alpha/\beta)_8$ -barrel architecture of the protein (PDB ID: 1A80). Combination of CD and fluorescence studies have contributed to the following three state acid induced unfolding pathway of DKGR.



where N, AI₁, and AI₂ are the native (pH 7.0), intermediate (pH 2.5), and second intermediate state at near pH 1.0. The acrylamide quenching data also shows two distinct curves for AI₁ and AI₂ indicating that these two are two distinct conformations, with the solvent exposure lying inbetween that of the natively folded state and completely denatured state. The AI₁ state shows molten globule (MG) like properties and has no tertiary structure but contains considerable secondary structure and strong ANS binding. Although, AI₂ also shows molten globule like properties (strong ANS binding and loss of tertiary structure etc.), it differ from AI₂ state in fluorescence properties (Figure 5.7). MG state of proteins is known to contain unstable secondary structure and is thought to expose hydrophobic patches, resulting in a tendency to aggregate due to hydrophobic interactions. The exposure of hydrophobic patches seems to shifts the equilibrium toward amyloid formation and intermolecular interactions are more favored compare to intermolecular interactions. The molten-globule state of the protein interacts

with molecular chaperon and assists in the folding process by avoiding formation of wrong conformation. As curcumin is also hydrophobic in nature, it seems that it prevents progression of amyloid formation by binding to exposed hydrophobic residues and thereby preventing intermolecular interactions. The molecular nature of the interactions of curcumin and the intermediate state is being studied in our laboratory. As the molten globule state of DKGR tends to aggregate, the stability effect could not be reliably measured in this particular condition. Curcumin shows marginal stabilizing effect on the protein possibly because it offers moieties for hydrogen bonding and ring-stacking interactions and may have stabilizing effect on protein. Thus, the inhibition of progression of amyloid formation is likely to be due to increase in activation barrier between MG_1 and amyloid.

The molten globule conformation was found in prion oligomerization and conformational transition of the human prion protein from a α -helical to a β -sheet-rich structure is believed to be the critical event in prion pathogenesis (Gerber *et al.*, 2007). Ceru *et al.* have recently reported that oligomeric molten globule state shows toxicity similar to prefibrillar oligomers (Ceru and Zerovnik, 2008).

Chiti *et al.* have performed analysis of more than 50 proteins to identify sequences which have greater amyloidogenic tendency and aggregate more rapidly than others, based on the physicochemical characteristics of the polypeptide chain, namely hydrophobicity, secondary structure propensity and charge (Chiti *et al.*, 2003). Based on this studies at the Heidelberg Laboratory of the EMBL have developed an algorithm, TANGO, that predicts which particular polypeptide sequences will aggregate or form amyloid (Fernandez-Escamilla *et al.*, 2004). Based on this algorithm, an online server, Waltz (<http://switpc7.vub.ac.be/cgi-bin/submit.cgi>) is also developed for predicting amyloidogenic regions in protein sequences at neutral pH and pH 2.6 (close to amyloidogenic condition of 2,5-Diketo-D-gluconate Reductase A). The analysis of 2,5-Diketo-D-gluconate Reductase A at pH 2.6 predicts two stretches of residues 45-51 (TAAIYGN) and 225-230 (GFVVFP) which may be involved in amyloid formation as shown in Figure 5.11.



Figure 5.12 Ribbon diagram of DKGR, showing the $(\alpha/\beta)_8$ -barrel architecture and the co-crystallized NADPH cofactor (PDB ID: 1A80). Residues which may involve in amyloid formation are shown in dark black (25-30) and green (225-230) and indicated between arrows.

5.6 Conclusions

In the present study we have shown that molten globule like intermediate state in DKGR plays an essential role in amyloidogenesis. Further, the current work shows the potential of curcumin as a common therapeutics against protein aggregation/amyloid diseases. It seems that curcumin directly interacts with the polypeptide chain and prevents its aggregation, acting like a chaperone. However, a more detailed study is required for deciphering mechanism of inhibition of amyloid formation by curcumin.

Chapter VI

Summary*

Correct folding of polypeptide chain to its native three dimensional conformations are a prerequisite for proper functioning of the protein. However, despite several cellular quality control mechanisms, proteins sometimes get kinetically trapped in local energy minima as misfolded structures. These misfolded conformations are the starting points of protein aggregation/amyloid formation. When these misfolded conformations accumulate, which can be due to reasons like destabilizing protein mutations, environmental conditions or defective cellular quality control, they interact among themselves through intermolecular interactions leading to amyloid formation. Deposition of insoluble protein aggregates in the tissues as amyloid has been the root cause of several degenerative diseases in human such as Alzheimer's disease, Parkinson disease, Type II diabetes and so on.

*Publications from current research: Sarkar *et al.* Process Biochemistry, **2011**, 46, 1179-1185 **2.** Sarkar *et al.* Biochimie, **2011**, 93, 962-968. **3.** Sarkar *et al.* Biological Chemistry, **2009**, 390, 1057-1061. **4.** Sarkar *et al.* Biochimica et Biophysica Acta- General Subjects, **2011**, DOI: 10.1016/j.bbagen.2011.06.012 **5.** Current Proteomics, **2010**, 7, 116-120

The conversion of soluble globular protein to insoluble fibrillar aggregates called “amyloid” is one of the most elusive problems of modern science which has gained immense clinical importance owing to its involvement in several degenerative diseases such as Alzheimer’s disease, Parkinson’s disease, Type II diabetes and so on. Till date over 20 different proteins have been identified which deposit in the tissues forming amyloid fibril and leading to different diseases. These amyloids are found to be highly similar in structural, immunological, toxicity and tinctorial properties despite having originated from polypeptide chains differing in sequence and tertiary structure. Considering the common structural, toxicity, immunogenic and tinctorial properties of amyloids, can it be possible to develop a common mode of therapy for all amyloid forming diseases? This was one of the questions I investigated during my PhD research. Further, recent studies have shown that amyloid formation to be an inherent property of all polypeptide chains when subjected to specific partially denaturing conditions. These studies made me more curious to research on possible common mode of therapy against amyloid diseases. Also, I explored the role of disulfide bonds in determining amyloid progression. Further, curcumin, principal curcuminoid of *Curcuma longa*, was reported to inhibit A β plaque deposition in brain. However, the mechanism of action of curcumin as not extensively investigated. This was also included as part of specific aim of my PhD research. In brief, my research work focuses on understanding critical parameters that modulate the transition of proteins from its natively folded conformation to misfolded, amyloidogenic conformation, identification of potential inhibitors of amyloidogenesis in vitro and understanding their underlying mechanism of action and further exploring the possibility of promiscuity of amyloid inhibitor.

Chapter 1:

Deposition of fibrillar protein aggregates in the tissues has been the root cause of several degenerative diseases. These fibrillar aggregates called “amyloids” exhibit highly ordered structures which are predominantly composed of cross β sheets. Recent studies have shown that amyloid formation is an inherent property of all polypeptide chains when subjected to partially denaturing conditions. In many cases, partially unfolded protein conformations with highly exposed hydrophobic surface have been found to initiate amyloidogenesis. Another interesting property of amyloids are they exhibit strikingly similar structural, toxicity, tinctorial and immunogenic property despite having

originated from polypeptide chains differing in amino acid sequence and tertiary structure. These similarities in amyloid fibrils irrespective of their source proteins invite the attention towards development of common therapeutics against amyloidosis. Thus compounds that can prevent aggregation of proteins leading to amyloid formation can serve as an effective therapeutic agent against amyloidosis¹.

Chapter 2:

We have studied the effect of few small molecule compounds e.g, clotrimazole, rottlerin and sulconazole towards amyloidogenesis of two model proteins- hen egg white lysozyme (HEWL) which forms amyloid in two pH conditions and cytochrome C from bovine heart (Cyt C). The inhibitory effect of these compounds towards amyloidogenesis was found to be both polypeptide chains as well as pH specific, suggesting that promiscuity of amyloid inhibitor seems to be elusive and further studies are required in this direction². In certain cases, stabilization of the amyloidogenic intermediate states of the proteins by the compounds suggest a possible thermodynamic mechanism of amyloid inhibition by increasing the energy barrier between the aggregation prone and the aggregated state. Further, compounds exhibiting amyloid inhibitory effect were found to reduce the surface hydrophobicity in proteins, suggesting a vital role of exposed hydrophobic surface in promoting amyloidogenesis. Docking studies also reveal that the inhibitor binds near the amyloidogenic region in the protein and prevents aggregation by blocking the hydrophobic residues.

Chapter 3:

Amyloids are known to highly stable structures which can not be easily reversed once formed. Here, using several biophysical methods like Atomic force microscopy (AFM), Fourier transform infrared spectroscopy (FTIR) and fluorescence measurements we have shown that rottlerin exhibits instantaneous disaggregation effect on HEWL fibrils. We have also monitored the conformational changes induced by rottlerin on the fibril in terms of surface hydrophobicity and secondary structure through 8-anilino-1-naphthalene sulfonic acid (ANS) fluorescence and FTIR study respectively. We have also attempted to elucidate the type of interaction between HEWL and rottlerin at pH 12.2 employing techniques like quenching study and FTIR³. These studies provide essential clues

regarding factors that stabilize amyloid fibrils, which may help in development of effective therapeutics against amyloidosis.

Chapter 4:

Effect of sodium tetrathionate (STT) towards HEWL amyloidogenesis was studied with an aim to understand the role of disulfide bonds in amyloidogenesis. STT was found to inhibit HEWL amyloidogenesis at 500 μ M concentration. However, amyloid inhibition was not accompanied by decrease in surface hydrophobicity in the protein, suggesting some other critical factor is also involved that decides amyloid progression. STT was found to facilitate intramolecular disulfide mixing in HEWL resulting in formation of HEWL species which is resistant to amyloid formation. These results essentially indicate the correct disulfide bond of an amyloidogenic protein is required for its amyloidogenic property and fibrillogenesis⁴.

Chapter 5:

Further, effect of curcumin towards amyloidogenesis of 2,5 Diketo Gluconate Reductase (DKGR) was studied, which belongs to $(\alpha/\beta)_8$ barrel class of protein. Curcumin was found to inhibit DKGR amyloidogenesis at 1:1 molar ratio, suggesting a possible mode of action of curcumin by directly interacting with the polypeptide chain and preventing aggregation. Further, molten globule like intermediate state in DKGR was found to play an important role in initiating amyloid formation⁵.

1. Sarkar et al. *Current Proteomics* (2010) 7, 116-120. 2. Sarkar et al. *Process Biochemistry* (2011) 46, 1179-1185. 3. Sarkar et al. *Biochimica et Biophysica Acta – General Subjects* (2011) DOI: 10.1016/j.bbagen.2011.06.012 4. Sarkar et al. *Biochimie* (2011) 93, 962-968. 5. Sarkar et al. *Biological Chemistry* (2009) 390, 1057-1061.

Bibliography

- Anfinsen CB, Haber E, Sela M, White FH Jr. The kinetics of formation of native ribonuclease during oxidation of the reduced polypeptide chain. *Proc Natl Acad Sci USA* 47, 1309–14 (1961).
- Anfinsen CB. Principles that govern the folding of protein chains. *Science* 181, 223–230 (1973).
- Arnaudov LN, Vries R. Thermally induced fibrillar aggregation of hen egg white lysozyme. *Biophys J* 88, 515-526 (2005).
- Artymiuk PJ, Blake CC. Refinement of human lysozyme at 1.5 Å resolution analysis of non-bonded and hydrogen-bond interactions, *J Mol Biol* 152, 737–762 (1981).
- Balasubramanian D, Kumar C. Recent studies of the circular dichroism and optical rotatory dispersion of biopolymers. *Appl Spectrosc Rev* 11, 223-286 (1976).
- Barral JM, Broadley SA, Schaffar G and Hartl F.U. Roles of molecular chaperones in protein misfolding diseases. *Semin Cell Dev Biol* 15, 17–29 (2004).
- Bench NF, Sampat RM, Kopito RR. Impairment of the ubiquitin-proteasome system by protein aggregation. *Science* 292, 1552-1555 (2001).
- Bertoncini CW, Fernandez CO, Griesinger C, Jovin TM, Zweckstetter M. Familial mutants of alpha-synuclein with increased neurotoxicity have a destabilized conformation. *J Biol Chem* 280, 30649–30652 (2005).

- Blake C, Koenig D, Mair G, North A, Phillips D, Sarma V. Structure of Hen Egg-White Lysozyme. A Three-Dimensional Fourier Synthesis at 2 Angstrom Resolution. *Nature* 206, 757-61 (1965).
- Bolognesi B, Kumita JR, Barros TP, Esbjorner EK, Luheshi LM, Crowther DC, Wilson MR, Dobson CM, Favrin G, Yerbury JJ. ANS binding reveals common features of cytotoxic amyloid species. *ACS Chem Biol* 5, 735-740 (2010).
- Booth DR, Sunde M, Bellotti V, Robinson CV, Hutchinson WL, Fraser PE, Hawkins PN, Dobson CM, Radford SE, Blake CCF, Pepsys MB. Instability, unfolding and aggregation of human lysozyme variants underlying amyloid fibrillogenesis. *Nature* 385, 787-793 (1997).
- Bouchard M, Zurdo J, Nettleton EJ, Dobson CM, Robinson CV. Formation of insulin amyloid fibrils followed by FTIR simultaneously with CD and electron microscope. *Protein Sci.* 9, 1960-1967 (2000).
- Bourassa P, Kanakis CD, Tarantilis P, Pollissiou MG, Tajmir-Riahi HA. Resveratrol, genistein, and curcumin bind bovine serum albumin. *J Phys Chem B* 114, 3348-54 (2010).
- Broome BM, Hecht MH. Nature disfavors sequences of alternating polar and non-polar amino acids: Implications for amyloidogenesis. *J Mol Biol* 296, 961-968 (2000).
- Bucciantini M, Giannoni E, Chiti F, Baroni F, Formigli L, Zurdo J, Taddei N, Ramponi G, Dobson CM, Stefani M. Inherent toxicity of aggregates implies a common mechanism for protein misfolding diseases. *Nature* 416, 507-511 (2002).
- Calamai M, Canale C, Relini A, Stefani M, Chiti F and Dobson CM. Reversal of protein aggregation provides evidence for multiple aggregated states. *J Mol Biol* 346, 603-616 (2005).
- Calloni G, Zoffoli S, Stefani M, Dobson CM And Chiti F. Investigating the effects of mutations on protein aggregation in the cell. *J Biol Chem* 280, 10607-13 (2005).
- Canale C, Torrassa S, Rispoli P, Relini A, Rolandi R, Bucciantini M, Stefani M and Gliozzi A. Natively folded HypF-N and its early amyloid aggregates interact with phospholipid monolayers and destabilize supported phospholipid bilayers. *Biophys J* 91, 4575-88 (2006).
- Carrell RW and Lomas DA. Mechanisms of disease. Alpha1-antitrypsin deficiency—a model for conformational diseases. *N Engl J Med* 346, 45-53 (2002).
- Carriò MM, Villaverde A. Construction and deconstruction of bacterial inclusion bodies. *J Biotechnol* 96, 3-12 (2002).
- Ceru S, Zerovnik E. Similar toxicity of the oligomeric molten globule state and the prefibrillar oligomers. *FEBS Lett* 582, 203-209 (2008).

- Chatani E, Goto Y. Structural stability of amyloid fibrils of β_2 -microglobulin in comparison with its native fold. *Biochim Biophys Acta Proteins Proteomics* 1753, 64-75 (2005).
- Chiti F, Calamai M, Taddei N, Stefani M, Ramponi G, Dobson CM. Studies of the aggregation of mutant proteins in vitro provide insights into the genetics of amyloid diseases. *Proc Natl Acad Sci USA* 99, 16419-26 (2002^a).
- Chiti F, Dobson CM. Protein misfolding, functional amyloid, and human disease. *Annu Rev Biochem* 75, 333–366 (2006).
- Chiti F, Stefani M, Taddei N, Ramponi G, Dobson CM. Rationalization of the effects of mutations on peptide and protein aggregation rates. *Nature* 424, 805–808 (2003).
- Chiti F, Taddei N, Baroni F, Capanni C, Stefani M, Ramponi G and Dobson CM. Kinetic partitioning of protein folding and aggregation. *Nat Struct Biol* 9, 137–143 (2002^b).
- Chiti F, Taddei N, Bucciantini M, White P, Ramponi G, Dobson CM. Mutational analysis of the propensity for amyloid by a globular protein. *EMBO J* 19, 1441-9 (2000).
- Cohen FE, Kelly JW. Therapeutic approaches to protein-misfolding diseases. *Nature* 426, 905-909 (2003).
- Cui W, Ma JW, Lei P, Wu WH, Yu YP, Xiang Y, Tong AJ, Zhao YF, Li YM. Insulin is a kinetic but not a thermodynamic inhibitor of amylin aggregation. *FEBS J* 276, 3365-3371 (2009).
- Das U, Hariprasad G, Ethayathulla AS, Manral P, Das TK, Pasha S, Mann A, Ganguli M, Verma AK, Bhat R, Chandrayan SK, Ahmed S, Sharma S, Kaur P, Singh TP, Srinivasan A. Inhibition of protein aggregation: supramolecular assemblies of arginine hold the key. *PLoS One* 2, e1176 (2007).
- Dill KA and Chan HS. From Levinthal to pathways to funnels. *Nat Struct Biol* 4, 10-19 (1997).
- Dobson CM. Protein folding and misfolding. *Nature* 426, 884-890 (2003).
- Dobson CM. Protein misfolding, evolution and disease. *Trends Biochem Sci* 24, 329–332 (1999).
- Doig AJ. Peptide inhibitors of β -amyloid aggregation. *Curr Opin Drug Discovery Dev* 10, 533-539 (2007).
- Dubey VK, Jagannadham MV. Differences in the unfolding of procerain induced by pH, GuHCl, urea and temperature. *Biochemistry* 42, 12287-97 (2003).
- Dubey VK, Lee J, Blaber M. Redesigning Symmetry-Related “Mini-Core” Regions of FGF-1 to Increase Primary Structure Symmetry: Thermodynamic and

- Functional Consequences of Structural Symmetry. *Protein Sci* 14, 2315-2323 (2005).
- Eisert R, Felau L, Brown LR. Methods for enhancing the accuracy and reproducibility of Congo red and thioflavin T assays. *Anal Biochem* 353, 144–146 (2006).
- Engel MFM. Membrane permeabilization by Islet Amyloid Polypeptide. *Chem Phys Lipids* 160, 1-10 (2009).
- Fandrich M, Fletcher MA, Dobson CM. Amyloid fibrils from muscle myoglobin. *Nature* 410, 165–166 (2001).
- Feng BY, Toyama BH, Wille H, Colby DW, Collins SR, May BCH, Prusiner SB, Weissman J, Shoichet BK. Small-molecule aggregates inhibit amyloid polymerization. *Nat Chem Biol* 4, 197-199 (2008).
- Fernández CO, Hoyer W, Zweckstetter M, Jares-Erijman EA, Subramaniam V, Griesinger C, Jovin TM. NMR of alpha-synuclein-polyamine complexes elucidates the mechanism and kinetics of induced aggregation. *EMBO J* 23, 2039-46 (2004).
- Fernandez-Escamilla AM, Rousseau F, Schymkowitz J, Serrano L. Prediction of sequence-dependent and mutational effects on the aggregation of peptides and proteins. *Nat Biotechnol* 22, 1302–1306 (2004).
- Fersht AR. A kinetically significant intermediate in the folding of barnase. *Proc Natl Acad Sci USA* 19, 14121-14126 (2000).
- Fischer H, Fukuda N, Barbry P, Illek B, Sartori C, Matthay MA. Partial restoration of defective chloride conductance in DeltaF508 CF mice by trimethylamine oxide. *Am J Physiol: Lung Cell Mol Physiol* 281, L52–L57 (2001).
- Flecha FLG, Levi V. Determination of molecular size of BSA by fluorescence anisotropy. *Biochem Mol Biol Educ* 31, 319-322 (2003).
- Friedler A, Hansson LO, Veprintsev DB, Freund SMV, Rippin TM, Nikolova PV, Proctor MR, Rüdiger S, Fersht AR. A peptide that binds and stabilizes p53 core domain: Chaperone strategy for rescue of oncogenic mutants. *Proc Natl Acad Sci USA* 99, 2937-2942 (2002).
- Garbuzynskiy SO, Lobanov MY, Galzitskaya OV. FoldAmyloid: a method of prediction of amyloidogenic regions from protein sequence. *Bioinformatics* 26, 326-32 (2010).
- Gerber R, Tahiri-Alaoui A, Hore PJ, James W. Oligomerization of the human prion protein proceeds via a molten globule intermediate. *J Biol Chem* 282, 6300–6307 (2007).
- Goda S, Takano K, Yamagata Y, Nagata R, Akutsu H, Maki S, Namba K, Yutani K. Amyloid protofibril formation of hen egg white lysozyme in highly concentrated ethanol solution. *Protein Sci* 9, 369-375 (2000).

- Goers J, Uversky VN, Fink AL. Polycation-induced oligomerization and accelerated fibrillation of human alpha-synuclein in vitro. *Protein Sci* 12, 702-7 (2003).
- Goldberg MS, Lansbury Jr PT. Is there a cause-and-effect relationship between alphasynuclein fibrillization and Parkinson's disease? *Nat Cell Biol* 2, E115–E119 (2000).
- Grindley JF, Payton MA, VAN DE Pol H, Hardy KG. Conversion of Glucose to 2-Keto-L-Gulonate, an Intermediate in L-Ascorbate Synthesis, by a Recombinant Strain of *Erwinia citreus*. *Appl Environ Microbiol* 54, 1770-1775 (1988).
- Groot NS, Ventura S. Amyloid fibril formation by bovine Cytochrome C. *Spectroscopy* 19, 199-205 (2005).
- Gruschus JM. Do Amyloid Oligomers Act As Traps for Misfolded Proteins? A Hypothesis. *Amyloid* 15,160-165 (2008).
- Gsponer J and Vendruscolo M. Theoretical approaches to protein aggregation. *Protein Pept Lett* 13, 287-293 (2006).
- Hardesty B and Kramer G. Folding of a nascent peptide on the ribosome. *Prog Nucleic Acid Res Mol Biol* 66, 41–66 (2001).
- Harper JD, Lieber CM, Lansbury PT Jr. Atomic force microscope imaging of seeded fibril formation and fibril branching by the Alzheimer's disease amyloid-beta protein. *Chem Biol* 4, 951-9 (1997).
- Hartley DM, Walsh DM, Ye CP, Diehl T, Vasquez S, Vassilev PM, Teplow DB, Selkoe DJ. Protofibrillar intermediates of amyloid beta-protein induce acute electrophysiological changes and progressive neurotoxicity in cortical neurons. *J Neurosci* 19, 8876-84 (1999).
- Heise H, Celej MS, Becker S, Riedel D, Pelah A, Kumar A, Jovin TM and Baldus M. Solid-State NMR Reveals Structural Differences between Fibrils of Wild-Type and Disease-Related A53T Mutant α -Synuclein. *J Mol Biol* 380, 444-450 (2008).
- Hendrick JP and Hart FU. The role of molecular chaperones in protein folding. *FASEB J* 9, 1559-69 (1995).
- Hermanson GT. Bioconjugate Techniques. *Academic Press* Chapter-1, 161-162 (2008).
- Higashimoto Y, Asanomi Y, Takakusagi S, Lewis MS, Uosaki K, Durell SR, Anderson CW, Appella E, Sakaguchi K. Unfolding, aggregation, and amyloid formation by the tetramerization domain from mutant p53 associated with lung cancer. *Biochemistry* 45, 1608-1619 (2006).
- Hiramatsu H, Kitagawa T. FT-IR approaches on amyloid fibril formation. *Biochim Biophys Acta Proteins Proteomics* 1753, 100-107 (2005).

- Hirota-Nakaoka M, Hasegawa K, Naiki H, Goto Y. Dissolution of β_2 -microglobulin amyloid fibrils by dimethylsulfoxide. *J Biochem* 134, 159-164 (2003).
- Hoang L, Bedard S, Krishna MM, Lin Y, Englander SW. Cytochrome c folding pathway: kinetic native-state hydrogen exchange. *Proc Natl Acad Sci USA* 99, 12173-8 (2002).
- Hollstein M, Sidransky D, Vogelstein B, Harris CC. p53 mutations in human cancers. *Science* 253, 49-53 (1991).
- Homchaudhuri L, Kumar S, Swaminathan R. Slow aggregation of lysozyme in alkaline pH monitored in real time employing fluorescence anisotropy of covalently labelled dansyl probe. *FEBS lett* 580, 2097-2101 (2006).
- Horwich A. Protein aggregation in disease: a role of folding intermediates forming specific multimeric interactions. *J Clin Invest* 110, 1221-32 (2002).
- Howard M and Welch WJ. Manipulating the folding pathway of Δ F508 CFTR using chemical chaperones. *Methods Mol. Med.* 70, 267–275 (2002).
- Hughes E, Burke RM, Doig AJ. Inhibition of toxicity in the β -amyloid peptide fragment β -(25-35) using N-methylated derivatives. *J Biol Chem* 275, 25109-115 (2000).
- Huong VT, Shimanouchi T, Shimauchi N, Yagi H, Umakoshi H, Goto Y, Kuboi R. Catechol derivatives inhibit fibril formation of amyloid- β peptides. *J Biosci Bioeng* 109, 629-634 (2010).
- Ikeda K, Okada T, Sawada S-i, Akiyoshi K, Matsuzaki K. Inhibition of the formation of amyloid beta-protein fibrils using biocompatible nanogels as artificial chaperones. *FEBS Lett* 580, 6587-6595 (2006).
- Ivanova MI, Sawaya MR, Gingery M, Attinger A, Eisenberg D. An amyloid-forming segment of beta2-microglobulin suggests a molecular model for the fibril. *Proc Natl Acad. Sci. USA* 101, 10584-10589 (2004)
- Jaroniec CP, MacPhee CE, Astrof NS, Dobson CM, Griffin RG. Molecular Conformation of a Peptide Fragment of Transthyretin in an Amyloid Fibril. *Proc Natl Acad Sci USA* 99, 16748–53 (2002).
- Kaganovich D, Kopito R and Frydman J. Misfolded proteins partition between two distinct quality control compartments. *Nature* 454, 1088-95 (2008).
- Kajava AV, Aebi U, Steven AC. The parallel superpleated beta-structure as a model for amyloid fibrils of human amylin. *J Mol Biol* 348, 247–52 (2005).
- Kalhor HR, Kamizi M, Akbari J, Heydari A. Inhibition of amyloid formation by ionic liquids: ionic liquids affecting intermediate oligomers. *Biomacromolecules* 10, 2468-2475 (2009).

- Kallberg Y, Gustafsson M, Persson B, Thyberg J, Johansson J. Prediction of amyloid fibril-forming proteins. *J Biol Chem* 276, 12945–50 (2001).
- Kayed R, Bernhagen J, Greenfield N, Khuloud S, Brunner H, Voelter W, Kapurniotu A. Conformational transitions of islet amyloid polypeptide (IAPP) in amyloid formation *in Vitro*. *J Mol Biol* 287, 781-796 (1999).
- Kayed R, Head E, Thompson JL, McIntire TM, Milton SC, Cotman CW and Glabe CG. Common structure of soluble amyloid oligomers implies common mechanism of pathogenesis. *Science* 300, 486–489 (2003).
- Kelly JW. Alternative conformations of amyloidogenic proteins govern their behavior. *Curr Opin Struct Biol* 6, 11–17 (1996).
- Khurana R, Gillespie JR, Talapatra A, Minert LJ, Ionescu-Zanetti C, Millett I, Fink AL. Partially folded intermediates as critical precursors of light chain amyloid fibrils and amorphous aggregates. *Biochemistry* 40, 3525-3535 (2001).
- Khurana R, Udgaonkar JB. Equilibrium unfolding studies of barstar: evidence for an alternative conformation which resembles a molten globule. *Biochemistry* 33, 106-115 (1994).
- Khurana S, Powers DB, Anderson S, Blaber M. Crystal structure of 2,5-diketo-D-gluconic acid reductase A complexed with NADPH at 2.1 Å resolution. *Proc Natl Acad Sci USA* 95, 6768-73 (1998).
- Kim J, Kobayashi M, Fukuda M, Ogasawara D, Kobayashi N, Han S, Nakamura C, Inada M, Miyaura C, Ikebukuro K, Sode K. Pyrroloquinoline quinone inhibits the fibrillation of amyloid proteins. *Prion* 4, 26-31 (2010).
- Krishnan R, Lindquist SL. Structural insights into a yeast prion illuminate nucleation and strain diversity. *Nature* 435, 765–72 (2005).
- Kumar S, Ravi VK, Swaminathan R. How do surfactants and DTT affect the size, dynamics, activity and growth of soluble lysozyme aggregates. *Biochem J* 415, 275-288 (2008).
- Kumar S, Ravi VK, Swaminathan R. Suppression of lysozyme aggregation at alkaline pH by tri-N-acetylchitotriose. *Biochim Biophys Acta, Proteins Proteomics* 1794, 913-920 (2009).
- Kwon YS, Koh JY, Song DK, Kim HC, Kwon MS, Choi YS, Wie MB. Danthron inhibits the neurotoxicity induced by various compounds causing oxidative damages. *Pharm Bull* 27, 723-26 (2004).
- Lakowicz JR. Principles of Fluorescence Spectroscopy. Plenum Press, New York, 1983.
- Lambert MP, Barlow AK, Chromy BA, Edwards C, Freed R, Liosatos M, Morgan TE, Rozovsky I, Trommer B, Viola KL, Wals P, Zhang C, Finch CE, Krafft GA, Klein WL. Diffusible, nonfibrillar ligands derived from A β 1-42 are potent

- central nervous system neurotoxins. *Proc Natl Acad Sci USA* 95, 6448-53 (1998).
- Lashuel HA, Hartley D, Petre BM, Walz T, Lansbury PT. Neurodegenerative disease: Amyloid pores from pathogenic mutations. *Nature* 418, 291 (2002).
- Lashuel HA. Membrane permeabilization: a common mechanism in protein-misfolding diseases. *Sci Aging Knowl Environ* 2005, 28 (2005).
- Leandro P and Gomes CM. Proteins misfolding in conformational disorders: rescue of folding defects and chemical chaperoning. *Mini Rev Med Chem* 8, 901-911 (2008).
- Lee VM. Amyloid binding ligands as Alzheimer's disease therapies. *Neuro Biol Aging* 23, 1039-1042 (2002).
- Levinthal C. Are there pathways for protein folding. *Journal de Chimie Physique et de Physico-Chimie Biologique* 65, 44-45 (1968).
- Li J, Zhu M, Manning-Bog AB, Di Monte DA, Fink AL. Dopamine and L-dopa disaggregate amyloid fibrils: implications for Parkinson's and Alzheimer's disease. *FASEB J* 18, 962-962 (2004).
- Li L, Darden TA, Bartolotti L, Kominos D, Pederson LG. An atomic model for the pleated β -sheet structure of A β amyloid protofilaments. *Biophys J* 76, 2871-2878 (1999).
- Liberek K, Lewandowska A and Zietkiewicz S. Chaperones in control of protein disaggregation. *EMBO J* 27, 328-335 (2008).
- Liu G, Men P, Harris PL, Rolston RK, Perry G, Smith MA. Nanoparticle iron chelators: A new therapeutic approach in Alzheimer disease and other neurologic disorders associated with trace metal imbalance. *Neurosci Lett* 406, 189-193 (2006).
- Liu X, Kim C, Yang J, Jemmerson R, Wang X. Induction of apoptotic program in cell-free extracts: requirement for dATP and cytochrome c. *Cell* 86, 147-57 (1996).
- Liu Y, Gotte G, Libonati M and Eisenberg D. A domain swapped RNase A dimer with implications for amyloid formation. *Nat Struct Biol* 8, 211-214 (2001).
- London J, Skrzynia C and Goldberg ME. Renaturation of *Escherichia Coli* tryptophanase after exposure to 8 M urea. *Eur J Biochem* 47, 409-415 (1974).
- Lorenzo A, Yanker BA. Beta-amyloid neurotoxicity requires fibril formation and is inhibited by Congo red. *Proc Natl Acad Sci USA* 91, 12243-47 (1994).
- Luheshi LM and Dobson CM. Bridging the gap: from protein misfolding to protein misfolding diseases. *FEBS Letts* 583, 2581-86 (2009).

- Lührs T, Ritter C, Adrian M, Riek-Loher D, Bohrmann B, Döbeli H, Schubert D, Riek R. 3D structure of Alzheimer's amyloid-beta (1-42) fibrils. *Proc Natl Acad Sci USA* 102, 17342-7 (2005).
- Malisauskas M, Weise C, Yanamandra K, Wolf-Watz M, Morozova-Roche L. Lability landscape and protease of human insulin amyloid: a new insight into its molecular properties. *J Mol Biol* 396, 60-74 (2009).
- McGovern SL, Helfand BT, Feng B, Shoichet BK. A Specific Mechanism of Nonspecific Inhibition. *J Med Chem* 46, 4265-4272 (2003).
- McLaurin J, Golomb R, Jurewicz A, Antel JP, Fraser PE. Inositol stereoisomers stabilize an oligomeric aggregate of Alzheimer's amyloid β peptide and inhibit A β -induced toxicity. *J Biol Chem* 275, 18495-18502 (2000).
- McParland VJ, Kad NM, Kalverda AP, Brown A, Kirwin-Jones P, Hunter MG, Sunde M and Radford SE. Partially unfolded states of β_2 -Microglobulin and amyloid formation in vitro. *Biochemistry* 39, 8735-46 (2000).
- Meinhardt J, Sachse C, Hortschansky P, Grigorieff N, Fändrich M. A β (1-40) fibril polymorphism implies diverse interaction patterns in amyloid fibrils. *J Mol Biol* 386, 869-77 (2009).
- Miller JV, Estell DA, Lazarus RA. Purification and Characterization of 2,5 diketo gluconate reductase from *Corynebacterium* Sp. *J Biol Chem* 262, 9016-9020 (1987).
- Mirkin N, Jaconcic J, Stojanoff V, Moreno A. High resolution X-ray crystallographic structure of bovine heart cytochrome c and its application to the design of an electron transfer biosensor. *Proteins* 70, 83-92 (2008).
- Mishra S, Palanivelu K. The effect of curcumin (turmeric) on Alzheimer's disease: An overview. *Ann Indian Acad Neurol* 11, 13-19 (2008)
- Morris GM, Huey R, Lindstrom W, Sanner MF, Belew RK, Goodsell DS, Olson AJ. AutoDock4 and AutoDockTools4: Automated docking with selective receptor flexibility. *J Comput Chem* 30, 2785-2791 (2009).
- Morshedi D, Rezaei-Ghaleh N, Ebrahim-Habibi A, Ahmadian S, Nemat-Gorgani M. Inhibition of amyloid fibrillation of lysozyme by indole derivatives- possible mechanism of action. *FEBS J* 274, 6415-6425 (2007).
- Nakanishi T, Yoshioka M, Moriuchi K, Yamamoto D, Tsuji M, Takubo T. S-sulfonation of transthyretin is an important trigger step in the formation of transthyretin-related amyloid fibril. *Biochim Biophys Acta, Proteins Proteomics* 1804, 1449-1456 (2010).
- Nakashima T, Higa H, Matsubara H, Benson AM, Yasunobu KT. The amino acid sequence of bovine heart cytochrome c. *J Biol Chem* 241, 1166-77 (1966).

- Nallamsetty S, Dubey VK, Pande M, Ambasht PK & Jagannadham MV. Accumulation of partly folded states in the equilibrium unfolding of ervatamin A: Spectroscopic description of the native, intermediate, and unfolded states. *Biochimie* 89, 1416-1426 (2007).
- Ng TP, Chiam PC, Lee T, Chua H-C, Lim L and Kua E-H. Curry Consumption and Cognitive Function in the Elderly. *Am J Epidemiol* 164, 898–906 (2006).
- Nilsson MR. Techniques to study amyloid fibril formation in vitro. *Methods* 34, 151-160 (2004).
- Oberg K, Chrnyk BA, Wetzel R and Fink AL. Native-like secondary structure in Interleukin-1.β. Inclusion bodies by attenuated Total Reflectance FTIR. *Biochemistry* 33, 2628-34 (1994).
- Otzen DE, Kristensen O, Oliveberg M. Designed protein tetramer zipped together with a hydrophobic Alzheimer homology: A structural clue to amyloid assembly. *Proc Natl Acad Sci USA* 97, 9907–12 (2000).
- Pace CN. Measuring and increasing protein stability. *Trends Biotechnol* 8, 93-98 (1990).
- Pai AS, Rubinstein I, Onyuksel H. PEGylated phospholipid nanomicelles interact with beta-amyloid (1-42) and mitigate its beta-sheet formation, aggregation and neurotoxicity in vitro. *Peptides* 27, 2858-2866 (2006).
- Papadopoulou A, Green RJ, Frazier RA. Interaction of Flavonoids with Bovine Serum Albumin: A Fluorescence Quenching Study. *J Agric Food Chem* 53, 158-163 (2005).
- Pedersen JS, Christensen G, Otzen DE. Modulation of S6 fibrillation by unfolding rates and gatekeeper residues. *J Mol Biol* 341, 575–588 (2004).
- Pedersen JS, Dikov D, Flink JL, Hjuler HA, Christiansen G, Otzen DE. Changing face of glucagon fibrillation: structural polymorphism and conformational imprinting. *J Biol Chem* 355, 501-23 (2006).
- Pepsys MB, Hawkins PN, Booth DR, Vigushin DM, Tennent GA, Soutar AK, Totty N, Nguyen O, Blake CCF, Terry CJ, Feest TG, Zalini AM, Hsuan JJ. Human lysozyme gene mutations cause hereditary systemic amyloidosis. *Nature* 362, 553-557 (1993).
- Perutz MF, Finch JT, Berriman J, Lesk A. Amyloid fibers are water-filled nanotubes. *Proc Natl Acad Sci USA* 99, 5591–95 (2002).
- Petkova AT, Ishii Y, Balbach JJ, Antzutkin ON, Leapman RD, Delaglio F and Tycko R. A structural model for Alzheimer's beta-amyloid fibrils based on experimental constraints from solid state NMR. *Proc Natl Acad Sci USA* 99, 16742-47 (2002).

- Porat Y, Abramowitz A, Gazit E. Inhibition of amyloid fibril formation by polyphenols: structural similarity and aromatic interactions as a common mechanism of inhibition. *Chem Biol Drug Des* 67, 27-37 (2006).
- Priller C, Bauer T, Mitteregger G, Krebs B, Kretzschmar HA, Herms J. Synapse formation and function is modulated by the amyloid precursor protein. *J Neurosci* 26, 7212–7221 (2006).
- Quintas A, Vaz DC, Cardoso I, Saraiva MJ, Brito RM. Tetrameric dissociation and monomer partial unfolding precedes protofibril formation in amyloidogenic transthyretin variants. *J Biol Chem* 276, 27207-27213 (2001).
- Radford SE, Dobson CM, Evans PA. The folding of hen lysozyme involves partially structured intermediates and multiple pathways. *Nature* 358, 302–307 (1992).
- Rambaran RN and Serpell LC. Amyloid fibrils- abnormal protein assembly. *Prion* 2, 112-117 (2008).
- Redfield C, Dobson CM. 1H NMR studies of human lysozyme: Spectral assignment and comparison with hen lysozyme, *Biochemistry* 29, 7201– 7214 (1990).
- Roberto S, Ineke Quality control in the endoplasmic reticulum protein factory. *Nature* 426, 891-894 (2003)
- Roux P, Delepierre M, Goldberg ME, Chaffotte A. Kinetics of Secondary Structure Recovery during the Refolding of Reduced Hen Egg White Lysozyme. *J Biol Chem* 272, 24843-24849 (1997).
- Saiki M, Honda S, Kawasaki K, Zhou D, Kaito A, Konakahara T, Morii H. Higher-order molecular packing in amyloid-like constructed with linear arrangements of hydrophobic and hydrogen-bonding side-chains. *J Mol Biol* 348, 983–98 (2005).
- Samuel D, Kumar TK, Ganesh G, Jayaraman G, Yang PW, Chang MM, Trivedi VD, Wang SL, Hwang KC, Chang DK, Yu C. Proline inhibits aggregation during protein refolding. *Protein Sci* 9, 344-52 (2000).
- Samuel D, Kumar TKS, Jayaraman G, Yang PW, Yu C. Proline is a protein stabilizing solute. *Biochem Mol Biol Int* 41, 235–242 (1997).
- Sarkar N, Dubey VK. Protein nano-fibrillar structure and associated diseases. *Curr Proteomics* 7, 116-120 (2010).
- Sarkar N, Singh AN, Dubey VK. Effect of curcumin on amyloidogenic property of molten globule-like intermediate state of 2,5-diketo-D-gluconate reductase A. *Biol Chem* 390, 1057-1061 (2009).
- Sawkar AR, Cheng WC, Beutler E, Wong CH, Balch WE, Kelly JW. Chemical chaperones increase the cellular activity of N370S β -glucosidase: a therapeutic strategy for Gaucher disease. *Proc Natl Acad Sci USA* 99, 15428–15433 (2002).

- Schiene C, Fischer G. Enzymes that catalyze the restructuring of proteins. *Curr Opin Struct Biol* 10, 40-45 (2000).
- Schlieker C, Bukau B, Mogk A. Prevention and reversion of protein aggregation by molecular chaperones in the E. coli cytosol: implications for their applicability in biotechnology. *J Biotechnol* 96, 13-21 (2002).
- Schmittschmitt JP, Scholtz JM. The role of protein stability, solubility, and net charge in amyloid fibril formation. *Protein Sci* 12, 2374-8 (2003).
- Schobert B, Tschesche H. Unusual solution properties of proline and its interaction with proteins. *Biochim Biophys Acta* 541, 270-77 (1978).
- Schubert U, Anton LC, Gibbs J, Norbury CM, Yewdell JW, Bennick JR. Rapid degradation of a large fraction of newly synthesized proteins by proteasomes. *Nature* 404, 770-774 (2000).
- Selkoe DJ. Folding proteins in fatal ways. *Nature* 426, 900-904 (2003).
- Semisotnov GV, Rodionova NA, Razgulyaev OI, Uversky VN, Gripas AF, Gilmanshin RI. Study of the molten globule intermediate state in protein folding by a hydrophobic fluorescent probe. *Biopolymers* 31, 119-128 (1991).
- Serpell LC, Berriman J, Jakes R, Goedert M and Crowther RA. Fiber diffraction of synthetic alpha-synuclein filaments shows amyloid-like cross-beta conformation. *Proc Natl Acad Sci USA* 97, 4897-4902 (2000).
- Serpell LC, Sunde M, Fraser PE, Luther PK, Morris EP, Sangren O, Lundgren E, Blake CC. Examination of the structure of the transthyretin amyloid fibril by image reconstruction from electron micrographs. *J Mol Biol* 254, 113-8 (1995).
- Shea TB, Robert DO, Nicolosi RJ, Kumar R, Watterson AC. Nanosphere-mediated delivery of vitamin E increases its efficacy against oxidative stress resulting from exposure to amyloid beta. *Journal of Alzheimers Disease* 7, 297-301 (2005).
- Shiraki K, Kudou M, Fujiwara S, Imanaka T, Takagi M. Biophysical effect of amino acids on the prevention of protein aggregation. *J Biochem (Tokyo)* 132, 591-95 (2002).
- Silow M, Tan Y, Fersht AR and Oliveberg M. Formation of short-lived protein aggregates directly from the coil in two-state folding. *Biochemistry* 38, 13006-12 (1999).
- Sonoyama T, Kobayashi K. Purification and properties of two 2,5-diketo-D-gluconate reductases from a mutant strain derived from *Corynebacterium* sp. *J Ferment Bioeng* 65, 311-317 (1987).
- Stefani M and Dobson CM. Protein aggregation and aggregate toxicity: new insights into protein folding, misfolding diseases and biological evolution. *J Mol Med* 81, 678-99 (2003).

- Stefani M. Protein misfolding and aggregation: new examples in medicine and biology of dark side of protein world. *Biochim Biophys Acta* 1739, 5-25 (2004).
- Stryer L. The interaction of a naphthalene dye with apomyoglobin and apohemoglobin. A fluorescent probe of non-polar binding sites. *J Mol Biol* 245, 525–530 (1965).
- Sunde M and Blake CCF. The structure of amyloid fibrils by electron microscopy and X-ray diffraction. *Adv Protein Chem* 50, 123–59 (1997).
- Sureshbabu N, Kirubakaran R, Thangarajah H, Padma Malar EJ and Jayakumar R. Lipid-induced conformational transition of Amyloid β peptide fragments. *J Mol Neurosci* 41, 368-82 (2010).
- Takahashi TT, Mihara HH. Peptide and Protein Mimetics Inhibiting Amyloid β -Peptide Aggregation. *Acc Chem Res* 41, 1309-1318 (2008).
- Tanaka M, Chien P, Yonekura K, Weissman JS. Mechanism of cross-species prion transmission: an infectious conformation compatible with two highly divergent yeast prion proteins. *Cell* 121, 49-62 (2005).
- Thomas PJ, Qu B-H, Pederson PL. Defective protein folding as a basis of human disease. *Trends Biochem Sci* 20, 456–459 (1995).
- Tomiyaama T, Kaneko H, Kataoka K, Asano S, Endo N. Rifampicin inhibits the toxicity of pre-aggregated amyloid peptides by binding to peptide fibrils and preventing amyloid-cell interaction. *Biochem J* 322, 859-865 (1997).
- Torok B, Dasgupta S, Torok M. Chemistry of small molecule inhibitors in self-assembly of Alzheimer's disease related amyloid-beta peptide. *Curr Bioact Compd* 4, 159-174 (2008).
- Tyedmeters J, Mogk A, Bukau B. Cellular strategies for controlling protein aggregation. *Nature* 11, 777-788 (2010).
- Uversky VN, Li J, Souillac P, Millett IS, Doniach S, Jakes R, Goedert M, Fink AL. Biophysical properties of the synucleins and their propensities to fibrillate: inhibition of alpha-synuclein assembly by beta- and gamma-synucleins. *J Biol Chem* 277, 11970-8 (2002).
- Wallace AC, Laskowski RA, Thornton JM. Ligplot: a program to generate schematic diagrams of protein–ligand interactions. *Prot Eng* 8, 127-134 (1995).
- Walsh DM, Lomakin A, Benedek GB, Condron MM and Teplow DB. Amyloid beta-protein fibrillogenesis. Detection of a protofibrillar intermediate. *J Biol Chem* 272, 22364–72 (1997).
- Wang SS, Chen P and Hung Y. Effects of p-benzoquinone and melatonin on amyloid fibrillogenesis of hen egg-white lysozyme. *J Mol Catal B:Enzym* 43, 49-57 (2006).

- Wang SS, Liu KN, Lee WH. Effect of curcumin on amyloid fibrillogenesis of hen egg white lysozyme. *Biophys Chem* 144, 78-87 (2009^a).
- Wang SS, Liu KN, Lu YC. Amyloid fibrillation by Hen Egg-White Lysozyme is inhibited TCEP. *Biochem Biophys Res Commun* 381, 639-642 (2009^b).
- West MW, Wang W, Patterson J, Mancias JD, Beasley JR, Hecht MH. De novo amyloid proteins from designed combinatorial libraries. *Proc Natl Acad Sci USA* 96, 11211-11216 (1999).
- Wilson MR, Easterbrook Smith SB. Clusterin is a secreted mammalian chaperone. *Trends Biochem Sci* 25, 95-98 (2000).
- Wright CF, Teichmann SA, Clarke J, Dobson CM. The importance of sequence diversity in the aggregation and evolution of proteins. *Nature* 438, 878-81 (2005).
- Yamamoto K, Yagi H, Ozawa D, Sasahara K, Naiki H, Goto Y. Thiol compounds inhibits the formation of amyloid fibrils by β_2 -microglobulin at neutral pH. *J Mol Biol* 376, 258-268 (2008).
- Yang F, Lim GP, Begum AN, Ubeda OJ, Simmons MR, Ambegaokar SS, Chen PP, Kaye R, Glabe CG, Frautsch SA, Cole GM. Curcumin inhibits formation of amyloid beta oligomers and fibrils, binds plaques, and reduces amyloid in vivo. *J Biol Chem* 280, 5892-901 (2005).
- Yang SG, Wang WY, Ling TJ, Feng Y, Du XT, Zhang X, Sun XX, Zhao M, Xue D, Yang Y, Liu RT. Alpha-tocopherol quinone inhibits beta-amyloid aggregation and toxicity, disaggregates preformed fibrils and decrease the production of reactive oxygen species, NO and inflammatory cytokines. *Neurochem Int* 57, 914-922 (2010).
- Yum DY, Lee BY, Pan JG. Identification of the yqhE and yafB genes encoding two 2,5 Diketo-D-Gluconate Reductases in *Escherichia coli*. *Appl Environ Microbiol* 65, 3341-46 (1999).
- Zhang L, Xing GQ, Barker JL, Chang Y, Maric D, Ma W, Li B-S, Rubiow DR. α -Lipoic acid protects rat cortical neurons against cell death induced by amyloid and hydrogen peroxide through the Akt signalling pathway. *Neurosci Lett* 312, 125-128 (2001).
- Zhang Q, Kelly JW. Cys10 mixed disulfides make transthyretin more amyloidogenic under mildly acidic condition. *Biochemistry* 42, 8756-8761 (2003).
- Zhu M, Rajamani S, Kaylor J, Han S, Zhou F, Fink AL. The flavonoid bicalcin inhibits fibrillation of alpha-synuclein and disaggregates existing fibrils. *J Biol Chem* 279, 26846-57 (2004).

Publications

Publications (In Peer Reviewed Journals)

Published/ Accepted

1. **Nandini Sarkar**, Manjeet Kumar and Vikash Kumar Dubey. Rottlerin dissolves pre-formed protein amyloid: A study on hen egg white lysozyme. *Biochimica et Biophysica Acta - General Subjects* (2011) DOI: 10.1016/j.bbagen.2011.06.012
2. **Nandini Sarkar**, Manjeet Kumar and Vikash Kumar Dubey. Effect of sodium tetrathionate on amyloid fibril: Insight in to the role of disulfide bond in amyloid progression. *Biochimie* (2011) 93, 962-968.
3. **Nandini Sarkar**, Manjeet Kumar and Vikash Kumar Dubey. Exploring possibility of promiscuity of amyloid inhibitor: Studies on effect of selected compounds on folding and amyloid formation of proteins. *Process Biochemistry* (2011) 46, 1179-1185.
4. **Nandini Sarkar**, Abhay Narain Singh and Vikash Kumar Dubey. Effect of curcumin on amyloidogenic property of molten globule like intermediate state of 2,5-Diketo-D-Gluconate Reductase A. *Biological Chemistry* (2009) 390, 1057-1061.
5. **Nandini Sarkar**, Vikash Kumar Dubey. Protein nano-fibrillar structure and associated diseases. *Current Proteomics* (2010) 7, 116-120.
6. **Nandini Sarkar**, Pramod Kumar Srivastava, Vikash Kumar Dubey. Understanding the language of Vitamin C. *Current Nutrition & Food Science* (2009) 5, 53-55.
7. Bishal Kumar Singh, **Nandini Sarkar** and Vikash Kumar Dubey. Modeled Structure of Trypanothione synthetase of *Leishmania infantum* for development of novel therapeutics for leishmaniasis. *Current Trends in Biotechnology and Pharmacy* (2008) 2, 390-395.
8. Bishal Kumar Singh, **Nandini Sarkar**, M.V. Jagannadham and Vikash Kumar Dubey. Modeled Structure of Trypanothione Reductase of *Leishmania infantum*. *Biochemistry and Molecular Biology Reports* (2008) 41, 444-447.
9. Vikash Kumar Dubey, Bishal Kumar Singh, **Nandini Sarkar**, Monu Pande and M.V Jagannadham. Biophysical characterization of Fibroblast Growth Factor homologous Factor-1b (FHF-1b): Sodium dodecyl sulfate promotes two state folding. *Protein & Peptide Letters* (2008) 15, 215-218.

Conference Presentations

- **Nandini Sarkar**, Abhay Narain Singh and Vikash Kumar Dubey. "Studies on 2,5 Di Keto D Gluconate Reductase : Identification of amyloid forming folding intermediate state in acidic condition". 77th Annual Meeting of Society of Biological Chemists India, held at IIT Chennai during 18-20 December 2008. **Awarded B.S NARASINGA RAO BEST POSTER AWARD.**
- **Nandini Sarkar**, Abhay Narain Singh, Vikash Kumar Dubey. "Identification of amyloidogenic folding intermediate state of 2,5-Diketo-D-Gluconate Reductase A: Effect of Curcumin on Amyloid formation". 21st IUBMB and 12th FAOBMB International Congress of Biochemistry and Molecular Biology held on 2-7 August 2009 and Young Scientist Program held on July30-August 2, 2009 in Shanghai, China. **(The work was selected for IUBMB full travel fellowship funding and Young Scientist Program Award).**
- **Nandini Sarkar** and Vikash Kumar Dubey. "Effect of small molecule aggregators on amyloid formation of proteins". Symposium on Recent Trends in Biophysics sponsored by Indian Biophysical Society, held at Benaras Hindu University, Varanasi, 13-15 February 2010.